TRANSIENT HEAT TRANSFER AND THERMAL PROPERTIES IN FOOD SYSTEMS

Thesis for the Degree of Ph. D.
MICHIGAN STATE UNIVERSITY

Isaiah J. Kopelman

1966

THESIS

This is to certify that the

thesis entitled

Transient Heat Transfer and Thermal

Properties in Food Systems

presented by

Isaiah J. Kopelman

has been accepted towards fulfillment
of the requirements for

Ph.D. degree in Food Science

Major professor

Date Feb. 21, 1966.

O-169

TH

TH

ABSTRACT

TRANSIENT HEAT TRANSFER AND THERMAL PROPERTIES IN FOOD SYSTEMS

by Isaiah J. Kopelman

The study of the transient state heat transfer is important in many food processing operations, from the designing as well as the evaluation of quality viewpoint. For the analytical treatment of heat transfer problems it will be useful to know more about transient heat transfer analysis and thermal properties. In this project both transient heat transfer and the evaluation of thermal properties were studied.

The project consisted of two studies: a theoretical study and a laboratory study. The theoretical part of the thesis in itself consisted of two parts; a study to extend the knowledge and use of the first term approximation (suggested by Ball, 1923) and an analysis of the thermal conductivity of two-component homogeneous dispersion systems. Specifically the theoretical study consisted of a dimensional analysis of f; derivation of a mathematical expression for the relationship of the body properties and the system properties as related to the magnitude of f and j as reflected in the design of an experiment and the evaluation of experimental data; derivation of a mathematical expression in which the mass average temperature is a function of the temperature at the

TH

geometric center; studying the heat transfer properties of low and high N_{Bi} and analysis of the thermal conductivity of a one, two and three dimensional, homogeneous two-component dispersion system. The laboratory study consisted of two parts: an investigation of the thermal conductivity of a foam, a two-component air-sucrose solution, and evaluation of the thermal diffusivity of several food products.

The expression developed for the thermal conductivity of the three dimensional two-component homogeneous isotropic system was evaluated experimentally using a transient heat transfer method in a high film coefficient system in which the thermal diffusivity of 1.5, 8, 16 and 24 percent by weight air-sucrose solutions foam having various amounts of air, in three sizes of stainless steel tubings (1", 1.5" and 2" O.D.) during heating from 36° F to 96° F and cooling from 96° F to 36° F were measured.

The analysis of the experimental data was carried out using a Control Data 3600 Digital Computer; the results showed that the values and the magnitude of the thermal conductivity of the foamed sucrose matrix compared with the values and particularly with the magnitude of the developed expression. The thermal diffusivity of several typical foodstuffs (raw potato flesh, raw and deaerated apple flesh, apple sauce and meat) was evaluated using the same experimental system.

The analysis of the thermal conductivity of a two-dimensional homogeneous anisotropic fibrous (or layered) system which showed that

TH

the thermal conductivity in the direction parallel to the fibers is always larger than the thermal conductivity in the direction perpendicular to the fibers was confirmed both by the results of the meat flesh experiments of this study and by the results of the extensive work related to the thermal conductivity of meat done by Lentz (1961) and Miller (1963).

TH

TRANSIENT HEAT TRANSFER AND THERMAL PROPERTIES IN FOOD SYSTEMS

By

Isaiah J. Kopelman

A THESIS

Submitted to
Michigan State University
in partial fulfillment of the requirements
for the degree of

DOCTOR OF PHILOSOPHY

Department of Food Science

1966

To my family

למשפחתי

TH

ACKNOWLEDGMENTS

The author wishes to express his sincere appreciation to Dr. I. J. Pflug (Food Science), a truly inspiring teacher and counselor; for his guidance and friendship during the course of this investigation.

Grateful appreciation is also extended to Dr. C. M. Cooper (Chemical Engineering), Dr. B. S. Schweigert (Food Science), Dr. L. E. Dawson (Food Science) and Dr. R. F. Gonzalez (Management) for serving on the author's guidance committee.

The author is indebted to the American Society of Heating, Refrigerating and Air-Conditioning Engineers (ASHRAE) for supporting project RP-42 of which this study is a part. I wish to express particular thanks to Mr. H. A. Whitesel and to the late Mr. M. A. Mayers, Directors of Research for ASHRAE and to Mr. E. J. Robertson, Chairman of the ASHRAE Task Group on Food Science and Refrigeration, for their interest in this project.

Thanks go to Dr. B. S. Schweigert, Chairman of the Food Science Department, for making available the graduate assistantship.

Grateful acknowledgment is extended to Mr. C. Borrero for spending much valuable time reviewing the manuscript and to Mr. R. K. Fisher and Mr. W. J. Marble for their assistance in the laboratory.

TABLE OF CONTENTS

THE

LIST OF TABLES

LIST OF FIGURES

THI

TH

NOMENCLATURE

A	constant in equation (5. 2. 2)	
A_r	surface area of the body	ft^2
AIR	amount of air (v/v) in percent	dimensionless
AVT	average time temperature	°F
a	volumetric fraction of air	dimensionless
B	constant in equation (5. 2. 2)	
b	constant in $k = b\ AIR + d$	
C	constant in equation (3. 5. 14)	
C_p	specific heat	Btu/lb °F
D	diameter of sphere or cylinder, or thickness of slab	ft
d	constant in $k = b\ AIR + d$	
E	$\log (f_1/f_2)/\log (R_1/R_2)$	dimensionless
e	Naperian base (= 2.71828)	
f	temperature response parameter; time required for the asymptote of the heating (or cooling) curve to cross one log-cycle, the time required for a 90% reduction of temperature on the linear portion of the heating (or cooling) curve	hr
g	gravitational constant	ft/hr^2
h	surface film coefficient	Btu/hr ft^2 °F

TH

j	lag factor $(T_a - T_1)/T_0 - T_1)$. j_c, lag factor at the geometric center, j_s, lag factor at the surface; j_m, lag factor for the mass average	dimensionless
$J_n(\beta_i)$	nth order, Bessel function of first kind for the argument β_i	dimensionless
K	j_m/j_c	dimensionless
k	thermal conductivity; k means thermal conductivity of the system; k_A, thermal conductivity of air; k_c, thermal conductivity of the continuous component; k_d, thermal conductivity of the dispersed component; k_E, the experimental thermal conductivity; k_L, thermal conductivity of sucrose solution; k_T, the predicted thermal conductivity; k_w, the thermal conductivity of water; $k_{\parallel}$, the thermal conductivity in the direction parallel to the fibers; $k_{\perp}$, the thermal conductivity in the direction perpendicular to the direction of the fibers	Btu/hr ft °F
L	characteristic length of product in the direction of the fluid flow	ft
M	parameter in the three dimensional dispersion system, M^3 = void fraction	dimensionless
N	parameter in the two dimensional dispersion system, N^2 = void fraction	dimensionless
N_{Bi}	Biot number $\frac{h R}{k}$	dimensionless
N_{Gr}	Grashof number $\frac{L^3 \rho^2 g \beta (T_1 - T_f)}{\mu^2}$	dimensionless

TH

N_{Pr}	Prandtl number $\frac{C_p \mu}{k_f}$	dimensionless
P	parameter in the one dimensional dispersion system, P = void fraction	dimensionless
q	rate of heat generated	Btu/ ton day
Q	constant (Table 3. 3)	dimensionless
R	radius of sphere or cylinder; half the thickness of slab	ft
r	distance from center to point of measurement in a sphere, cylinder or slab	ft
S	sucrose concentration, percent w/ w	dimensionless
SJ	the ratio between the experimental lag factor and the predicted lag factor, $j_c / T j_c$	
ST	the ratio between the experimental thermal conductivity and the predicted thermal conductivity, k_E / k_T	dimensionless
T	temperature; T_0, initial temperature, T, product temperature; T_1, temperature of cooling or heating media; T_a, the apparent initial temperature as defined by the linear portion of the cooling curve, that is, the ordinate value of the asymptote of cooling curve; T_{ac} for center, T_{am} for mean and T_{as} for surface; T_f, temperature of fluid film, $(T_s + T_1)/2$ where T_s is the surface temperature	°F
t	time	hr
V	volume	ft^3

TH

W	k_d/k_c	dimensionless
w	the ratio between the thermal conductivity of the foamed sucrose solution, k_E, and the thermal conductivity of the same sucrose solution having zero air $k_E/(k_E)_{0\%\ air}$	dimensionless
x, y, z	rectangular coordinates	ft
α	thermal diffusivity $k/C_p\ \rho$; α_E, the experimental thermal diffusivity; α_T, the predicted thermal diffusivity	ft^2/hr
β	thermal coefficient of volumetric expansion	$1/°F$
β_n	nth root of the boundary equation	dimensionless
ξ	exponent in equation (3.1.2)	
δ	exponent in equation (3.1.2)	
ε	exponent in equation (3.1.2)	
η	exponent in equation (3.1.2)	
θ	angle in cylindrical or spherical coordinates	radians
λ	constant in equation (3.1.2)	
μ	viscosity	lb/hr ft
π	pi = 3.14159	
ϕ	angle in spherical coordinates	radians
ρ	density: ρ, density of the system; ρ_A, density of air; ρ_L, density of sucrose solution	lb/ft^3
ψ	indicating function	

1. INTRODUCTION, LITERATURE REVIEW AND OBJECTIVES

Most processed foods are subjected to a heat treatment, either heating or cooling, moderate or severe, once or several times. Both desirable and undesirable changes in the food product are produced by the heat treatment. Understanding the heat flow mechanism and knowledge of the thermal properties of the food product are essential in making analytical studies of food processes such as heating, cooling, or dehydrating. Analytical heat processing studies are very useful in designing new processing systems and in improving existing food processing systems.

In handling and storage of perishable food products, knowledge of heat transfer and thermal properties are as important or may even be more important than for processed foods since produce quality may be directly related to the heat process.

Information regarding the three conduction heat transfer thermal properties; thermal conductivity, specific heat, and density, for particular food substances is limited and frequently conflicting; of these three thermal properties, the thermal conductivity is the most elusive and variable. Where data do exist, information is often lacking regarding the composition of the sample, or specifications of the experiments, temperature difference, and structure of the sample in respect to heat flow. In some cases the reporters apparently failed to fully understand

TH

the mathematical models and their results based on misinterpretation of their data are misleading.

Excluding the information on the specific heat of foodstuffs based on the work of Siebel (1892), the first recent basic data related to thermal properties of foodstuffs was evaluated by Gane (1936). In addition important data have been generated within the past decade by workers such as Lentz (1961) and Miller (1963) where the thermal conductivity of meats and fats mostly in the frozen state was determined using the guarded hot plate method (steady state conditions); Turrell and Perry (1957) and Poppendiek (1953) reported specific heat and thermal conductivity of citrus, assuming a spherical geometric shape; Bennett (1962, 1964) reported the thermal conductivity of Valencia orange and Marsh grapefruit using the Fitch (1935) method; the Fitch method was also used by Walters (1963) to determine the thermal conductivity of chicken breast muscle and skin in the frozen state; the thermal conductivities of beef, fruit tissue and fish during freeze-drying were determined under quasi-steady-state conditions by Harper (1962) and Graham et al. (1964). Dickerson (1955) used a system in which the $\frac{\partial T}{\partial t}$ of the sample was kept constant to determine the thermal diffusivity of food substances under transient heat flow conditions. Charm (1963) presented a trial-and-error method to calculate the thermal conductivity of frozen food using the heat penetration curve.

The specific heat is relatively an easier property to measure than

TH

thermal conductivity since it is independent of direction or shape. Measurement of the specific heat dates back to Siebel (1892). Since then some of the important work has been done by: Short et al. (1942), Ordinanz (1946), Staph (1949), Staph and Woolrich (1951), Mannheim et al. (1955), Janson and Long (1955), Moline et al. (1961), and others. Their results may be found tabulated in such books as ASHRAE Guide and Data Book, Anderson (1959), and Charm (1963).

Pflug et al. (1965) observed that thermal diffusivity calculated using thermal conductivity by the Anderson (1959) equation (equation 6.1.5) is unreasonably high for apples. The difference is probably due to intercellular air which may occupy approximately 20 to 25% of the volume of the fruit (Smock and Neubert, 1950; Reeve and Leinbach, 1965) and which the Anderson equation does not take into account. The Anderson thermal conductivity prediction equation agrees with the sucrose solution data of Riedel (1951) and presumably agrees with data for other foodstuff solutions. If an apple was a homogeneous solution of components--without air--the Anderson equation probably would give satisfactory results. However, since as much as 25% of the apple volume may be intercellular air spaces, a new approach to predicting the thermal conductivity is needed. This point, discussed in detail by Kopelman et al. (1965), was the initiation point for this study. It was concluded that in order to study the basic phenomena and the role of the air in fixing the thermal conductivity, we ought to go to a foodstuff model

TH

system. A model system makes it possible to vary the composition of the solid phase and at the same time the amount of dispersed air with greater stability and a more precise geometrical shape.

This project consisted of two studies; a laboratory study performed first followed by a theoretical study. (In this thesis the theoretical study is presented first for greater continuity in the thesis.)

The objective of the experimental phase of this study was divided into two parts:

1. To investigate the thermal conductivity of air-foamed sucrose solutions. Specifically to develop an expression for the overall thermal conductivity of the system and to check it experimentally using air-foamed and stabilized sucrose solutions, in which the overall system thermal conductivity is a function of the known parameters, i.e., function of the thermal conductivity of the continuous and the discontinuous phases, and their volumetric proportion.

2. To determine the thermal conductivity of several typical foodstuffs (raw potato flesh, raw and deaerated apple flesh, apple sauce and meat).

The objective of the second phase of this study was to conduct a further investigation of the first term approximation theory and to analyze the thermal conductivity of dispersion systems. Specifically, to make a dimensional analysis of f; derive a mathematical expression for the relationship between the body properties and the system properties as

TH

related to the magnitude of f and j as reflected in the design of an experiment and the evaluation of experimental data; to derive a mathematical expression in which the mass average temperature is a function of the temperature at the geometric center; to study the heat transfer properties of low and high N_{Bi} and to analyze the thermal conductivity of a one, two and three dimensional homogeneous dispersion systems.

The accuracy of the solution of any heat transfer problem depends to a great extent on the accuracy of the thermal property values used in the analysis. The properties involved in conduction heat transfer are: thermal conductivity, k; specific heat, C_p; and density, ρ. As far as density and specific heat are concerned, their determination is a comparatively simple process. The thermal diffusivity α is of the utmost importance; however, it is derived from the three thermal properties, $\alpha = k/C_p\,\rho$.

There are many methods which at one time or another have been used for measuring thermal conductivity. The thermal properties of any material occur in various combinations which may be regarded as characteristic of, and measured by, different experimental situations. The methods can be classified under two categories: steady and transient state. The former usually determines thermal conductivity, and the latter thermal diffusivity. In fact, most transient state experiments, in principle, not necessarily in practice, make possible determination of both k and α. Steady state methods often involve the

measurement of the quantity of heat transferred and since heat losses cannot be entirely eliminated, this often presents a difficult problem; also, the time required for reaching equilibrium and completion of the test is rather long.

In transient methods, changing temperatures in respect to time are measured instead of the quantity of heat. These methods suffer from the disadvantage that it is difficult to know how closely the actual boundary conditions in an experiment agree with those postulated in the theory; the effect of a discrepancy of this sort, for example, a contact resistance at the boundary, is more difficult to allow for, and may be more important than in steady state experiments. In transient methods errors in the timing of temperature measurement and in thermocouple response may produce appreciable error. On the other hand, transient methods have the advantage of being relatively rapid. Some methods may be used in situ without removing a sample to the laboratory, which is very desirable in studying the thermal properties of materials such as soils and rocks. In a few of the transient methods only the latter part of the temperature-time curve, in which the solution consists of a single exponential term, is used.

2. THEORY

2.1 General heat conduction equations

The general differential equation governing the temperature distribution in a solid body or stationary fluid in rectangular coordinates is

$$\rho C_p \frac{\partial T}{\partial t} = k \left(\frac{\partial^2 T}{\partial x^2} + \frac{\partial^2 T}{\partial y^2} + \frac{\partial^2 T}{\partial z^2} \right) \tag{2.1.1}$$

The C_p and ρ are mainly independent of direction and for most of the liquids and solids neither of them varies substantially with temperature. The magnitude of thermal conductivity, on the other hand, is not only a function of temperature but may vary with direction (anistropic material) or may vary from point to point (heterogeneous material). If k varies with direction, equation (2. 1. 1) can be generalized to

$$\rho C_p \frac{\partial T}{\partial t} = \frac{\partial}{\partial x} \left(k_x \frac{\partial T}{\partial x}\right) + \frac{\partial}{\partial y} \left(k_y \frac{\partial T}{\partial y}\right) + \frac{\partial}{\partial z} \left(k_z \frac{\partial T}{\partial z}\right) \tag{2.1.2}$$

If heat energy is developed in the differential element in the amount of q (where q is the heat energy developed in unit volume per unit time) equation (2. 1. 1) becomes

$$\rho C_p \frac{\partial T}{\partial t} = k \nabla^2 T + q \tag{2.1.3}$$

It will be shown later (see 5. 4) that the value of q is negligible in our system. (In living fruits and vegetables q is mainly associated with the heat of respiration.)

For an infinite slab, which is one dimensional heat flow

$(\frac{\partial T}{\partial y} = \frac{\partial T}{\partial z} = 0)$, the general differential equation may be reduced to

$$\frac{\partial T}{\partial t} = \alpha \frac{\partial^2 T}{\partial x^2} \qquad (2.1.4)$$

where $\alpha = \frac{k}{C_p \rho}$ (2.1.5)

The differential equation for one dimensional heat flow in cylindrical (equation 2.1.6) and spherical (equation 2.1.7) coordinates can be found by transformation of coordinates in equation (2.1.1) and plugging $\frac{\partial T}{\partial z} = \frac{\partial T}{\partial \theta} = 0$ and $\frac{\partial T}{\partial \theta} = \frac{\partial T}{\partial \phi} = 0$ respectively or by energy balance on the differential element.

cylindrical coordinates $$\rho C_p \frac{\partial T}{\partial t} = k \left(\frac{1}{r} \frac{\partial T}{\partial r} + \frac{\partial^2 T}{\partial r^2}\right) \qquad (2.1.6)$$

spherical coordinates $$\rho C_p \frac{\partial T}{\partial t} = k \left(\frac{2}{r} \frac{\partial T}{\partial r} + \frac{\partial^2 T}{\partial r^2}\right) \qquad (2.1.7)$$

2.2 The mathematical and physical meaning of the infinite body with respect to heat flow

Mathematically the term infinite slab means that $\frac{\partial T}{\partial y} = \frac{\partial T}{\partial z} = 0$ which means that we do not have a temperature drop along the y and z axis, therefore there is no heat flow in these directions. Practically, infinite slab condition can be obtained either when the y and z directions are fairly large with respect to x or when the planes x-y and x-z are thermally insulated.

The infinite cylinder is a similar concept to the infinite slab where $\frac{\partial T}{\partial z} = \frac{\partial T}{\partial \theta} = 0$, consequently there is only radial heat flow. Practical

TH

infinite cylinder conditions exist when the ratio of the length of the cylinder to its diameter is fairly high (see 2.5) or by thermally insulating both ends of the cylinder. At this point we can observe that in a cylinder where $\frac{\partial T}{\partial \theta} = \frac{\partial T}{\partial r} = 0$ the heat flow is parallel to the main axis; this system is mathematically an infinite slab.

The sphere is always a one dimensional heat flow body (unless unevenly heated or partially insulated), because of the symmatrical nature of all the points having the same radius ($\frac{\partial T}{\partial \theta} = \frac{\partial T}{\partial \phi} = 0$).

The infinite slab, infinite cylinder and sphere, because they have only one characteristic dimension, are three geometric shapes in which unsteady state heat flow is a function of only two variables, time and geometric dimension. The solution of unsteady state heat flow problem in a two variables system is much easier than the solution for a geometric shape having two or three geometric variables (finite cylinder, cube, etc.). However, it will be shown later (see 2.5) that the solution of the unsteady state heat flow of geometric shapes (finite cylinder, cube, rectangular) which are geometric products of simpler shapes (infinite slab, infinite cylinder) can be expressed as a product of solutions of the simpler shapes.

2.3 Solution of the differential equation of the infinite slab, infinite cylinder and sphere

As a matter of convenience the origin of the coordinates system will be taken as the geometric center of the object; the x, y, z coordinates

TH

will be square to the axes of the object; the thickness of the infinite slab and the diameter of the infinite cylinder and the sphere will be 2 R.

The boundary and initial conditions for objects of any of these three geometries that are initially at a uniform temperature, T_0, and are suddenly exposed to an environment of constant temperature T_1 are:

Initial conditions are:

$$T = T_0 \qquad \text{at} \qquad t = 0 \qquad \text{for all } r \tag{2.3.1}$$

Boundary conditions are:

$$\frac{\partial T}{\partial r} = 0 \qquad \text{at} \qquad r = 0 \qquad \text{for } t \geq 0 \tag{2.3.2}$$

$$\frac{\partial T}{\partial r} = \frac{h}{k}(T - T_1) \qquad \text{at} \qquad r = R \qquad \text{for } t > 0 \tag{2.3.3}$$

The first boundary condition results from temperature symmetry at the geometric center. The second boundary condition is the surface heat flux and it is obtained by comparing the rate of heat transfer through the surface $hA_r(T_1 - T)$ to Newton's law of heat flux at the surface $- A_r k \frac{\partial T}{\partial r}$. The exact solution of the differential equation for unsteady state one dimensional heat flow in an infinite slab (equation 2.1.4), infinite cylinder (equation 2.1.6) and sphere (equation 2.1.7) all having the initial and boundary conditions stated in equations (2.3.1), (2.3.2), (2.3.3) as given in Schneider (1957) are listed below:

For the infinite slab:

$$\frac{T - T_1}{T_0 - T_1} = \sum_{i=1}^{\infty} \frac{2 \sin \beta_i}{\beta_i + \sin \beta_i \cos \beta_i} \cos\left(\beta_i \frac{r}{R}\right) e^{-\frac{\beta_i^2 \alpha t}{R^2}} \tag{2.3.4}$$

where the β_i and the roots of the transcendental equation

$$N_{Bi} = \beta_i \tan \beta_i \tag{2.3.5}$$

For the infinite cylinder:

$$\frac{T - T_1}{T_0 - T_1} = \sum_{i=1}^{\infty} \left(\frac{2}{\beta_i}\right) \frac{J_1(\beta_i)}{J_0^2(\beta_i) + J_1^2(\beta_i)} J_0\left(\beta_i \frac{r}{R}\right) e^{-\frac{\beta_i^2 \alpha t}{R^2}} \tag{2.3.6}$$

where the β_i are the roots of the transcendental equation

$$N_{Bi} = \beta_i \frac{J_1(\beta_i)}{J_0(\beta_i)} \tag{2.3.7}$$

For the sphere:

$$\frac{T - T_1}{T_0 - T_1} = \sum_{i=1}^{\infty} \frac{2(\sin \beta_i - \beta_i \cos \beta_i)}{\beta_i - \sin \beta_i \cos \beta_i} \frac{\sin\left(\beta_i \frac{r}{R}\right)}{\beta_i \frac{r}{R}} e^{-\frac{\beta_i^2 \alpha t}{R^2}} \tag{2.3.8}$$

where the β_i are the roots of the transcendental equation

$$N_{Bi} = 1 - \beta_i \cot \beta_i \tag{2.3.9}$$

The Biot Number, N_{Bi}, is a dimensionless number which is physically a ratio of the thermal resistance $\frac{R}{k}$ of the interior part of the system and the thermal resistance $\frac{1}{h}$ of the exterior part of the system, $N_{Bi} = \frac{h R}{k}$. In a system where the N_{Bi} can be only approximated, it is much easier to evaluate that part of the system that will dominate the heat flow, and in many cases, especially in low and high N_{Bi} values, to have a simple algebraic relationship between the physical and geometric properties of the system and the heat flow (see 3.5).

All the exact solutions for heat flow in the infinite slab, infinite cylinder and sphere (equations 2.3.4, 2.3.6, 2.3.8) are series type solutions, having the following form

$$\frac{T - T_1}{T_0 - T_1} = \sum_{i=1}^{\infty} j\, e^{-\frac{\beta_i^2 \alpha t}{R^2}} \qquad (2.3.10)$$

The location parameter is in j and the exponential term contains the time function, the physical and geometric properties of the body and surface heat transfer coefficient. Applying Cauchy test for convergency $\lim \frac{M_{n+1}}{M_n}$ shows that all the three series solutions mentioned above do converge (the $\lim \frac{M_{n+1}}{M_n}$ turns out to be 0) but are not continuous at $t = 0$. The number of terms needed for certain convergency depends mainly on t; the smaller the t the more terms are needed for the same convergency.

Generally it is known that this type of series, because of its exponential nature, will converge rapidly and after a certain time, all the terms after the first become negligible.

McAdams (1954) gives the Hottel and Gurney-Lurie charts which describe the transient conduction solutions for the infinite slab, infinite cylinder and sphere by plotting the log of the unaccomplished temperature change versus a relative time $\frac{\alpha t}{R^2}$ for a constant N_{Bi} and a certain radius ratio r/R.

2.4 First term approximation

In the transient heating or cooling of a system beyond a certain time the temperature as a function of the time and location can be described by the first term of equation (2.3.10).

Th

$$\frac{T - T_1}{T_0 - T_1} = j\, e^{-\frac{\beta_1^2 \alpha}{R^2}} \qquad (2.4.1)$$

Equation (2. 4. 1) will give a straight line when the log of the unaccomplished temperature or log $(T - T_1)$ is plotted versus t. If 10-base logarithms are used equation (2. 4. 1) can be rearranged into the following straight line form.

$$\log \frac{T - T_1}{T_0 - T_1} = \log j - \frac{\beta_1^2 \alpha t}{2.303 R^2} \qquad (2.4.2)$$

$$\log (T_0 - T_1) = \log [j (T - T_1)] - \frac{\beta_1^2 \alpha t}{2.303 R^2} \qquad (2.4.3)$$

Equation (2. 4. 3) is a straight line having a slope and an intercept of:

$$\text{slope} = \frac{-\beta_1^2 \alpha}{2.303 R^2} \qquad (2.4.4)$$

$$\text{intercept} = j \qquad (2.4.5)$$

By introducing a new term f (which is the negative reciprocal of the slope of the straight line described by equation (2. 4. 3) we get:

$$f = \frac{2.303 R^2}{\beta_1^2 \alpha} \qquad (2.4.6)$$

This approximate asymptotic solution (only one term of the series solutions is used) was suggested by Ball (1923). A summary of the various analytical approaches is given by Pflug and Blaisdell (1963).

The slope or f of the straight line, semi-logarithmic heating curve, is independent of location of the point of measurement since the slope term does not contain a geometric variable. The equation for f is the same for the three geometric shapes (infinite slab, infinite

cylinder and sphere). The j term, however, does depend on location. There are three j's, center, surface and mass average that are important.

geometric center $j_c = |j|_{r=0}$

surface $j_s = |j|_{r=R}$

mass average $j_m = \frac{1}{m}\int_0^m j\,dm$ where m = mass

Values for j_c, j_s and j_m for infinite slab, infinite cylinder and sphere are tabulated and plotted in Appendix 1.

The importance of the various j's is that once the straight line of the heating curve plotted in semi-log fashion is established we can determine the lowest (heating) or highest (cooling) temperature of the body, the surface temperature and the mass average temperature as a function of time by using j_c, j_s, and j_m respectively.

2.5 Temperature-time solution of geometric shapes which are a combination of an infinite slab and/or infinite cylinder

In many cases the temperature-time solution for two or three dimensional heat flow is a product of the solutions of one dimensional heat flow systems, and thus can be written down immediately if these are known.

As an example we will show that the temperature-time solution for a rectangular parallelepiped can be expressed as the product of the temperature-time solution of three infinite slabs each normal to the other.

The equation for the three dimensional conduction heat flow in a rectangular parallelepiped is

$$\frac{\partial^2 T}{\partial x^2} + \frac{\partial^2 T}{\partial y^2} + \frac{\partial^2 T}{\partial z^2} = \frac{1}{\alpha}\frac{\partial T}{\partial t} \tag{2.5.1}$$

which its solution is $u = \psi(x, y, z, t)$.

Consequently the temperature-time solution for the three one dimensional heat flow infinite slabs in their respective axes are:

$u_x = \psi(x, t)$; (2.5.2) $u_y = \psi(y, t)$; (2.5.3) $u_z = \psi(z, t)$ (2.5.4)

and each solution satisfies its respective differential equation

$\frac{\partial^2 u_x}{\partial x^2} = \frac{1}{\alpha}\frac{\partial u_x}{\partial t}$; (2.5.5) $\frac{\partial^2 u_y}{\partial y^2} = \frac{1}{\alpha}\frac{\partial u_y}{\partial t}$; (2.5.6) $\frac{\partial^2 u_z}{\partial z^2} = \frac{1}{\alpha}\frac{\partial u_z}{\partial t}$ (2.5.7)

In the following steps it will be shown that the temperature-time solution $u = \psi(x, y, z, t)$ for the rectangular parallelepiped is the simple product of the temperature-time solution of the three infinite slabs. In other words

$$u = u_x u_y u_z \tag{2.5.8}$$

By differentiating the solution (2.5.8) with respect to x, y, z and t respectively we get:

$$\frac{\partial^2 u}{\partial x^2} = u_y u_z \frac{\partial^2 u_x}{\partial x^2} \tag{2.5.9}$$

$$\frac{\partial^2 u}{\partial y^2} = u_x u_z \frac{\partial^2 u_y}{\partial y^2} \tag{2.5.10}$$

$$\frac{\partial^2 u}{\partial z^2} = u_x u_y \frac{\partial^2 u_z}{\partial z^2} \qquad (2.5.11)$$

$$\frac{\partial u}{\partial t} = u_y u_z \frac{\partial u_x}{\partial t} + u_x u_z \frac{\partial u_y}{\partial t} + u_x u_y \frac{\partial u_z}{\partial t} \qquad (2.5.12)$$

Replacing the values of $\frac{\partial u_x}{\partial t}$; $\frac{\partial u_y}{\partial t}$ and $\frac{\partial u_z}{\partial t}$ from equations (2.5.5), (2.5.6) and (2.5.7) in equation (2.5.12) we obtain

$$\frac{\partial u}{\partial t} = \alpha \left(u_y u_z \frac{\partial^2 u_x}{\partial x^2} + u_x u_z \frac{\partial^2 u_y}{\partial y^2} + u_x u_y \frac{\partial^2 u_z}{\partial z^2}\right) \qquad (2.5.13)$$

The substitution of equations (2.5.9), (2.5.10) and (2.5.11) in the appropriate places in equation (2.5.13) will yield $\frac{\partial u}{\partial t} = \alpha \left(\frac{\partial^2 u}{\partial x^2} + \frac{\partial^2 u}{\partial y^2} + \frac{\partial^2 u}{\partial z^2}\right)$ which is the differential equation for heat conduction in rectangular parallelepipeds.

A similar procedure can be used to show that the solution for an infinite cylinder is the simple product of an infinite cylinder and an infinite slab.

Since the three solutions, u_x, u_y and u_z have the form (see 2.4) $j\, e^{-t/f}$, the product solution u will therefore be

$$u = \left|j\, e^{-t/f}\right|_x \left|j\, e^{-t/f}\right|_y \left|j\, e^{-t/f}\right|_z \qquad (2.5.14)$$

After rearranging we get

$$u = j_x j_y j_z\, e^{-t(1/f_x + 1/f_y + 1/f_z)} \qquad (2.5.15)$$

This product solution has the form $j\, e^{-t/f}$ as the single solution and has, therefore, the same properties with respect to j and f. It can be immediately seen from equation (2.5.15) that

T

$$j_u = j_x\, j_y\, j_z \tag{2.5.16}$$

$$\frac{1}{f_u} = \frac{1}{f_x} + \frac{1}{f_y} + \frac{1}{f_z} \tag{2.5.17}$$

The practical meaning is that the j and 1/f value for any rectangular parallelepiped is the product of the j and the summation of the reciprocal of the f of the three infinite slabs. The j and the 1/f value for the finite cylinder, for instance, will be the product of the j for the infinite cylinder and the j for infinite slab and the summation of the reciprocal of the f respectively.

The question may be asked regarding what is "infinitely long" and how can we estimate the error introduced when we assume a finite geometrical shape to be infinite in one or two directions. As a first consideration it can be noted that any direction whose perpendicular surface is thermally insulated can be considered to be infinitely long, since no heat will be flowing in that direction. A finite cylinder of very small length, for example, if perfectly insulated at both ends can be considered an infinite cylinder as far as heat flow is concerned. The contribution of the noninsulated sides in the various directions to the temperature change of any point depends on the location of the point with respect to the appropriate surface. Again, if we are referring to a cylinder, the larger the ratio of the length of a finite cylinder to its diameter the smaller error is introduced by assuming that the finite cylinder is an infinite cylinder. In Table 2.1 numerical values in the

relationship between the length/ diameter ratio and the ratio of the calculated f assuming an infinite cylinder geometry to be correct f are shown. The values in the table were calculated for $N_{Bi} \rightarrow \infty$, however, the magnitude of the results will be the same for any N_{Bi}. Of course any finite cylinder having both ends thermally insulated is, as far as heat conduction, an infinite cylinder. However, it can be seen from Table 2.1 that practically when the ratio of the length to the diameter is 4 the error is about 2.67% and it becomes less than 1% when the ratio exceeds 7.

Table 2.1. Comparison of the f value for an infinite cylinder and a finite one.

N_{Bi} assumed to be infinite

Length of Cylinder / Diameter of Cylinder	f Assuming Infinite Cylinder / f Correct
1.00	1.4267
1.10	1.3526
1.20	1.2963
1.30	1.2525
1.40	1.2177
1.50	1.1896
1.60	1.1667
1.70	1.1476
1.80	1.1317
1.90	1.1182
2.00	1.1067
3.00	1.0474
4.00	1.0267
5.00	1.0171
6.00	1.0119
7.00	1.0087
8.00	1.0067
9.00	1.0053
10.00	1.0043
11.00	1.0035
12.00	1.0030

3. FURTHER INVESTIGATION OF THE FIRST TERM APPROXIMATION THEORY AND ANALYZING THE THERMAL CONDUCTIVITY IN DISPERSION SYSTEMS

3.1 Dimensional analysis of f

The value of f in its simple physical definition indicates the time required for the asymptote of the heating curve to cross one log-cycle, the time required for a 90% reduction of temperature on the linear portion of the heating curve.

The f value is a very useful term. From the analytical standpoint it incorporates into a single term all the transient thermal properties of the body, its geometrical characteristic and the thermal property of the external system appearing in transient heat conduction. In other words, the f term, which is expressed in units of time, shows the overall results of the body response to temperature change with respect to the external system. In other words f is the temperature response parameter of the body with respect to the external system. We would like to emphasize that by saying "the body transient thermal properties" we mean the body properties which are functioning in the transient stage, i.e. the property of the body to conduct the heat, the thermal conductivity, as well as its property to store it, ρC_p. From the practical standpoint the f term is quite useful, as it can be used to describe, compare, and predict the character of the temperature response of the

body exposed to certain exterior heat transfer conditions.

By inspection and simple reasoning of the physical meaning of the simple definition of f we can see that its value is a function of the following parameters:

1. The geometric parameter of the body, R (magnitude--the larger the geometric parameter the slower is the temperature response).
2. The ability of the body to store heat, ρC_p (magnitude--the larger the ρC_p the slower the temperature response).
3. The ability of the body to conduct heat, k (magnitude--the larger the thermal conductivity the faster the the temperature response).
4. The exterior film coefficient, h (magnitude--the larger the film coefficient the faster the temperature response).

So far, those independent variables of the dependent f were obtained by simple reasoning of a temperature change of a body exposed to certain heat transfer conditions.

In order to express the f value as a function of the above parameters we should try to find the total parameters of the system in form of dimensionless groups. The advantage of dimensionless groups is quite clear both from the design of experiments and presentation of data.

If ψ represents any function we can write

$$f = \psi [R, (\rho C_p), k, h] \tag{3.1.1}$$

or that

$$f = \lambda R^{\xi} (\rho C_p)^{\delta} k^{\varepsilon} h^{\eta} \tag{3.1.2}$$

T

where the coefficient λ and the exponents ξ, δ, ε and η are constants.

The dimensional quantities are as follows:

I	for length
t	for time
T	for temperature
H	for thermal energy

hence

the dimension of f is t

the dimension of R is I

the dimension of ρC_p is $HT^{-1} I^{-3}$

the dimension of k is $Ht^{-1} I^{-1} T^{-1}$

the dimension of h is $Ht^{-1} I^{-2} T^{-1}$

Substituting the dimensional quantities into equation (3.1.2) we obtain

$$t^1 = I^{\xi}(H\ T^{-1}\ I^{-3})^{\delta}\ (H\ t^{-1}\ I^{-1}\ T^{-1})^{\varepsilon}\ (H\ t^{-1}\ I^{-2}\ T^{-1})^{\eta} \qquad (3.1.3)$$

For the homogeneity of t, I, T and H respectively we find from equation (3.1.3)

$$\begin{aligned} &\text{for } t && 1 = -\varepsilon - \eta \\ &\text{for } I && 0 = \xi - 3\delta - \varepsilon - 2\eta \\ &\text{for } T && 0 = -\delta - \varepsilon - \eta \\ &\text{for } H && 0 = \delta + \varepsilon + \eta \end{aligned} \qquad (3.1.4)$$

Solving the relationships in equation (3.1.4) we obtain

$$\delta = 1$$

$$\xi = 2 + \eta \qquad (3.1.5)$$

$$\varepsilon = -1 - \eta$$

Substitution of δ, ξ and ε as obtained in equation (3.1.5) into equation (3.1.2) we obtain

$$f^1 = \lambda\ R^{2+\eta}\ (\rho C_p)^1\ k^{-1-\eta}\ h^\eta$$

$$= \lambda \left(\frac{R^2 \rho C_p}{k}\right)^1 \left[\frac{hR}{k}\right]^\eta \qquad (3.1.6)$$

Since $\alpha = \frac{k}{\rho C_p}$ and $N_{Bi} = \frac{h R}{k}$ we obtain

$$\frac{f \alpha}{R^2} = \lambda\ N_{Bi}^{\ \eta} \qquad (3.1.7)$$

$$\frac{f \alpha}{R^2} = \psi (N_{Bi}) \qquad (3.1.8)$$

Therefore we see that the system consists of two dimensional groups $\frac{f \alpha}{R^2}$ and N_{Bi}.

As a matter of fact Pflug et al. (1965) plotted and tabulated values in which the j_c, j_s and j_m and $\frac{f \alpha}{R^2}$ according to Ball's approximate asymptote solution were presented as a function of N_{Bi}.

The dimensional analysis shows the dimensionless group of the system, but obviously gives no information of any kind about the coefficients or the exponentials of the system. In our case we have no idea of the value of the coefficient λ or the exponential η their magnitude or dependency. Such information can be obtained only from the exact

solution, experimental data, reasoning or sometimes intuition. In fact, while analyzing some properties of the heat penetration curves in low and high N_{Bi}, we showed (see equation 3.5.7) that when N_{Bi} approaches 0 $\frac{f\alpha}{R^2}$ approaches $2.303 \left(\frac{V}{RA_r}\right) \frac{1}{N_{Bi}}$.

Equating the above equation to equation (3.1.7) when N_{Bi} approaches 0 will yield

$$\lambda \rightarrow 2.303 \left(\frac{V}{RA_r}\right)$$

$$\eta \rightarrow 1$$

In equation (3.5.1) we showed that when N_{Bi} approaches ∞, $\frac{f\alpha}{R^2}$ approaches a constant value (which is dependent on the body configuration). This means that when N_{Bi} is large

$$\lambda \rightarrow \text{constant*}$$

$$\eta \rightarrow 0$$

It is interesting to see that not only the coefficient λ and the exponential η are functions of N_{Bi}, but that the value of η is between -1 and 0, $0 \geq \eta \geq -1$.

3.2 Some properties of f and j

Theoretically both the terms f and j can be used independently

---

*The value of the constant is dependent on the configuration of the body, and for an example, is equal to $\frac{2.303}{\pi^2}$; $\frac{2.303}{2.405^2}$; $\frac{2.303}{(\pi/2)^2}$ for sphere, infinite cylinder and infinite slab respectively.

of each other for the evaluation of either of the physical properties of a system (f for the determination of α and j for the determination of k) or in the case where the physical properties are known, to evaluate the system properties (such as film coefficient, h, or N_{Bi}). However, we want to strongly emphasize that because of possible experimental errors, the f value is much more reliable. For example, the experimental j value will be affected by the initial temperature distribution or an error in location of the temperature sensing element; the experimental f is not succeptible to either of these errors. Any errors in conduction along the thermocouple wires will have a critical influence on the experimental j value but a small effect on the experimental f value. Any inaccuracies in timing in respect to the sudden change of temperature will cause the ordinate to shift. This obviously will have a big influence on the experimentally evaluated j value, but will not at all affect the value of the slope, f. Another point that should be taken into consideration is that the change of j_c in respect to N_{Bi} for $.5 < N_{Bi} > 10$ is so slight that its use becomes doubtful, even if the other possibilities for experimental errors in its determination were eliminated.

A final point is that unless the heating or cooling experiment yields a good "straight" line, drawing of the straight line becomes very subjective and any variation in the way the straight line is drawn will cause relatively small changes in the f value but may cause very large changes in j.

3.3 The relationship between the N_{Bi}, the thermal diffusivity α, and the root value β_1 in form of total derivatives

The relationship between N_{Bi}, α and β_1 in form of total derivatives is important as it gives us the ability to calculate the magnitude of the effect of change in N_{Bi} on β_1 and α (or between any other parameters) for any region of N_{Bi} in the following manner.

The basic equation $f\,\alpha / R^2 = 2.303 / \beta_1^2$ holds for all values of N_{Bi}. Taking the derivative of α with respect to β_1:

$$\frac{d\alpha}{d\beta_1} = \frac{2.303}{f} R^2 \left(\frac{-2}{\beta_1^3}\right)$$

$$= \frac{-2\alpha}{\beta_1} \qquad (3.3.1)$$

as $\beta_1^2 \quad = \dfrac{2.303\, R^2}{f\,\alpha}$

Next, by taking, for example, the derivative of the transcendental equation for the infinite slab $N_{Bi} = \beta_1 \tan\beta_1$ we get:

$$\frac{dN_{Bi}}{d\beta_1} = \tan\beta_1 + \frac{\beta_1}{\cos^2\beta_1} \qquad (3.3.2)$$

we obtain an expression that shows the tremendous rate of change of N_{Bi} with respect to β_1 in the neighborhood of $\pi/2$, where both terms $\tan\beta_1$ and $\beta_1^2/\cos^2\beta_1$ tend to become infinite. In low N_{Bi} $\cos\beta_1 \rightarrow 1$ and $\tan\beta_1 \approx \beta_1$, therefore $\dfrac{dN_{Bi}}{d\beta_i} \approx 2\,\beta_1$.

The most important derivative is probably $\dfrac{dN_{Bi}}{d\alpha}$, which shows the relationship of a change in the overall heat transfer properties of the total system and a change in the thermal diffusivity. $\dfrac{dN_{Bi}}{d\alpha}$ can be

obtained by dividing equation (3.3.2) with equation (3.3.1)

$$\frac{dN_{Bi}}{d\alpha} = \frac{\tan\beta_1 + \dfrac{\beta_1}{\cos^2\beta_1}}{-\dfrac{2\alpha}{\beta_1}}$$

$$= -\left[\frac{\beta_1 \tan\beta_1 + \left(\dfrac{\beta_1}{\cos\beta_1}\right)^2}{2\alpha}\right] \tag{3.3.3}$$

$$= -\left[\frac{N_{Bi} + \left(\dfrac{\beta_1}{\cos\beta_1}\right)^2}{2\alpha}\right]$$

Equation (3.3.3) again shows the tremendous change of N_{Bi} with respect to α when dealing with large N_{Bi}, and demonstrates clearly how in a high N_{Bi} system a small error in the physical properties can cause a large error in N_{Bi}.

On the other hand, $\frac{d\alpha}{dN_{Bi}}$ in the high N_{Bi} will be very small, and the change in α due to a change in N_{Bi} will be very small.

The negative sign in front of equation (3.3.3) is obvious as the α will decrease when the N_{Bi} increases.

Following the same reasoning for sphere we find that the derivative of the transcendental equation $N_{Bi} = 1 - \beta_1 \cot\beta_1$, is:

$$\frac{dN_{Bi}}{d\beta_1} = -\left[\cot\beta_1 - \frac{\beta_1}{\sin^2\beta_1}\right] \tag{3.3.4}$$

$\frac{dN_{Bi}}{d\beta_1}$, in this case, will be very large and approaches ∞ when β_1 approaches π, where $\cot\beta_1 \to -\infty$ and $\sin\beta_1 \to 0$.

$\frac{dN_{Bi}}{d\alpha}$ for a sphere can be obtained by dividing equation (3.3.4) by equation (3. 3. 1)

$$\frac{dN_{Bi}}{d\alpha} = \frac{-\cot \beta_1 + \dfrac{\beta_1}{\sin^2 \beta_1}}{-\dfrac{2\alpha}{\beta_1}}$$

$$= \frac{-\beta_1 \cot \beta_1 + \left(\dfrac{\beta_1}{\sin \beta_1}\right)^2}{-2\alpha} \tag{3. 3. 5}$$

$$= -\frac{N_{Bi} - 1 + \left(\dfrac{\beta_1}{\sin \beta_1}\right)^2}{2\alpha}$$

Thus we can observe from equation (3. 3. 5) that for a sphere the maximum change, $\frac{dN_{Bi}}{d\alpha}$ will occur when β_1 approaches π where $N_{Bi} \rightarrow \infty$ and $\sin \beta_1 \rightarrow 0$.

The mechanism for the infinite cylinder is more laborious since we have to take the derivatives of the series expression of the $J_0(\beta_1)$ and $J_1(\beta_1)$, and the infinite cylinder solution will not be presented here. The magnitude of $\frac{dN_{Bi}}{d\beta_1}$ and $\frac{dN_{Bi}}{d\alpha}$ are the same as for the sphere and infinite slab. The maximum change in this case of the infinite cylinder will take place when β_1 approaches 2. 4048 . . . .

3. 4 Evaluation of thermal properties or system film coefficient using experimental data

From Ball's first term approximation we saw that the thermal properties (such as h) can be theoretically evaluated under any condition from the heating data (f) and the physical and geometrical

properties of the body. Also, from the h, f and the geometrical dimension we can evaluate the physical property, α. However, in order to avoid possible misinterpretation of the data which consequently may lead to wrong results, it is very important that we understand the overall heat transfer properties of the system, and specifically the possible errors due to the high $\frac{dN_{Bi}}{d\alpha}$ in high N_{Bi}.

When the objective of the experiment is to determine physical properties, it is preferable to determine f under conditions where β_1 is insensitive to changes in h and, therefore, in the Biot number. When β_1 approaches π (for a sphere), the N_{Bi} increases so fast (equation 3. 3. 4) that large changes in h have a negligible effect on β_1 and, therefore, on the thermal diffusivity. In other words we have to look for a system where $\frac{dN_{Bi}}{d\alpha}$ is as large as possible--and from equation (3. 3. 5) it can be seen that this ratio increases with increasing N_{Bi}. This can be illustrated by considering three spherical shaped products of 0. 1 - ft. radius of widely different thermal diffusivities. Let the materials have properties near those of copper, water, and insulation material with thermal conductivities of 229 Btu/hr ft °F, respectively. The data in Table 3. 1 indicate that it is practically impossible to obtain N_{Bi} values corresponding to β_1 values as large as 3. 0 for materials, such as copper, which have large k values. For products having thermal conductivities similar to water, as do most foodstuffs, the h value resulting from heat transfer to or from water at moderate velocities will produce an N_{Bi} and β_1 value greater than 3.0; for example, if h is between 300 and 500 Btu/hr ft^2 °F, the β_1 root value is between 3.11 and 3.12. If we arbitrarily pick the value of 3.115, the error introduced in the diffusivity calculation (equation 2.4.6) is at most $(3.115^2 - 3.11^2)/3.11^2 \times 100 = 0.33\%$. The f and j values for materials with low k values are less sensitive to changes in h. If condensing steam is employed in heating food products, the exterior film coefficient obtained will be sufficiently large; thus, for any material that has a thermal conductivity equal to or less than water, the β_1 value can be assumed to be π. For such conditions, the accuracy of ρ and C_p are equally important in the determination of k. Due to the nature of highly conductive materials such as copper, the N_{Bi} encountered in practice will generally be low and the internal temperature will consequently be nearly uniform. Since the internal temperature gradient is negligible, the heating or cooling rate parameter f will be directly proportional to the C_p and ρ and inversely proportional to the film coefficient h (see 3.5).

When the purpose of the experiment is to determine the film coefficient, the system should have a low N_{Bi}, or the $\frac{dN_{Bi}}{d\alpha}$ should be as small as possible. Any attempt to determine the film coefficient of a system where water is the heat transfer media h = 200 $\frac{\text{Btu}}{\text{hr ft}^2 \text{ °F}}$ using a water based model will lead to erroneous results. It can be seen immediately from $f\,\alpha/R^2 = \ln 10/\beta_1^2$, that a change of 2% in f or

α or a change of 1% in R will cause a change of 1% in β_1. Since the N_{Bi} of such a system is about 60 we can see from Table 2.1 that a 1% change in β_1 will have a tremendous effect on the N_{Bi} and therefore, on h. If a copper model is used instead of the water-based model the N_{Bi} will be about .0885 and a similar error of 1% will only cause a 2% error in the N_{Bi}, and in h.

In summary we can conclude that: the film coefficient should be evaluated in a system where the N_{Bi} is as small as possible! When the N_{Bi} is high (> 10), the N_{Bi}, and therefore the evaluated h becomes very sensitive to any change either in the physical or geometric properties of the overall system. On the other hand, evaluation of the thermal diffusivity should be done in a system with a very high N_{Bi} so the root value β_1 is insensitive to N_{Bi} (or h).

3.5 Some properties of the heat penetration curves in low and high N_{Bi}.

In systems having either low or high N_{Bi} it is possible to derive simple useful correlations between the physical and the geometric properties of the system and its temperature change. The reason for seeking either low or high N_{Bi} is that in these ranges there is only one dominating thermal resistance. As a general rule of thumb a $N_{Bi} > 50$ can be considered to be high while $N_{Bi} < .3$ can be considered to be low.

Most of the heat transfer systems involving food or food products have low N_{Bi} when air is the heat transfer medium and high N_{Bi} when water is the heat transfer medium.

Table 3.1. The relationship between the β_1, N_{Bi} and h for low and high N_{Bi} for three materials of widely differing k values.

	β^1	N_{Bi}	h, Btu/hr ft^2 °F		
			Copper	Water	Expanded Polystyrene
Low N_{Bi}	.4	5.40×10^{-2}	1.23×10^{2}	1.78×10^{-1}	2.11×10^{-2}
	.6	1.23×10^{-1}	2.81×10^{2}	4.05×10^{-1}	4.82×10^{-2}
	.8	2.23×10^{-1}	5.10×10^{2}	7.35×10^{-1}	8.74×10^{-2}
	1.0	3.57×10^{-1}	8.19×10^{2}	1.18×10^{0}	1.40×10^{-1}
	1.2	5.33×10^{-1}	1.22×10^{3}	1.76×10^{0}	2.09×10^{-1}
	1.4	7.58×10^{-1}	1.73×10^{3}	2.50×10^{0}	2.97×10^{-1}
	⋮	⋮	⋮	⋮	⋮
High N_{Bi}	3.00	3.08×10^{1}	7.06×10^{4}	1.02×10^{2}	1.20×10^{0}
	3.08	5.09×10^{1}	1.17×10^{5}	1.68×10^{2}	2.00×10^{0}
	3.10	7.55×10^{1}	1.73×10^{5}	2.49×10^{2}	2.95×10^{0}
	3.11	9.94×10^{1}	2.28×10^{5}	3.28×10^{2}	3.90×10^{0}
	3.12	1.45×10^{2}	3.33×10^{5}	4.80×10^{2}	5.70×10^{0}
	3.13	2.71×10^{2}	6.20×10^{5}	8.94×10^{2}	1.06×10^{1}
	3.14	1.97×10^{3}	4.51×10^{6}	6.51×10^{3}	7.73×10^{2}
	π	∞	∞	∞	∞

High N_{Bi} systems

In the high N_{Bi} system the root value β_1 approaches its maximum value of π, 2.404826 . and $\pi/2$ for a sphere, infinite cylinder and infinite slab respectively. Since $\frac{f\,\alpha}{R^2} = \frac{2.303}{\beta_1^2}$ we can see that the ratio between the f value for a sphere, infinite cylinder and infinite slab having the same characteristic dimensions will be

$$\frac{1}{\pi^2} \quad : \quad \frac{1}{(2.405)^2} \quad : \quad \frac{1}{(\pi/2)^2}$$

$$1 \quad : \quad 1.705 \quad : \quad 4$$

respectively. If we try to find the relationship between the f value and the dimension within the shape itself we observe that in high N_{Bi} the value of $\frac{f\,\alpha}{R^2}$ becomes a constant the value of which is different, of course, for each shape.

$$\frac{f\,\alpha}{R^2} = \text{constant} \qquad (3.5.1)$$

From equation (3.5.1) in high N_{Bi} systems we observe the following:

1) The f value is inversely proportional to the thermal diffusivity.

2) The f value is independent of the N_{Bi} (the root value β_1 is constant) and the film coefficient h, which means that increasing h does not improve the total heat transfer in the high N_{Bi} system.

3) The f value for a defined geometry is proportional to the square of the characteristic dimension.

Low N_{Bi}

In the low N_{Bi} region, the exterior resistance dominates $(\frac{1}{h} \gg \frac{R}{k})$. Therefore the interior temperature can be considered to be uniform. In this case the heat balance may be written as follows:

$$V \rho C_p \frac{dT}{dt} = A_r h (T_1 - T) \qquad (3.5.2)$$

$$\frac{V \rho C_p}{A_r h} \left(\frac{dT}{T_1 - T}\right) = dt$$

And after integration:

$$- \frac{V \rho C_p \, 2.303}{A_r h} \log [T_1 - T]_{T'}^{T''} = [t]_{t'}^{t''} \qquad (3.5.3)$$

$$- \frac{V \rho C_p \, 2.303}{A_r h} \log \frac{T_1 - T''}{T_1 - T'} = t'' - t' \qquad (3.5.4)$$

by definition $t'' - t' = f$ when $\frac{T_1 - T''}{T_1 - T'} = .1$ or $\log \frac{T_1 - T''}{T_1 - T'} = -1$.

By inserting this value into equation (3.5.4), we obtain:

$$\frac{-2.303 \, V \rho C_p}{A_r h} (-1) = f$$

$$f = \frac{2.303 \, V \rho C_p}{A_r h} \qquad (3.5.5)$$

Equation (3.5.5) and the following derivations are important in understanding and interpreting the heat flow mechanism in the low N_{Bi} system.

We shall prove that equation (3.5.5) which was derived on the single assumption that no temperature gradient exists in the interior of the body, can be derived from the exact unsteady solution for the sphere, infinite cylinder and infinite slab.

Multiplying and dividing equation (3.5.5) by factor of R^2/k yields

$$f = \frac{2.303 \frac{V}{A_r} \frac{\rho C_p R^2}{k}}{\frac{h R}{k} R} \tag{3.5.6}$$

since $\frac{\rho C_p}{k} = \frac{1}{\alpha}$ and $\frac{h R}{k} = N_{Bi}$ by rearranging equation (3.5.6) we obtain:

$$\frac{f \alpha}{R^2} = \frac{2.303}{N_{Bi} R} \frac{V}{A_r} \tag{3.5.7}$$

The respective value $(\frac{V}{A_r})$ for a sphere, infinite cylinder and infinite slab are:

$$\frac{\frac{4}{3} \pi R^3}{4 \pi R^2} = \frac{R}{3}; \qquad \frac{\pi R^2 \ell}{2 \pi R \ell} = \frac{R}{2}; \qquad \frac{2 a_1 b_1 R}{2 a_1 b_1} = R$$

(3.5.8) (3.5.9) (3.5.10)

Plugging the value of $(\frac{V}{A_r})$ into equation (3.5.7) yields:

$$\frac{f \alpha}{R^2} = \frac{2.303}{3 N_{Bi}} \quad \text{sphere} \tag{3.5.11}$$

$$\frac{f \alpha}{R^2} = \frac{2.303}{2 N_{Bi}} \quad \text{infinite cylinder} \tag{3.5.12}$$

$$\frac{f \alpha}{R^2} = \frac{2.303}{N_{Bi}} \quad \text{infinite slab} \tag{3.5.13}$$

The general form will be $\frac{f \alpha}{R^2} = \frac{2.303}{C N_{Bi}}$ (3.5.14)

Now we will proceed to evaluate the effect from the exact solutions standpoint. The equation $\frac{f\alpha}{R^2} = \frac{2.303}{\beta_1^2}$ which was derived from the exact solution holds for the three mentioned shapes for any N_{Bi}. This equation is very similar to equation (3.5.14) but the β_1^2 is replaced by $C\,N_{Bi}$ (C = 3, 2, 1 for sphere, infinite cylinder, and infinite slab respectively).

We will proceed to develop the relationship between the N_{Bi} and β_1^2 for low N_{Bi}.

Sphere

Transcendental equation $N_{Bi} = 1 - \beta_1 \cot \beta_1$. By expanding $\cot \beta_1$ we get:

$$N_{Bi} = 1 - \beta_1 \left(\frac{1}{\beta_1} - \frac{\beta_1}{3} - \frac{\beta^3}{45} \ldots\right)$$

when β_1 is small, $\beta_1^3 \ll \beta_1$ and therefore

$$N_{Bi} = 1 - 1 + \frac{\beta_1^2}{3} = \beta_1^2/3$$

$$\beta_1^2 \approx 3N_{Bi} \qquad (3.5.15)$$

Infinite cylinder

Transcendental equation $N_{Bi} = \beta_1 \frac{J_1(\beta_1)}{J_0(\beta_1)}$ where $J_0(\beta_1)$ and $J_1(\beta_1)$ are Bessel functions of the first kind of order zero and one respectively. For small value of β_1 the values are calculated (Hildebrand, 1963) from $J_p(\beta) \approx \frac{1}{2^p p!}\beta^p$, and therefore, when β_1 approaches zero, $J_0(\beta_1) \rightarrow 1$ and $J_1(\beta_1) \rightarrow \beta_1/2$, which means that

$N_{Bi} \approx \beta_1(\beta_1/2)$

$$\beta_1^2 \approx 2\ N_{Bi} \qquad (3.5.16)$$

Infinite slab

Transcendental equation $N_{Bi} = \beta_1 \tan \beta_1$. When β_1 is small, $\beta_1 \approx \tan \beta_1$ and therefore $N_{Bi} \approx \beta_1^2$. (3.5.17)

Inserting the β_1^2 values for the sphere, infinite cylinder and infinite slab as functions of N_{Bi} as they appear in (3.5.8), (3.5.9), (3.5.10) into $\frac{f\,\alpha}{R^2} = \frac{2.303}{\beta_1^2}$ will yield:

$$\frac{f\,\alpha}{R^2} = \frac{2.303}{3\ N_{Bi}} \qquad \text{sphere} \qquad (3.5.18)$$

$$\frac{f\,\alpha}{R^2} = \frac{2.303}{2\ N_{Bi}} \qquad \text{infinite cylinder} \qquad (3.5.19)$$

$$\frac{f\,\alpha}{R^2} = \frac{2.303}{N_{Bi}} \qquad \text{infinite slab} \qquad (3.5.20)$$

We obtain a result identical to that obtained in (3.5.11), (3.5.12), and (3.5.13).

From the above analysis we may conclude the following regarding the effect of low N_{Bi}.

1) From equation (3.5.5) $f = \frac{2.303\ \rho\, C_p\, V}{h\, A_r}$ we observe that under the same conditions (h, α, and N_{Bi} are constant) the ratio between the f values of various bodies, no matter how odd their shape, is

proportional to the ratio between their volume/surface area. If we compare the f value of a sphere, infinite cylinder and infinite slab having the same characteristic dimension we find the ratio to be equal to 1 : 1.5 : 3 respectively, which can be observed immediately through inspection of equations (3.5.11), (3.5.12), (3.5.13).

2) For the same geometry the f will be proportional to any chosen, but fixed, characteristic dimension to the power of 1 (rather than the power of 2 as in the case of high N_{Bi} systems).

3) From equation (3.5.5) we can see that the f is proportional to the heat capacity $C_p \rho$ (rather than the $\frac{\rho C_p}{k} = \frac{1}{\alpha}$ in case of high N_{Bi} systems), which shows that in low N_{Bi} systems a temperature-change comparison between two bodies should be made with respect to their heat capacity, ρC_p rather than their thermal diffusivity, α. In an air-cooled room (air flow by natural convection) for example, it will take copper, in spite of its well-known high thermal conductivity, k, and thermal diffusivity, α, about the same time to cool as an apple, both having the same dimension. If we compare a 3" diameter apple assumed to have $\rho = 50$ lb/ft^3, $C_p = .85$ Btu/lb °F, $k = .2$ Btu/hr ft °F with a copper sphere having the same diameter and assumed to have $\rho = 559$ lb/ft^3, $C_p = .0915$ Btu/lb °F and $k = 223$ Btu/hr ft °F both cooling under natural convection condition (assumed $h = 1.0$ Btu/hr ft^2 °F)

f value for the exact solution is about 4.9 hr and 4.6 hr for the copper and the apple respectively.

4) f is inversely proportional to the h (the f was independent of the h in the case of high N_{Bi} systems), showing the importance of improving the exterior film coefficient in order to increase the overall rate of heat flow.

5) From inspection of equations (3.5.11), (3.5.12), (3.5.13) we can observe that all have the general form $\frac{f\alpha}{R^2} = \frac{2.303}{C\,N_{Bi}}$. Taking the log of both sides we have:

$$\log \frac{f\alpha}{R^2} = -\log N_{Bi} + \log \frac{2.303}{C} \qquad (3.5.21)$$

or that when $\frac{f\alpha}{R^2}$ is plotted versus N_{Bi} we get in low N_{Bi} a straight line (slope = -1) (see Figure A.4 in Appendix 1).

6) We can describe $\frac{f\alpha}{R^2}$ versus N_{Bi} on log-log scale for any odd shape by simply choosing an arbitrary characteristic dimension used consistently for the computation of $\frac{f\alpha}{R^2}$, N_{Bi} and $(\frac{V}{A_r})$. The lines for the different shapes will be parallel with a slope of -1, each having a different intercept with the ordinate. To calculate the curve for the cube we can choose the characteristic dimension, a, to be half the thickness. We find that

$$\frac{V}{A_r} = \frac{(2R)^3}{6\,(2R)^2} = \frac{R}{3}$$

and as

$$\frac{f\alpha}{R^2} = \frac{2.303\,\frac{V}{A_r}}{N_{Bi}\,R}$$

we find that $\frac{f\,\alpha}{R^2} = \frac{2.303}{3\,N_{Bi}}$ (3.5.22)

which as a matter of fact is the same as the curve for a sphere.

The validity of the equation for the cube can be proved from a different approach by finding the solution for a cube from the product solution of three infinite slabs having the same thickness. The line equation for the infinite slab is

$$\frac{f\,\alpha}{R^2} = \frac{2.303}{N_{Bi}} \qquad \text{or} \qquad \frac{1}{f} = \frac{\alpha\,N_{Bi}}{2.303\,R^2}$$

The product solution will be

$$\frac{1}{f_{cube}} = \sum_{i=1}^{3} \frac{1}{f_i}$$

and as the thickness of the three infinite slabs forming the cube is the same, their N_{Bi} will also be the same, and the product solution will be, therefore,

$$\frac{1}{f_{cube}} = \frac{3}{f_{infinite\ slab}}$$

$$= \frac{3\,\alpha\,N_{Bi}}{2.303\,R^2} \qquad \text{or} \qquad \left(\frac{f\,\alpha}{R^2}\right)_{cube} = \frac{2.303}{3\,N_{Bi}}$$

which is exactly the same as equation (3.5.22).

A comparison of the most important properties in low N_{Bi} and high N_{Bi} conditions are summarized in Table 3.2.

Table 3.2. Some properties of low and high N_{Bi} systems

	High N_{Bi} $N_{Bi} > 50$			Low N_{Bi} $N_{Bi} < .3$		
$\frac{f\alpha}{R^2}$	constant			$\frac{2.303}{C\,N_{Bi}}$		
f	independent of N_{Bi} or h			inversely proportional to N_{Bi} or h		
f	proportional to $\frac{C_p\,\rho}{k}$			proportional to $C_p\,\rho$		
f	proportional to R^2			proportional to R		
η	0			-1		
	Sphere	Infinite cylinder	Infinite slab	Sphere	Infinite cylinder	Infinite slab
C				3	2	1
f ratio between the 3 shapes	1	1.7	4	1	1.5	3
β_1 approaches	π	2.405	$\pi/2$	0	0	0
N_{Bi} approaches	∞	∞	∞	$\beta_1^2/3$	$\beta_1^2/2$	β_1^2

3.6 <u>The mass average temperature as a function of the temperature at the geometric center, T_c</u>

In many cases knowing the mass average temperature (equation 3.6.1) of a body exposed to transient heat transfer, is important: from the standpoint of heat process design and the evaluation of the probable quality change of the product.

$$T_m = \frac{1}{m} \int_0^m T \, dm \qquad \text{where } m = \text{mass} \tag{3.6.1}$$

The average mass temperature, T_m, can be used to show the total heat removed, with respect to time, from the object. In the case of cooling processed cans, for example, the evaluation of the mass average temperature will determine the hazard of undercooling, where a high mass average temperature in the can after processing will cause discoloration or softening of the product or in the case of high pH vegetables, it may promote spoilage by providing temperature conditions under which surviving thermophiles may grow. In the case of overcooling, where the mass average temperature of the container is too low, not enough evaporation of the water on the outside of the container will take place; thus rusting may take place.

The geometric center is, in conduction heating products, the most common location to measure the temperature because it represents the slowest heating (or cooling) point, and because technically it is the easiest location to place the temperature-measuring device. Therefore, it is important to develop some kind of expression where the mass average temperature is a function of the temperature at the geometric center. In the following development we shall assume that sufficient time has elapsed and that we are dealing with a one term approximation, i.e., in the straight line region. In this case, all the heating (or cooling) curves are parallel and different from each other only at the point of intersection with the ordinate.

Since the general equation of the straight line semi-logarithmic curve is:

$$\log (T_1 - T) = -\frac{t}{f} + \log [j (T_1 - T_0)] \qquad (2.4.3)$$

We can write the expression for the temperature at the geometric center and the mass average temperature respectively as follows:

$$\log (T_1 - T_c) = -\frac{t}{f} + \log [j_c (T_1 - T_0)] \qquad (3.6.2)$$

$$\log (T_1 - T_m) = -\frac{t}{f} + \log [j_m (T_1 - T_0)] \qquad (3.6.3)$$

Subtracting equation (3.6.2) from equation (3.6.3) we get

$$\log \frac{T_1 - T_m}{T_1 - T_c} = \log \frac{j_m (T_1 - T_0)}{j_c (T_1 - T_0)} \qquad (3.6.4)$$

or $$\frac{T_1 - T_m}{T_1 - T_c} = \frac{j_m}{j_c} = K \qquad (3.6.5)$$

after rearranging equation (3.6.5) we get

$$T_m = T_1 - K (T_1 - T_c) \qquad (3.6.6)$$

The constant $K = \frac{j_m}{j_c}$ is a function of the shape and the N_{Bi} and can be evaluated from the appropriate j tables (see Appendix 1).

Example 1

A can of food, a finite cylinder, is heated in water or steam or cooled in water. The N_{Bi} is large enough so that the $\frac{j_m}{j_c}$ will be as follows:

$$K = \frac{[j_{\text{infinite cylinder}}\ j_{\text{infinite slab}}]_m}{[j_{\text{infinite cylinder}}\ j_{\text{infinite slab}}]_c} = \frac{.70 \times .81}{1.60 \times 1.27} = .279$$

And if $T_1 = 250°$ F the mass average temperature when the temperature at the center, $T_c = 240°$ F, is

$$T_m = 250 - .279\ (250 - 240)$$
$$= 250 - 2.79 = 247.2° F$$

Example 2

5" cube of meat having $\alpha = .005\ ft^2/hr$, $k = .29$ Btu/hr ft °F cooled in a room where the $h = 5$ Btu/hr ft² °F. The $N_{Bi} = \frac{5 \times 2.5}{.29 \times 12} = 3.6$. The j_m and j_c of $N_{Bi} = 3.6$ for infinite slab is .93 and 1.22 respectively. As we know, from product solution that $j_{cube} = j^3_{\text{infinite slab}}$ we find that $k = \frac{j_m}{j_c} = \frac{.93^3}{1.22^3} = .444$. If $T_1 = 36°$ F the mass average temperature at the center is 45° F will be

$$T_m = 36 - .444\ (36 - 45)$$
$$= 36 + .444 \times .9 = 40° F$$

j_m/j_c reaches its minimum value when $N_{Bi} \to \infty$, and approaches 1 (no internal temperature gradient) when $N_{Bi} \to 0$.

It should be mentioned that Stumbo (1964) derived an equation in the same form as equation (3.6.6). In his technique, however, in order to find the constant K he used a laborious graphical integration using some of his previous graphical data related to iso - j lines in cylindrical cans and which was only valid for specific case: body having a cylindrical shape exposed to a media which was either steam or water (which is for foodstuffs a high N_{Bi} system). By the graphical integration method for this specific case he found the average value of the constant, K to be .27 (we found it to be .279).

In this section we have presented the general solution for the mass average temperature as a function of the temperature at the geometric center, T_c, (equation 3.6.6) and have proven that the constant, K, in this equation is a function of the shape of the object and the N_{Bi} of the system and is equal to $\frac{j_m}{j_c}$.

3.7 Analyzing the thermal conductivity of three dimensional, two dimensional and one dimensional dispersion systems

Materials whose properties do not vary with respect to direction are called isotropic materials, in contrast to anisotropic materials whose properties vary with respect to direction. Thus, whether the material is isotropic or anisotropic, is a function of structure. These materials should not be confused with homogeneous materials whose respective properties do not change from point to point nor be confused with heterogeneous materials which are materials whose properties do change from point to point. Being a homogeneous or a heterogeneous material is a function of uneven distribution of compounds, for example, wood or layered type material, are anisotropic - homogeneous materials, while meat flesh having uneven distribution of fat will be considered to be an anisotropic - nonhomogeneous material. Ground beef in which the fat is unevenly distributed is isotropic but nonhomogeneous material. Insulation materials are homogeneous isotropic materials.

Generally speaking we can say that the static thermal property, the specific heat, is independent of the direction of the heat flow or the pattern of the individual components. In any homogeneous system (either isotropic or anisotropic) the specific heat, C_p can be considered to be

$$C_p = \Sigma\, C_{p_i} \times (\text{fraction weight})_i$$

The thermal conductivity which is the transport property, is direction dependent and may vary significantly with arrangement of the individual components.

Many materials consist of various components, and other materials consist of more than one phase. Many other materials may have structural patterns which may cause the thermal conductivity of the system to vary with respect to the direction of heat flow. The overall thermal conductivity of such systems is by reasoning, a function of the thermal conductivity of the individual components, their proportion and their pattern. In the following pages we shall try to analyze a few homogeneous systems and to find the overall thermal conductivity of the system as a function of the individual component thermal properties and their relative pattern.

The analysis will be made using a model system having the properties as follows:

1. The model will be a 1 unit cube, $x = y = z = 1$.
2. Heat flow will be by conduction only.
3. The discontinuous component and the continuous component may have the same state or may form two phases.
4. The size of the dispersed particles is small in comparison to the system size.
5. The dispersed component is randomly distributed.
6. The dis~~t~~continuous component is dispersed in the continuous component in the macro level and not in the atomic or molecular levels. For example, alloys or impurities in metals are excluded.

For this model system analysis:

k - overall thermal conductivity of the system

k_c - thermal conductivity of the continuous component

k_d - thermal conductivity of the dispersed component

We shall analyze three basic models:

A. Two-component - three dimensional - isotropic system (the two components may form two phases) where one component is randomly dispersed in the other to form the non-continuous phase (Figure 3.1A).

This model is most important to us since it represents the experimental model of this study--the air-sucrose solutions foam. However it is typical of other systems such as butter (water dispersed in fat), ice cream or apple flesh (air dispersed in liquid). We would

like again to point out that this model cannot represent alloys or impurities in metal. In such cases we get random distribution at the atom level rather than in the macro level, which yields a different crystallographic pattern. Since the mechanism of heat flow in metals is due to the outer electron shell, a change or new pattern in the crystallographic configuration will change the value of the thermal conductivity. It is an established fact that the thermal conductivity of alloys or impure metals is usually lower than the thermal conductivities of the principal metals.

B. Two-component - two dimensional - anisotropic fibrous system (the two components may form two phases) in which the fibers are parallel to each other and randomly distributed. In this case the dispersed component (the fibers) are continuous in one direction and the random dispersion will be two dimensional. (See Figure 3.2A.)

This system is an anisotropic system, and the thermal conductivity will vary with direction. This model is typical to all fibrous systems such as meat flesh, wood, fibrous vegetable. This system will be characterized with two thermal conductivities.

$k_{\parallel}$ - the thermal conductivity in the direction parallel to the fibers

$k_{\perp}$ - the thermal conductivity in the direction perpendicular to the fibers

C. Two (or more) components - one dimensional - anisotropic layered system (the components may form more than one phase) in which the components are arranged in parallel layers to form some kind of a composite layer (figure 3.3A). In this case random distribution is not necessary and all the components are equal with respect to the continuous phase (both are continuous in two directions). The dispersion will be a one dimensional dispersion.

This is an anisotropic system which is typical of all the cases where the system consists of a composite layered pattern such as fat layer above the flesh, packed material with respect to the packing materials and plywood.

In the analysis we shall use the following rules concerning the computation of the total conductance of conductors connected in series or parallel.

Total conductance of conductors connected in parallel

$$k = \Sigma\, k_i \times \left(\frac{\text{cross section}}{\text{length}}\right)_i$$

Total conductance of conductors connected in series

$$\frac{1}{k} = \Sigma \frac{1}{k_i \times \left(\frac{\text{cross section}}{\text{length}}\right)_i}$$

Because our overall system has a unit cross section and length, the total system conductance will be the same as the system conductivity.

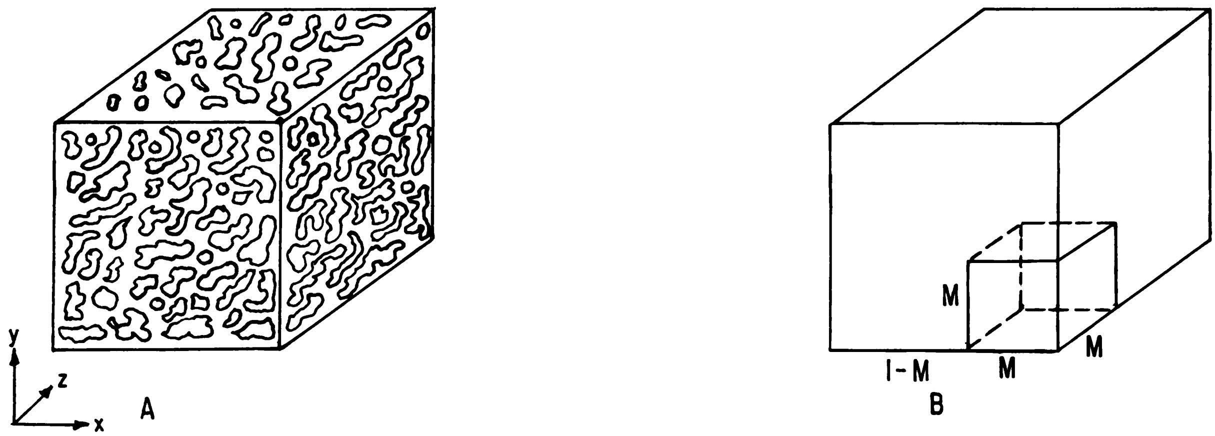

Figure 3.1. The diagram of the two component homogeneous three dimensional dispersion system. A. Natural random state. B. The rearrangement of the components.

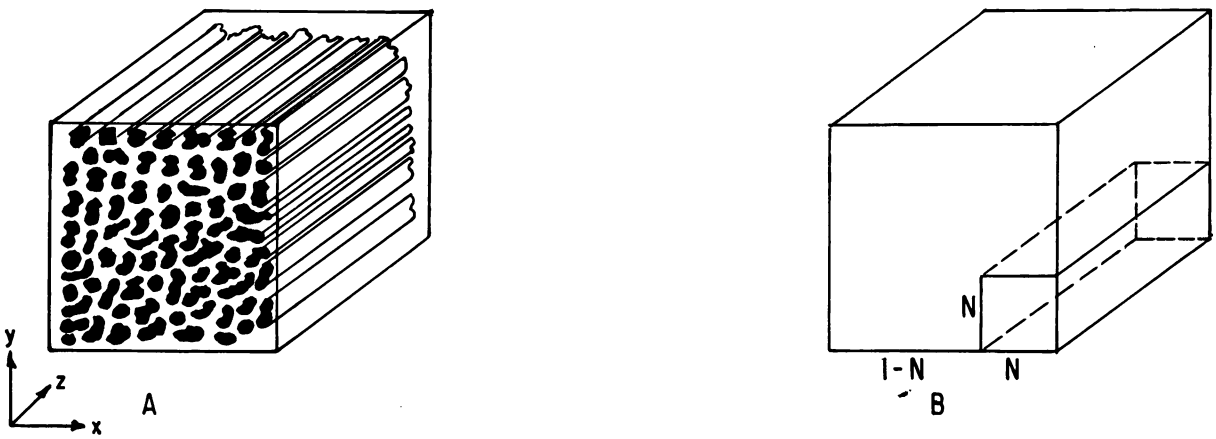

Figure 3.2. The diagram of the two component homogeneous two dimensional fibrous system. A. Natural random state. B. The rearrangement of the components.

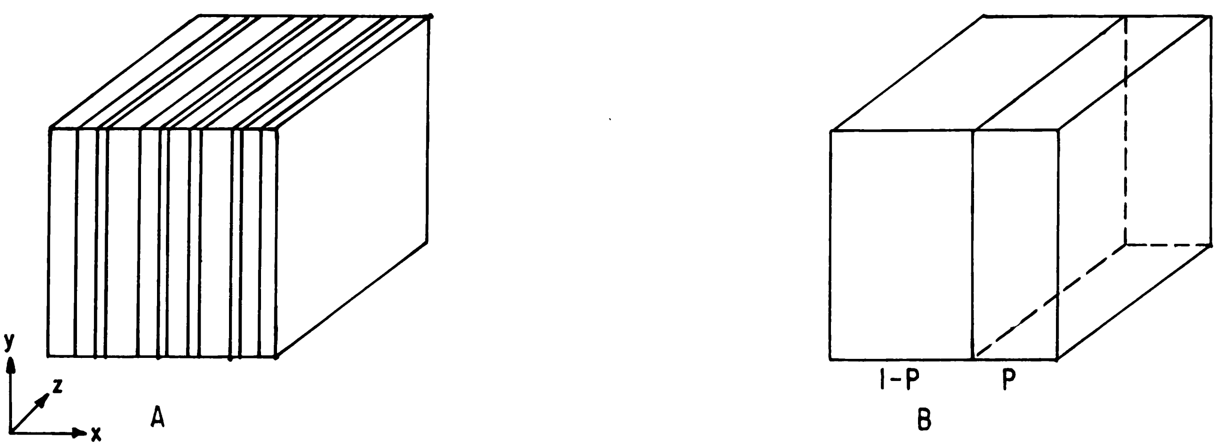

Figure 3.3. The diagram of the two component homogeneous one dimensional layered system. A. Natural random state. B. The rearrangement of the components.

A. Two-component - three dimensional isotropic system

In this case one component is randomly dispersed in the other to form the discontinuous phase (see Figure 3.1A). Let us assume that the cube (Figure 3.1A) is sliced in the x-y plane into very thin layers. The thermal conductivity of one single layer in the three directions will not be changed if all areas of the discontinuous phase are combined and rearranged to form a square area M^2. Based upon additive thermal resistance when areas are connected in series, the combined rearranged layers will not change the total thermal resistance. When the discontinuous phase is composed of small enough particles randomly distributed, it is clear that from a symmetrical standpoint M^2 is not only equal for each layer cut in the x-y plane, but its fraction with respect to the total cross sectional area is independent of the cutting plane. All other thin parallel layers cut in the y-z plane will have after rearrangement, the same cross section of discontinuous phase M^2.

Collecting all the discontinuous particles randomly distributed in the three dimensions will yield a cube (Figure 3.1B). Since the total value of the system is one unit, the volume of this cube M^3 is the void fraction of the discontinuous phase.

The overall thermal conductivity of the system can be computed in the following manner: The thermal conductivity of one layer in the x-y plane in the z direction will be

$$k_c (1 - M^2) + k_d M^2 \tag{3.7.1}$$

and as we have many similar layers (connected in series) along distance M, the thermal conductivity in the z direction of the unit cube from z = 0 to z = M will be

$$\frac{k_c (1 - M^2) + k_d M^2}{M} \qquad (3.7.2)$$

The thermal conductivity of the rest of the cube (which is the continuous component in the three directions from z = M up to z = 1) is added in series and, the overall thermal conductivity is computed as follows:

$$\frac{1}{k} = \frac{M}{k_c (1 - M^2) + k_d M^2} + \frac{1 - M}{k_c} \qquad (3.7.3)$$

$$\frac{1}{k} = \frac{M}{k_c - M^2 (k_c - k_d)} + \frac{1 - M}{k_c}$$

$$k = \frac{k_c [k_c - M^2 (k_c - k_d)]}{k_c M + k_c - M^2 (k_c - k_d) - M k_c + M^3 (k_c - k_d)}$$

$$k = \frac{k_c - M^2 (k_c - k_d)}{1 - M^2 (1 - k_d/k_c) + M^3 (1 - k_d/k_c)}$$

$$k/k_c = \frac{1 - M^2 (1 - k_d/k_c)}{1 - M^2 (1 - k_d/k_c)(1 - M)} \qquad (3.7.4)$$

$$= \frac{1 - Q}{1 - Q (1 - M)} \qquad (3.7.5)$$

where $Q = M^2 (1 - k_d/k_c)$

When $k_c \gg k_d$ equation (3.7.4) is simplified to

$$\frac{k}{k_c} = \frac{1 - M^2}{1 - M^2 (1 - M)} \qquad (3.7.6)$$

Equation (3.7.5) gives us the overall thermal conductivity of the two components system as a function of the thermal conductivity of the individual components and the void fraction.

Because of the symmetrical nature of the system the overall thermal conductivity is independent of direction.

The two-component - isotropic - three dimensional dispersion system is the basic model for the experimental work of this study.

Example: Calculation of the thermal conductivity of an apple. In this case the continuous component will be glucose-water solution while the dispersed component (about 25% v/v) is air.

k_c (of 15% glucose-water solution) = .3 Btu/hr ft °F

k_d (of air) = .0146 Btu/hr ft °F

$k_d/k_c = .0145/.3 = .0487$

M^3 (void fraction) = .25

$M^2 = .25^{2/3} = .393$

$M = .25^{1/3} = .63$

Inserting the values of M^2, M, k_c and k_d into equation (3.7.4) will give:

$$\frac{k}{.3} = \frac{1 - .393\,(1 - .0487)}{1 - .393\,(1 - .0487)(1 - .63)} = \frac{1 - .373}{1 - .138} = .728$$

$k = .3 \times .728 = .218$ Btu/hr ft °F

If we assume $k_d \ll k_c$ we get (equation 3.7.6)

$$\frac{k}{.3} = \frac{1 - .393}{1 - .393\,(1 - .63)} = \frac{.607}{.854} = .71$$

$k = .3 \times .71 = .213$ Btu/hr ft °F

B. Two-component - two dimensional anisotropic fibrous system

The fibers in this model are parallel to each other in the z direction (see figure 3.2A) We shall try to find the thermal conductivity, $k_{\parallel}$, which is the thermal conductivity in the direction parallel to the fibers, i.e. in the z direction, and the thermal conductivity, $k_{\perp}$, which is the thermal conductivity in the direction perpendicular to the fibers, i.e. in the x (or y) direction.

By the same reasoning used in the three dimensional dispersion system, we can see that by slicing the cube we can collect the fibrous material in one corner, now forming a rectangle which has the dimensions of N : N : 1 in the x, y, and z directions respectively, without changing the overall thermal conductivity in the respective direction (figure 3.2B).

Obviously void fraction = $N^2 \times 1$.

Based upon the additive property of the thermal conductivities when they are connected in parallel we find that the thermal conductivity parallel to the fibers (z direction),

$$k_{\parallel} = (1 - N^2)\, k_c + N^2 k_d$$

$$k_{\parallel}/k_c = (1 - N^2) + N^2 k_d/k_c$$

$$= 1 - N^2 (1 - k_d/k_c) \qquad (3.7.7)$$

$$= 1 - N\,Q \text{ where } Q = N\,(1 - k_d/k_c)$$

If $k_d \ll k_c$ we get that

$$k_{\parallel} / k_c = 1 - N^2$$

$$= 1 - \text{void fraction} \tag{3.7.8}$$

The thermal conductivity, $k_{\perp}$ (perpendicular to the fibers in the x or y directions), is found as follows: First, based upon the additive property of the thermal conductivities when they are connected in parallel we can find the thermal conductivity in the y direction from y = 0 up to y = N (figure 3.3B) is:

$$\frac{(1 - N)\, k_c + N\, k_d}{N} \tag{3.7.9}$$

Second, the thermal conductivity of the rest of the one unit cube, which is the continuous component in the y direction from y = N up to y = 1 will be:

$$\frac{k_c}{1 - N} \tag{3.7.10}$$

By adding the thermal conductivities, equations (3.7.9) and (3.7.10) when the conductors are connected in series we find:

$$\frac{1}{k_{\perp}} = \frac{N}{(1 - N)\, k_c + N\, k_c} + \frac{1 - N}{k_c} \tag{3.7.11}$$

$$\frac{k_c}{k_{\perp}} = \frac{N}{1 - N + N\, k_d / k_c} + 1 - N$$

$$= \frac{N + (1 - N)\, [1 - N\, (1 - k_d / k_c)]}{1 - N\, (1 - k_d / k_c)}$$

and by rearrangement we get

$$k_{\perp} / k_c = \frac{1 - Q}{1 - Q\, (1 - N)} \tag{3.7.12}$$

where $Q = N\,(1 - k_d/k_c)$

if $k_d \ll k_c$ we get (3.7.13)

$$k_\perp/k_c = \frac{1 - N}{1 - N + N^2} \qquad (3.7.14)$$

We would like to call the attention of the reader to the similarity of (3.7.12) to (3.7.5) which was obtained for the three dimensional randomly dispersed particles.

In the following steps we will find the ratio between the thermal conductivity in the direction parallel to the fibers, $k_\parallel$, and the thermal conductivity in the direction perpendicular to the fiber, $k_\perp$. If we divide $k_\perp$ (equation 3.7.9) by $k_\parallel$ (equation 3.7.14) we get

$$\frac{k_\parallel}{k_\perp} = \frac{1 - N\,Q}{\dfrac{1 - Q}{N + (1 - N)(1 - Q)}}$$

$$= \frac{(1 - N\,Q)(1 - Q + N\,Q)}{1 - Q}$$

$$= \frac{1 - N + N\,Q - N\,Q + N\,Q^2 - N^2\,Q^2}{1 - N}$$

$$= \frac{1 - Q + N\,Q^2\,(1 - N)}{1 - Q}$$

$$= 1 + \frac{N\,Q^2\,(1 - N)}{1 - Q} \qquad (3.7.15)$$

Equation (3.7.15) shows the ratio between the overall thermal conductivity in the direction parallel to the fibers, $k_\parallel$, and the overall thermal conductivity in the direction perpendicular to the fibers, $k_\perp$, as a function of the thermal conductivity of the individual components

and their proportion.

In the following step we show that the ratio $\frac{k_{\parallel}}{k_{\perp}}$ is always greater or equal to 1. As N is always a positive number smaller than 1 $(0 \leq N \leq 1)$ and k_d/k_c is always a positive number, Q (see equation 3.7.13) is a number within the following boundaries $1 \geq Q \geq -\infty$. By inspection of equation (3.7.18) which describes the ratio $\frac{k_{\parallel}}{k_{\perp}}$ we can see that as N, (1 - N), Q^2 and (1 - Q) must be positive numbers this ratio is greater than 1. Only when $k_c = k_d$, Q will be 1, resulting that $k_{\parallel} = k_{\perp}$.

This means that regardless of the values of the thermal conductivities of the components or their proportion, the thermal conductivity in the parallel direction, $k_{\parallel}$, in the fibrous system, is always larger than the thermal conductivity in the perpendicular direction, $k_{\perp}$. They will be equal only when $k_c = k_d$ or obviously in the trivial cases $N = 1$, $N = 0$.

Let us check the properties of the function $k_{\parallel}/k_{\perp}$ vs k_d/k_c (equation 3.7.18) with respect to its maximum or minimum value.

$$k_{\parallel}/k_{\perp} = 1 + \frac{N\,Q^2\,(1 - N)}{1 - Q} \qquad (3.7.15)$$

The first derivative is:

$$\frac{d(k_{\parallel}/k_{\perp})}{dQ} = \frac{2N\,Q\,(1 - N)(1 - Q) + N\,Q^2\,(1 - N)}{(1 - Q)^2}$$

$$= \frac{(1 - N)\,N\,(2Q - 2Q^2 + Q^2)}{(1 - Q)^2} = \frac{(1 - N)\,N\,(2Q - Q^2)}{(1 - Q)^2}$$

The second derivative is:

$$\frac{d^2(k_{\|}/k_{\perp})}{dQ^2} = \frac{(1 - N)\, N\, [(1 - Q)^2\, (2 - 2Q) + (2Q - Q^2)\, 2\, (1 - Q)]}{(1 - Q)^4}$$

$$= \frac{(1 - N)\, N\, (1 - Q)\, [2 + 2Q^2 - 4Q + 4Q - 2Q^2]}{(1 - Q)^4}$$

$$= \frac{2\, (1 - N)\, N\, (1 - Q)}{(1 - Q)^4}$$

Since $(1 - N)$ N and $(1 - Q)$ are positive numbers, the second derivative has a positive value. This means that the function has a minimum value. The minimum value can be found by equating the first derivative to zero.

$$\frac{d(k_{\|}/k_{\perp})}{dQ} = \frac{(1 - N)\, N\, (2Q - Q^2)}{(1 - Q)^2} = 0$$

There are four solutions to the above equation

1. $N = 0$
2. $N = 1$
3. $Q = 2$
4. $Q = 0$

The first and the second solutions are meaningless because when N equals 1 or 0 we have only one component. The third solution where $Q = 2$, is impossible as $Q < 1$, ($Q > 1$ means that either k_c or k_d has a negative value). The only solution possible is, therefore, $Q = 0$, in other words $k_c = k_d$. So the value of $k_{\|}/k_{\perp}$ as a function of k_d/k_c for any void fraction, has a <u>minimum</u> value of (= 1) when $k_c = k_d$.

C. <u>Two-component - one dimensional - anisotropic layered system</u>

In this case the components are arranged in parallel layers to form some kind of composite layer system (see figure 3. 3A).

From figure (3. 3A) we can see that we can collect all the layers of the same component to form a rectangle which has the dimensions of P : 1 : 1 in the x, y, and z directions, respectively (see Figure 3. 3B).

Obviously the void fraction = $1 \times 1 \times P$. Adding the thermal conductivities of the areas when they are parallel to each other we get

$$k_{\parallel} = k_c (1 - P) + k_d P$$

$$\frac{k_{\parallel}}{k_c} = 1 - P (1 - k_d/k_c) \qquad (3.7.16)$$

The thermal conductivity in the parallel direction will be

$$\frac{1}{k_{\perp}} = \frac{P}{k_d} + \frac{1 - P}{k_c}$$

or

$$\frac{k_{\perp}}{k_c} = \frac{k_d}{P k_c + k_d (1 - P)}$$

Dividing by k_d and rearrangement we get

$$\frac{k_{\perp}}{k_c} = \frac{1}{1 - P (1 - k_c/k_d)} \qquad (3.7.17)$$

The controlling effect of one of the components having a relatively low thermal conductivity in a perpendicular flow system in contrast to its lesser importance in the parallel flow case can be observed by inspection of equation (3.7.17) and equation (3.7.16) respectively.

(Note the similarity between equations (3.7.16) and (3.7.17). If we divide $k_{\parallel}$ by $k_{\perp}$ we get

$$\frac{k_{\parallel}}{k_{\perp}} = [1 - P(1 - k_d/k_c)]\,[1 - P(1 - k_c/k_d)]$$

$$= 1 - P(1 - k_c/k_d) - P(1 - k_d/k_c) + P^2(1 - k_d/k_c)(1 - k_c/k_d)$$

$$= 1 + P(-2 + k_c/k_d + k_d/k_c) - P^2(-2 + k_c/k_d + k_d/k_c)$$

$$= 1 + (1 - P)\,P\,(-2 + k_c/k_d + k_d/k_c) \qquad (3.7.18)$$

Since the term $(-2 + k_c/k_d + k_d/k_c)$ is always positive (unless $k_d = k_c$ in which case it becomes zero), regardless of the value of k_d and k_c, and since P is positive and smaller than 1 it turns out that $(1 - P)P(-2 + k_c/k_d + k_d/k_c)$ is always positive which consequently causes $\frac{k_{\parallel}}{k_{\perp}} > 1$. This means that in the layered pattern system as in the fibrous system the thermal conductivity in the parallel direction is always larger than the thermal conductivity in the perpendicular direction. The actual magnitude depends upon the values of the thermal conductivities of the individual components and their proportion.

Let us check the properties of the function $k_{\parallel}/k_{\perp}$ vs k_d/k_c (equation 3.7.18) with respect to its maximum value.

$$k_{\parallel}/k_{\perp} = 1 + (1 - P)\,P\,(-2 + k_c/k_d + k_d/k_c) \qquad (3.7.18)$$

The first derivative is

$$\frac{d(k_{\|}/k_{\perp})}{dW} = (1 - P)\, P\, (-\frac{1}{W^2} + 1)$$

where $W = k_d/k_c$

The second derivative is

$$\frac{d^2(k_{\|}/k_{\perp})}{dW^2} = (1 - P)\, P\, (\frac{2}{W^3})$$

Since $0 \leq P \leq 1$ and W is positive the second derivative is positive too. This means that the function has a minimum value. The minimum value can be found by equating the first derivative to zero.

$$\frac{d(k_{\|}/k_{\perp})}{dW} = (1 - P)\, P\, (1 - \frac{1}{W^2}) = 0$$

There are **four** solutions to the above equation

1. $P = 1$
2. $W = -1$
3. $W = 1$
4. $P = 0$

The **solutions** $P=0$, $P = 1$, is meaningless and the second solution, $W = -1$, is impossible as it shows that one of the components has a negative thermal conductivity. The only real solution possible is, therefore, $W = 1$, or in other words, $k_c = k_d$. So the value of $k_{\|}/k_{\perp}$ as a function of k_d/k_c for any void fraction has a minimum value $(= 1)$ when $k_c = k_d$.

Let us check the properties of the $k_{\|}/k_{\perp}$ equation (equation 2.7.18) with respect to the void fraction P.

The first derivative is

$$\frac{d(k_{\parallel}/k_{\perp})}{dP} = (-2 + k_c/k_d + k_d/k_c)(1 - P - P)$$

The fact that the second derivative is negative indicates that the function has a maximum. The maximum is obtained by equating the first derivative to zero. By doing so we found that $P = 1/2$. This means that if we vary the void fraction P, the ratio between the thermal conductivity in the parallel direction to the thermal conductivity in the perpendicular direction in the layered system will reach a maximum value when the void fraction is .5, i.e. the two components are of equal volume.

We would like to point out that in fibrous and layered systems by measuring the thermal conductivity in each of the two directions, parallel and perpendicular, and knowing two of the three parameters, k_c, k_d or void fraction it is possible to compute the third.

All the equations (3.7.4), (3.7.7), (3.7.12), (3.7.16) and (3.7.17) developed for the overall thermal conductivity of the system in the direction parallel and perpendicular for the three models (three dimensional, two dimensional and one dimensional dispersion system) must and do satisfy the following limits:

1. When $M = N = P = 1$ $\quad k = k_d$
2. When $M = N = P = 0$ $\quad k = k_c$
3. When $k_c = k_d$ $\quad k = k_c = k_d$

In Table 3. 3 we present the condensed table for the overall thermal conductivity of three dimensional, two dimensional and one dimensional homogeneous dispersion systems.

In this section we analyzed and presented the overall thermal conductivity of a three dimensional isotropic system, a two dimensional anisotropic fibrous system and one dimensional anisotropic layered system as a function of the thermal conductivity of the individual components, their proportion and relative pattern. We have shown that in the case of the anisotropic fibrous or layered system the thermal conductivity in the direction parallel to the fibers or layers is always larger than the thermal conductivity in the direction perpendicular to the fibers or layers.

Table 3.3. The overall thermal conductivity of three dimensional, two dimensional and one dimensional homogeneous dispersion systems

<table>
<tr><th></th><th>Three dimensional isotropic system</th><th>Two dimensional anisotropic fibrous system</th><th>One dimensional anisotropic layered system</th></tr>
<tr><td>Dimension of the rectangular</td><td>M : M : M</td><td>1 : N : N</td><td>1 : 1 : P</td></tr>
<tr><td>Void fraction</td><td>M^3</td><td>N^2</td><td>P</td></tr>
<tr><td></td><td>$Q = M^2 (1 - k_d/k_c)$</td><td>$Q = N (1 - k_d/k_c)$</td><td></td></tr>
<tr><td>$\frac{k_{\parallel}}{k_c}$</td><td rowspan="2">$\frac{1 - Q}{1 - Q (1 - M)}$</td><td>$1 - N Q$</td><td>$1 - P (1 - k_d/k_c)$</td></tr>
<tr><td>$\frac{k_{\perp}}{k_c}$</td><td>$\frac{1 - Q}{1 - Q (1 - N)}$</td><td>$\frac{1}{1 - P (1 - k_c/k_d)}$</td></tr>
<tr><td>$\frac{k_{\parallel}}{k_{\perp}} \geq 1$</td><td></td><td>$1 + \frac{N Q^2 (1 - N)}{1 - Q}$</td><td>$1 + (1 - P) P (-2$
$+ k_c/k_d + k_d/k_c)$</td></tr>
</table>

4. THE EXPERIMENTS

In this study we shall evaluate the thermal diffusivity of the experimental samples using a transient heat conduction method. The thermal diffusivity, α, has almost the same basic significance in transient heat conduction as the thermal conductivity, k, has in steady-state heat conduction. In the steady-state heat conduction system, the thermal conductivity is the only body thermal property that should be known (or that can be determined) in order to evaluate the experimental heat transfer data, while for transient heat conduction both the thermal diffusivity, α, and the thermal conductivity, k, must be known (or can be determined).

In many cases, especially in high N_{Bi} systems, as was discussed in the previous section, because of the lack of sensitivity of the root value β_1 to N_{Bi}, it is not necessary to know the thermal conductivity to analyze the transient system nor is it possible to determine the thermal conductivity directly.

4.1 Considerations in the selection of the experimental method

Measurements of the thermal conductivity, k, by the accurate guarded hot-plate method was ruled out because of the large size sample (8" $\times$ 8") required by this method. This method can be applied usually for solid, hard materials that can be machined to a smooth and relatively incomprisable uniform plate. Because of the limitation in the sample preparation techniques, this method could have been applied only to foodstuffs in the frozen state (Lentz, 1961; Miller, 1963).

The measurement of the thermal conductivity, k, by the Cenco-Fitch method which was used by Bennet (1962, 1964), Walters (1963), was attempted. This method is based on the measurement of heat quantities with respect to time, flowing in a one dimensional direction from a constant temperature source through the sample to the heat sink. At the start of this project a Cenco-Fitch type apparatus having a 180 gr heat sink which is 1-1/4" diameter chrome-plated copper plug as shown in Figure 4.1 was constructed and tested. Calibration of this apparatus using a 1/4" thickness of 50-Silastic Silicone Rubber as a standard, showed that the error due to the end effect and heat losses from the sink were more than 15%. This magnitude of the error is approximatly the same as that found by the above mentioned authors. It was decided to reject this method because of the following:

1) One of the necessary conditions for the Cenco-Fitch technique is to have no significant surface thermal resistance, i.e. good contact between the source and the sink metal surfaces at the top and bottom surfaces of the sample. This can be accomplished by applying pressure which may cause unpredictable errors due to such effects as extrusion of liquid, changing the thickness and changing the physical properties.

2) In the Cenco-Fitch technique the heat flow is assumed to be one

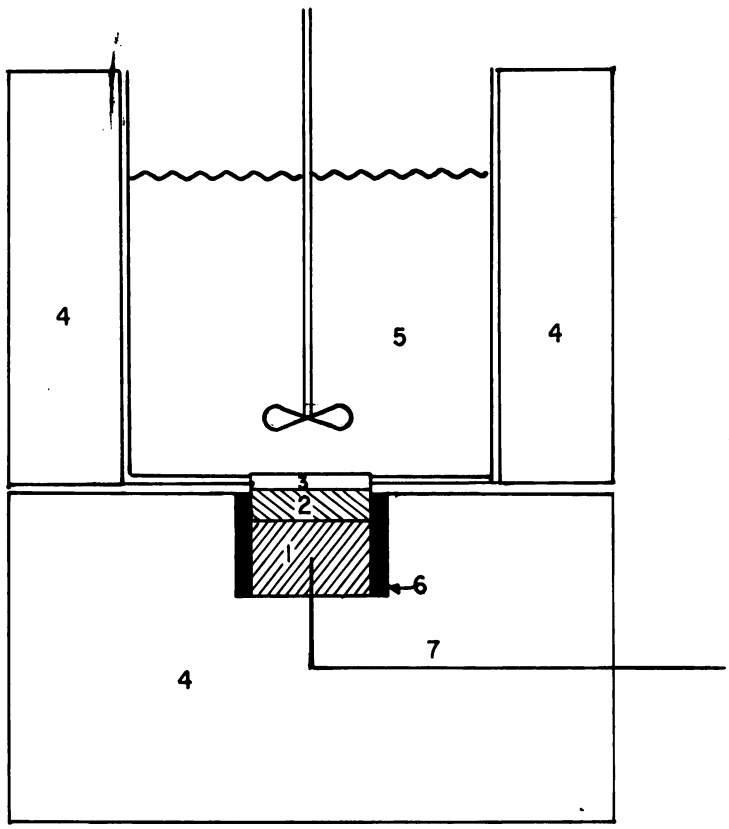

I. COPPER SINK
2. SAMPLE
3. CONSTANT TEMPERATURE COPPER SOURCE
4. STYROFOAM
5. CONTROLLED TEMPERATURE BATH
6. PRESPEX SLEEVE
7. 30"-GAGE COPPER-CONSTANTAN THERMOCOUPLE

Figure 4. 1. Modified Cenco-Fitch apparatus.

dimensional and, therefore, must be one dimensional from the source to the sink throughout the sample. The larger the ratio of the dimension which is perpendicular to heat flow to the dimension which is parallel to the heat flow the smaller the heat losses throughout the ends. In this technique the maximum practical ratio that can be obtained in a food sample will be in the neighborhood of 1 1/4 : 1/4. This ratio is quite poor, and the unpredictable heat losses could be expected to be fairly high.

3) Because heat flow is measured with respect to time (unsteady state), any heat loss from the sink itself, which is unavoidable and practically unmeasureable, will cause an error.

In summary, it appeared to us that this method has the combined major handicaps of steady state and transient methods.

4.2 The selected method

The method used in this study was a transient heat conduction method, by which the thermal diffusivity was determined directly by measuring the temperature change at the geometric center with respect to time of an initially uniform temperature sample suddenly exposed to a constant temperature.

For simplicity with respect to the sample itself and the general design of the apparatus, a cylindrical configuration of the specimen was chosen.

The basic differential equation for the infinite cylinder initially at a uniform temperature and suddenly exposed to an environment of constant temperature is stated in equation (2.1.6). The exact solution and the boundary conditions which must be satisfied are stated in equations (2.3.6), (2.3.1), (2.3.2) and (2.3.3) respectively. By following the discussion in section (2.4) we can see that by measuring the temperature at the geometric center, taking into account only the first term of equation (2.3.6) and plotting the logarithm of the unaccomplished temperature difference vs time, we can get the following relationship.

$$\alpha = \frac{(\ln 10)\, R^2}{f\, \beta_1^2} \qquad (4.2.1)$$

The derivation of the equations impose certain conditions which must be fulfilled experimentally:

1. Equation (2.3.6) holds only for one dimension radial heat flow, i.e. $\frac{\partial T}{\partial z} = 0$), and required, theoretically that the cylinder be infinitely long. We fulfill this requirement by a) having a large ratio *

$$\frac{\text{length of cylinder}}{\text{diameter of cylinder}}$$

b) thermally insulating the ends.

2. Equation (2.3.6) requires that the initial temperature of the sample be uniform. This requirement is accomplished by submerging the

---

* Ratio value between 6 to 12 in the air-sucrose solutions foam.
Ratio value between 3 to 6 in the foodstuffs.

sample in a controlled temperature environment for an adequate period of time (at least three f values).

In spite of the fact that we intend to determine the film coefficient of the system (in order to evaluate the N_{Bi}), we tried to build our system in such a way that the film coefficient and therefore the N_{Bi} will be as large as possible. It is quite obvious that in a large N_{Bi} system the β_1 is insensitive to the N_{Bi}, so any change or error in the film coefficient h (and therefore in N_{Bi}) will cause only a slight change in β_1, and therefore in the thermal diffusivity α. (See also sections 3.3 and 3.4). A few of the impressive advantages of this method are: 1) No heat quantities are measured. 2) The exact location of the thermocouple is not critical. The thermocouple was placed at the geometric center because it was convenient. 3) The timing of the sudden change of temperature is not critical.

4.3 The experimental system (see Figures 4.2 and 4.3)

The main components of the experimental apparatus were:

Temperature controlled water tanks. 30" × 30" × 28" 12-guage steel tanks having 3" standard nipple as the outlet standing on four 6" high 2" × 2" × 1/4" legs--these tanks were fabricated and were used as the hot and cold water baths.

Top tank. 35" × 25" × 10" 12-gauge steel standing on three 42" long 2" × 2" × 1/4" legs, having two 6" diameter 12" long outlets for discharge into the two temperature controlled tanks located below the top tank.

Test section. Forty inch long 4 1/2" diameter standard water pipe was welded to the top tank. About 10" from the bottom a 3" long cone end bronze support with conical end was supported vertically in the middle of the pipe by two 5" long perpendicular machine bolts 2" apart. This conical end bronze support is the lower support for the sample.

Piping. The suction part of the piping system consisted of 3" pipes. The discharge part was gradually increased from 2" discharge to the 4 1/2" size of the vertical main pipe. A set of valves was installed in such a way that the water flow could either pass through or by-pass the rotameter. The temperature controlled water tanks were connected to the pump by a 3" three-way bronze plug valve.

Pump. The pump was a 3 Hp, 1750 RPM centrifugal pump manufactured by Delco, and has a maximum capacity of 175 GPM. Because of the relatively low pressure drop throughout the system the value of 175 GPM flow rate was the same for all three sizes of stainless steel tubes.

Temperature controls. The heat supply to the high temperature tank was obtained by adding hot tap water directly from the main building supply system. The actual flow of the hot water was controlled within .5° F by a Foxboro Type F-37 proportioned valve activated by a 0-200° F Brown Potentiometer Model 152P13P-63-11 controller. The temperature in the cold temperature tank was maintained throughout the test by

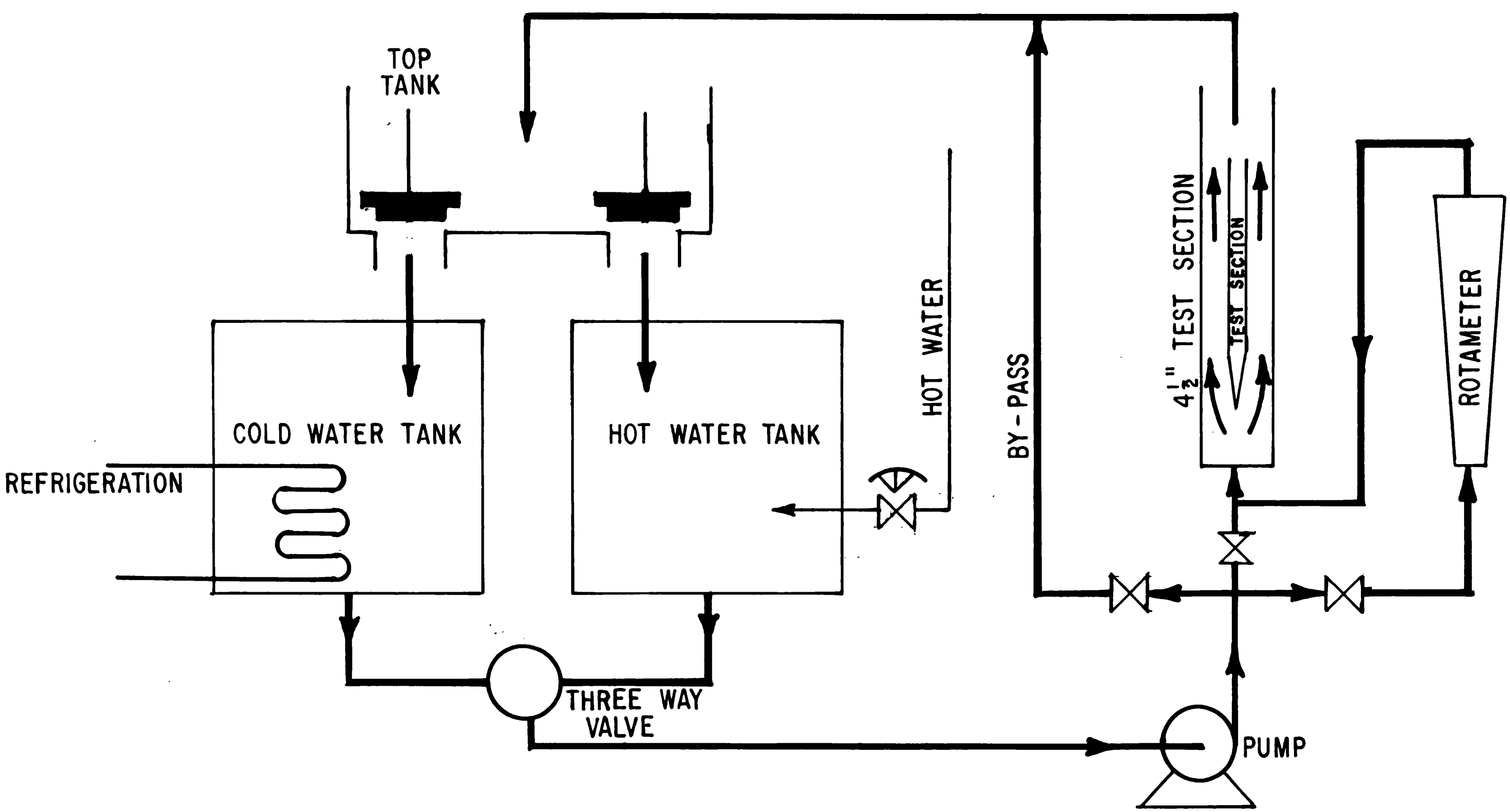

Figure 4.2. Schematic diagram of the experimental system.

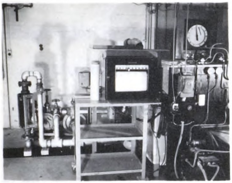

A

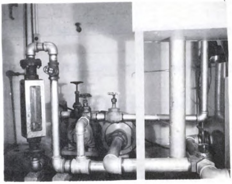

B

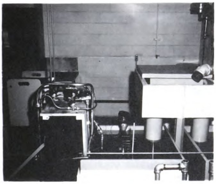

C

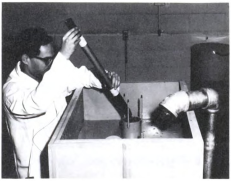

D

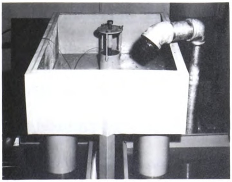

E

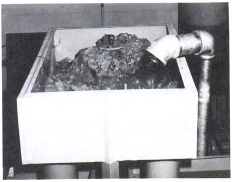

F

Figure 4.3. The experimental system. A. Overall view of the experimental system. B. Piping system and rotameter. C. Refrigeration coils and their controls. D. Inserting the assembled sample. E. View of top tank after the sample was installed. F. View of top tank once the test has begun.

a refrigeration system which consisted of a 3 Hp, R-12 condensing unit and two 50 ft long 1/2" I.D. copper coils. The temperature was controlled within .5° F by a Minneapolis-Honeywell Transistorized Amplifier Relay Temperature Controller Model L7038 having a range of 10 to 80° F.

Temperature measurements. The temperatures in all the experiments except the metal cylinders were measured and recorded with a 12 point 3 minute cycle temperature recording potentiometer, -40° F to +140° F span, 1° F least division Model 153X64P12-X-71, manufactured by Minneapolis-Honeywell. The temperature change of the metal cylinders was measured and recorded every 1 second by a multi-channel one minute cycle recording potentiometer. All of the thermocouples used in this study were No. 30 gauge copper-constantan wire, with enameled glass wrapped, fiberglass overwrapped insulation.

4.4 The experimental procedure

The specific tests in this study were:

a. Air-sucrose solution. The air-sucrose two-phase system, "a foam", was studied using 1.5, 8, 16, 24 percent sucrose concentration each having about 4 different air concentrations.

b. Fresh apple tissue.

c. Deaerated apple tissue.

d. Raw potato.

e. Beef lean meat.

The tubes used in this study, for supporting the samples, were 1" 1 1/2" and 2" O.D. stainless steel type 316 having a wall thickness of .012".

Each of the samples was run in a 1", 1 1/2" and 2" stainless tube (except for the apple tissue which was run in 1" and 1 1/2" only).

Each sample in the stainless steel tube was heated from 36° F to 96° F (heating), and cooled from 96° F to 36° F (cooling). These two temperatures encompass the range of temperatures encountered in the cooling and precooling of fruits and vegetables.

Preparation of the foamed sucrose solutions

To have an immobilized system it was necessary to add a solidification agent. Agar, a polysaccharide, was added in the amount of 1.5% w/w to all the tests throughout this study. For the purpose of calculation it was assumed that the agar has the same thermal properties as sugar; therefore, an 8% sugar solution consists of 6.5% sugar and 1.5% agar, and a 1.5% sugar sample contained only agar.

All foamed sucrose solutions were prepared in a Waring Blender Model PB-5A equipped with a standard 1 quart calibrated blending bowl. Six hundred gr of the appropriate sucrose solution having 1.5% w/w agar were placed in the blending glass. During blending the foam inducer D-100* was added from a 10% aqueous solution and air was

---

* Manufactured by Gunther Products Inc., Galesburg, Illinois.

incorporated. After the designed volume and specific gravity were reached, the viscous solution was quickly poured into the 1", 1 1/2" and 2" stainless steel tubes. The tubes were sealed with 1 1/2" thick plug of Polystyrene foam insulation and corked by the bakelite plug (see Figure 4.5). After the thermocouple lead wire was fastened to the bakelite plug, the assembled unit was immersed in a 36° F bath to accelerate solidification. The temperature of the sugar solution and the liquified agar were such that the temperature during blending was about 90° F. It was important to maintain this temperature because if the temperature was too low, the solution could solidify before pouring, and if the temperature of the solution was too high, the solution may not be viscous enough to prevent the air bubbles from rising. Control of the amount of air incorporated during blending was achieved by controlling the foam density, which was measured by withdrawing 100 ml of foam in a tared graduated cylinder and weighing it to the nearest .1 gr.

To avoid any microbiological activity 25 ppm of $HgCl_2$ was added to the sucrose and agar stock solutions.

After finishing a heat penetration experiment, the gel was pushed gently from the stainless steel tube and by accurate determination of the weight and volume of the gel the true specific gravity and the actual amount of air was calculated.

Preparation of the raw potato samples

Procedure. 1" 1 1/2" and 2" raw potato plugs were formed by pushing the stainless steel tubes through a whole raw potato. Both ends of plugs were cut square and packed carefully end to end into the stainless steel tubes to form a combined plug of about 7" length. A thermocouple was placed in a hypodermic needle and by using a bakelite guide-plug, corked into the top end of the stainless tube steel, the hypodermic needle was inserted down to the geometric center of the 7" long potato plug, then, holding the thermocouple the hypodermic needle was pulled back. Three inches of polystyrene foam insulation were packed into both ends of the 7" potato plug followed by the top and bottom bakelite plugs.

Analysis of the potato.

Total solids (by vacuum A.O A.C. 1960)	18.45% w/w
Density (by water displacement A.O.A.C. 1960)	1.07 gr/cm^3

Preparation of the raw apple samples

Procedure. MacIntosh apples were cut in halves. A plug was made by pushing a stainless steel tube through the apple flesh. The end of the plug was cut square. From each half one plug was put aside for the deaeration process. The other plug was packed into the stainless steel tube. The process was repeated until the total length of the combined apple flesh plugs was 7". The loading procedure was repeated for the deaerated plugs. The thermocouple placement procedure was the same as for the raw potato flesh.

Apple flesh deaeration procedures. The apple flesh plugs were submerged in a 15% sucrose-water solution in a desiccator. The desiccator was connected to a water-vacuum pump and a 28" Hg vacuum was applied. It was found that in order to get complete deaeration and replacement of the air spaces by the sucrose solution in a 3/4" thickness of apple plug, the 28" Hg vacuum should be applied for a few hours. There is an excellent visual criterion for the progress of deaeration: when the vacuum is released the solution penetrates immediately into all of the deaerated spaces and the spaces become translucent. When complete deaeration is achieved, the slice is completely translucent and now has the same specific gravity as the solution. The escape of the expanding air did not change the shape nor the strength of the apple plug, on the contrary, the deaerated translucent apple slices were firmer than the raw apple.

The leaching losses during deaeration were considered to be negligible since the infiltration medium and the apple had the same carbohydrate concentration (Reeve, 1953).

In order to avoid any microbiological activity during deaeration 500 ppm of benzoic acid was added to the solution. Browning was eliminated because of the apple plugs being submerged and the use of high vacuum.

Analysis of the raw apples.

Total solids (by vacuum A.O.A.C. 1960) 14.4 w/w

Average density (by water displacement A.O.A.C. 1960)	.773 gr/cm^3
Amount of air (using equation 5.2.5)	26.5% v/v

Preparation of the beef meat samples

Procedure. The 1", 1 1/2" and 2" beef lean meat plugs were formed by pressing a special cutter with a hydraulic press (see Figure 4.4C) through a square (square in respect to the meat grain) piece of frozen lean meat. Two sets of 1", 1 1/2" and 2" meat plugs were obtained; one set where the cutting plane was parallel to the grain, the second set where the cutting plane was perpendicular to the grain.

The meat plugs were packed end to end into the 1", 1 1/2" and 2" stainless tubes to form approximately a 7" combined plug. The tubes were placed in a lathe and a 5/64" drill was used to drill a hole to the geometric center. The procedure for the thermocouple placement was the same as for raw potato.

Analysis of the beef lean meat

Density (by water displacement A.O.A.C. 1960)	1.08 gr/cm^3

The chemical analysis for moisture content and fat were done on the ground meat by the methods described by Howard and Aurand (1963).

Moisture content	71.5% w/w
Fat	5.6% w/w
Protein (by difference)	22.9% w/w

Preparation of the apple sauce samples

Procedure. The 1", 1 1/2" and 2" apple sauce samples were prepared using 2 qt jar commercial apple sauce (brand name "Musselman").

Analysis of the apple sauce.

Density (by weighing 100 ml of apple sauce in volumetric flask)	1.07 gr/cm^3
Total soluble solids (as sucrose) (by refractometer)	19.5% w/w
Total solids (by vacuum A.O.A.C. 1960)	21.2% w/w
Acidity (expressed as dehydrous citric acid)	.41% w/w

The procedure for a test run

The procedure for a test run was the following: After submerging the sample in the temperature-controlled tank in order to equilibrate it at a uniform initial temperature, say 36° F, it was transfered to the main 4.5" test section, placed and fastened vertically in the center of the test section. The pump was turned on with the 36° F water flowing through the test section for about 5 minutes to assure a uniform initial temperature. The temperature of the heating medium was changed suddenly by turning the direction of the three-way valve, thus pumping the 96° F water by the sample. In order to avoid a sizable change of temperature of the temperature controlled tanks the first portion of water pumped right after the sudden change was drained from the top tank. After this portion was discarded, the drain outlet was sealed and the adequate 6" outlet of the top tank was opened to maintain cycling of the water. The experiment was terminated when the temperature at the geometric center was within 3° F of the medium temperature.

4.5 Metal cylinders

In order to determine the film coefficient applicable to samples evaluated throughout this study, 6" long copper and aluminum cylinders of 1", 1 1/2" and 2" diameter were made (see Figure 4.4). These metals were chosen because of their high purity, machinability, high thermal diffusivity and respectively moderate change in thermal properties with temperature. A 5/64" hole was drilled to the geometric center. A 30 gauge copper-constantan thermocouple was placed in a hypodermic needle with a square-cut end which was inserted into the hole to the geometric center, then, holding the thermocouple in place, the hypodermic needle was pulled back. A small amount of the (copper or aluminum) filings were poured into the hole, then pressed down by the hypodermic needle around the thermocouple wire. The hypodermic needle was then pulled back and more filings were added. The same process was repeated until the hole was completely filled and the thermocouple packed tightly. The top of the hole was sealed with a drop of electrical dope. To assure good contact between the thermocouple junction and the cylinder a drop of SAE No. 5 instrument oil was placed into the bottom of the hole at the beginning of the packing procedure.

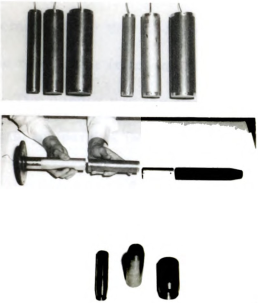

A

B

C

Figure 4.4. A. The metal cylinders. B. Assembling a metal cylinder. C. Cutter for preparing meat sample.

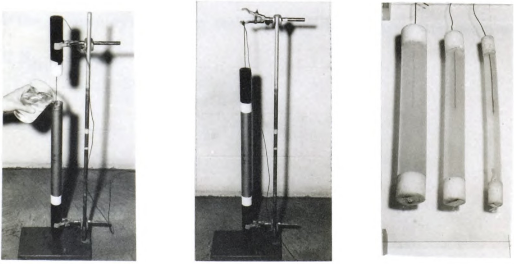

A B C

Figure 4.5. A. Pouring the sucrose solution. B. The assembled sample. C. The sucrose solution gel.

The various electrical resistances were measured before and after placement of the thermocouple, and no detectable difference (< .1 ohms) in the resistance (max. of 12 ohm) was noted.

The copper and the aluminum were assumed to have the following thermal properties (McAdams, 1954).

	ρ	k	C_p	α
	lb/ft^3	Btu/hr ft °F	Btu/lb °F	ft^2/hr
Copper	559	223	.0915	4.360
Aluminum	169	117	.2140	3.235

A computer program was written for the calculation of the first term approximation of the relationship between the f and the film coefficient, h, for the infinite cylinder for the three sizes of copper and aluminum for all N_{Bi} ranges.

5. BASIS FOR ANALYSIS OF DATA

In this section 1) we shall define the limits of the straight line semi-logarithmic curve and the time-average temperature. 2) We shall compute by the least square method the specific heat and the thermal conductivity of air as a function of the temperature. 3) We shall show the way the film coefficient of the system was evaluated. 4) We shall show the magnitude of the generated heat during the experiment. 5) We shall show the magnitude of the free convection. 6) We shall show the size of the air foamed bubbles. All the computations throughout this study such as the heat transfer computations, generating Bessel functions, the computation of the statistical least square fitting curve and the analysis of the results were done on the Control Data 3600 Digital Computer.

5.1 Defining the limits of the straight line semi-logarithmic curve and the time-average temperature

Here we shall first define the limits of the straight line semi-logarithmic curve and we shall draw the straight line between those limits for the determination of the slope and the intersection with the ordinate. Second, we shall find the temperature correspondent to the average time of those limits, the time-average temperature.

It was observed that the best points suitable for drawing the straight line semi-logarithmic heating or cooling curve are those where the time value, t, is between the limits $.4 \times f \leq t \leq 1.08 \times f$. In this region the straight line is already established, but yet it is far enough from the zone where the unaccomplished temperature becomes small enough that the fluctuation of the media temperature may introduce some error. We assume that the N_{Bi} is large enough (which it is--see Table 6.1) that the j_c value for the infinite cylinder can be taken to be 1.6. It can be seen either graphically or mathematically that the temperatures corresponding to $t = .4\,f$, and $t = 1.08\,f$ (which are the limits of the straight line semi-logarithmic curve where the straight line portion is drawn) are independent of the diameter of the infinite cylinder or its f value, and will be the same for all the cylinders regardless of their f value providing that the j value and the initial and media temperature are the same. The limits of this region can be found by inserting the appropriate values of $T_1 = 96°F$, $T_0 = 36°F$ and $T_1 = 36°F$, $T_0 = 96°F$ for heating and cooling respectively, and the value of t/f of .4 and 1.08 for the lower and upper limits respectively into the equation of the straight line semi-logarithmic curve:

$$\log (T_1 - T) = -\frac{t}{f} + \log [j(T_1 - T_0)]$$

The results are:

	lower limit	upper limit
heating	T = 57.8° F	T = 88° F
cooling	T = 74.2° F	T = 46° F

The average time-temperature of those limits will be the temperature corresponding to the average t/f of the upper and lower limits, i.e. $(\frac{t}{f})$ average $= \frac{.4 + 1.08}{2} = .74$. Using the above equation this average temperature was found to be 78.5° F for heating and 53.5° F for cooling. Throughout this study the thermal properties will be evaluated and compared at T = 78.5° F for heating and at T = 53.5° F for cooling.

5.2 Evaluation of the physical constants

Here we show the source and the way we evaluated the film coefficient of the system, the thermal properties of the air (the dispersed component), and the thermal properties of the air-sucrose solutions foam needed for the analysis of the data.

Sucrose solutions

Specific heat, C_p. An equation for the specific heat of an aqueous sucrose solution as function of per cent sucrose was computed by the least square method, using the following data given by Honig (1935) for 68° F.

% sucrose	0	10	30	50	65
$C_p \frac{Btu}{lb\ °F}$	1.00	.9428	.8299	.7213	.6406

The equation was found to be

$$C_p = 3.746 \times 10^{-6} S^2 - 5.77 \times 10^{-3} S + 1.000 \qquad (5.2.1)$$

S - percent sugar by weight

Density. The density of the aqueous sucrose solutions was taken for 20°C from Honig (1953), Table 16.

Thermal conductivity, k_L. Honig (1953 - Table 11) tabulates the values of the thermal conductivity, k_L, of aqueous sucrose solutions ranging from 0 percent sucrose up to 60 percent for a temperature range of 32° F to 144° F (at intervals of 18° F). Using these values, equations were computed using the least square method where the thermal conductivity of sucrose solutions, k_L, was a function of the sucrose concentration for a given temperature. The general form was $k_L = A\,S + B$ (equation 5.2.2), and each temperature has different values of A and B. The value of A and B for heating (average-time temperature = 78.5° F) and cooling (average-time temperature = 53.5° F) were found to be:

heating	$A = -.189 \times 10^{-2}$	$B = .351$
cooling	$A = -.181 \times 10^{-2}$	$B = .337$

$$k_L = A\,S + B \tag{5.2.2}$$

Air

Thermal conductivity, k_A. The thermal conductivity of air, k_A, was calculated as a function of temperature according to the equation (International Critical Tables, 1929):

$$k_A = k_{A0}\left(\frac{273 + 125}{T_c + 125}\right)\left(\frac{T_c}{273}\right)^{1.5} \tag{5.2.3}$$

T_c = absolute temperature, °K

k_{A0} = thermal conductivity of air at 0° C = .0140 Btu/hr ft °F

Air-sucrose solutions foam

Density. The amount of air (v/v) in the air-sucrose solutions foam was evaluated by determining the density of the foam as follows: The foamed sample was removed from the stainless tubing and the volume and weight of the gel were determined. After knowing the density, the amount of air was determined by the following material balance:

$$\rho_L (1 - a) + \rho_A a = \rho\ 1 \tag{5.2.4}$$

where

ρ_L - density of the sucrose solution

ρ_A - density of the air

ρ - density of the air sucrose solution foam

a - volume fraction of air

as $\rho_A \ll \rho_L$ we get by rearrangement of equation (5.2.4)

$$a = \frac{\rho_L - \rho}{\rho_L} \tag{5.2.5}$$

Specific heat. The specific heat of any system is a function of the product of the weight fraction of the individual components and their respective individual specific heat. It is well justified to say that in most of the systems having gaseous components as well as liquid and/or solid components, the specific heat of the total system, due to the relatively low density of the gaseous phase (and therefore its low weight fraction) will be the specific heat of the non-gaseous components. Since the weight of the foaming air in any of our experiments is very small with respect to the weight of the sucrose solution, the specific heat of the foamed sucrose solutions can be justified to be taken as the specific heat of a sucrose solution having the same sucrose concentration.

5.3 Film coefficient values

The film coefficients of the system for each stainless steel tube size for cooling and heating were evaluated by using the copper and aluminum cylinders (they are shown in Figure 4.4A). The temperature-time change at the geometric center was measured every second by a multi-channel one-minute cycle recording potentiometer. The f value was converted into the equivalent h values. The film coefficient, h, obtained by the two different metals agreed within 5%. The two film coefficients, h, obtained from the copper and aluminum were averaged and used in the computation of the experimental thermal conductivity, k_E. The average film coefficient value evaluated from the copper and aluminum cylinders for cooling and heating are tabulated in Table 5.1. The general magnitude of these film coefficients was anticipated and was quite satisfactory, both from the flow cross section aspect when a comparison was made with respect to the tube diameter, since the larger tube provides higher velocity, or in equal flow where comparison is

Table 5.1. Film coefficient, h, Btu/hr ft^2 °F as related to size and media

	Tube diameter		
	1"	1.5"	2"
Heating	1170	1270	1380
Cooling	797	855	1170

made with respect to the medium since the viscosity is larger in cooling then in heating.

5.4 Magnitude of the generated heat during the experiment

The conduction equation (equation 2.3.6) which is used in this study for the computation of the thermal diffusivity is based on the assumption that no heat is generated in the system. We shall show that the generated heat in our system can be neglected compared with the rate of heat removed by conduction.

The possibility of generated heat arises in this study only in those cases where living biological materials are involved, specifically raw apple and potato flesh.

We shall assume that we are dealing with the straight line portion of the semi-logarithmic curve and as an example we shall compare the heat removed with the heat generated at the average-time temperature, i.e., 78.5° F for heating and 53.5° F for cooling.

Role of heat removed. The equation of the straight line of the semi-logarithmic curve is

$$\log (T_1 - T) = -\frac{t}{f} + \log [j (T_1 - T_0)] \tag{5.4.1}$$

by differentiating the temperature, T, with respect to time, t, we get:

$$\frac{dT}{T_1 - T} = -\frac{dt}{f}$$

$$\frac{dT}{dt} = -\frac{(T_1 - T)}{f} \tag{5.4.2}$$

Taking the f of an 1.5" stainless steel tube packed with apple flesh to be about 20 minutes, we find, using equation (5.4.2) that

$$\frac{dT}{dt} = \pm \frac{17.5}{20} = \pm .875° \text{ F/min}$$

In other words +.875° F/min and -.875° F/min are the rates evaluated in 78.5° F and 53.5° F for heating and cooling respectively.

Rate of heat generated. If we take the $q_{10°C}$ of an apple to be 2.5; the C_p = .85 Btu/lb °F as the respiration reference point at 60° F, we find the respiration rate at the average-time temperature of heating and cooling as follows:

$$q_{78.5° F} = q_{60° F} \times 2.5^{(78.5 - 60)/18} = 7750 \text{ Btu/day ton}$$

$$q_{53.5° F} = q_{60° F} \times 2.5^{(53.5 - 60)/18} = 2160 \text{ Btu/day ton}$$

From the above it can be seen that

$$\left(\frac{dT}{dt}\right)_{78.5°F} = \frac{7750}{24 \times 60 \times .85 \times 2000} = .00316° F/min$$

$$\left(\frac{dT}{dt}\right)_{53.5°F} = \frac{2160}{24 \times 60 \times .85 \times 2000} = .000882° F/min$$

Comparison of the rate of temperature change due to heat flow by conduction from the media with the rate of temperature change due to biological respiration, shows that the latter is by far smaller (.33% for heating and .1% for cooling) for the 1.5" tube. This contrast is even higher if the analysis is made using the 1" tube.

The small contribution of the heat of respiration at the average time justifies neglecting the heat of respiration throughout the test. In low N_{Bi} (such as cooling in low air velocity) in which the probable f is larger, or in systems exposed to respiration-favorable temperatures having a small temperature driving force the relative contribution of the heat of respiration will be much larger and probably should be taken into account.

In cases where the elapsed time since t = 0 until comparison is made is short, the necessity of taking into account more than one term in the general temperature distribution solution should be considered. The method and the significance of comparing the heat of respiration to the conductive heat transfer is mainly dependent on the values of j, Q_{10}, t and the actual temperature distribution at the time the comparison is made.

5.5 Magnitude of free convection

In all the experiments throughout this study we are assuming that by using or creating immobilized water in our system heat was flowing due to conduction heat transfer only. In cases where air spaces are involved it is necessary that we prove that the air spaces are small enough that natural convection can be neglected.

Briggs (1954) showed that if the product of the Grashof and Prandtl numbers is less than 600 in self-consistent units, convection will not occur.

$$\left(\frac{L^3 \rho^2 g \beta \Delta t}{\mu^2}\right)\left(\frac{C_p \mu}{k}\right) \leq 600 \tag{5.5.1}$$

In our system the most favorable conditions for convection in the air spaces, as far as the above criteria are concerned, will be:

1. On the surface. It is only at surface that our maximum Δt of 60° F can occur. This maximum value of Δt = 60° F at the surface occurs only in the starting of the experiment and decreases immediately.

2. During the cooling cycle (due to higher viscosity in cooling).

The maximum size of the air space which under the conditions stated above yields $N_{Gr} \leq 600$ can be calculated as follows:

$$\left(\frac{\rho^2 g \beta C_p}{\mu k}\right)_{\text{air at } T = 496°R} = 2 \times 10 \quad \frac{1}{ft^3 \, °F} \quad \text{(McAdams, 1954)}$$

$$2 \times 10^6 \times \Delta t \times L^3 \leq 600$$

$$2 \times 10^6 \times 60 \times L^3 \leq 600$$

$$L_{min} = .0171 \text{ ft} = 5.2 \text{ mm}$$

This minimum L of 5.2 mm is of course far larger than the air spaces in any of our experiments (see 5.6); it is interesting to note that in computation of the magnitude of natural convection in spaces containing sucrose solution (apple flesh), the maximum $N_{Gr} N_{Pr}$ taking the average cell size to be about 500 micron (Reeve, 1953) was found to be less than 100. Therefore, for the experimental conditions stated, as for this system, the convection heat transfer may be considered to be negligible.

5.6 Size of the air-foamed bubbles

Photographs of sections of a few of the air-sucrose solutions foam were made and two of them are shown in Figure 5.1. The size distribution of the bubbles was found as follows:

20% of the bubbles have a diameter smaller than .05 mm

15% of the bubbles have a diameter between .05 mm to .1 mm

50% of the bubbles have a diameter about .1 mm

15% of the bubbles have a diameter larger than .1 mm

The bubbles have a spherical shape and seemed randomly distributed. As noted in section 3.7 the size of the bubbles, as long as they are small and randomly distributed, should not affect the overall thermal properties of the system.

% sucrose 24, % air 8

% sucrose 8, % air 16

scale (mm) 0 1 2 3 4

Figure 5.1. Cross section of air-foamed sucrose solution gel.

6. RESULTS AND DISCUSSION

In this section we shall give the results of the experimental part of the study and its related discussion. The major computer program (program COND) was used for the computations of:

1. The predicted thermal conductivity, k_T, and the predicted thermal diffusivity, α_T, for all tests using equation (equation 3.7.5) developed for three dimensional homogeneous isotropic system.

2. The experimental thermal conductivity, k_E, and its standard deviation using the experimental data by solving and satisfying the root equation of the cylindrical transcendental equation. This experimental thermal conductivity, k_E, which is an unknown value, cannot be calculated directly from the equation (4.2.1) which relates its value to the experimental data. The equation $f \frac{k_E}{C_p \rho} / R^2 = \ln 10/\beta_1^2$ can only be solved simultaneously by trial and error with the transcendental equation $N_{Bi} = \frac{h R}{k_E} = \beta_1 \frac{J_1(\beta_1)}{J_0(\beta_1)}$. Those steps are shown in the block diagram (Figure 6.1). As it can be noted from Figure 6.1 the computation of a single experiment is terminated when the value of the assumed thermal conductivity, k_E, is within .1% of the thermal conductivity evaluated using the transcendental equation.

An expression was developed (equation 3.7.5) in this study where the overall thermal conductivity of a two-component three-dimensional homogeneous-isotropic dispersion system, k_E, is a function of the

Figure 6.1. Block diagram for the computation of the experimental thermal conductivity, k_E

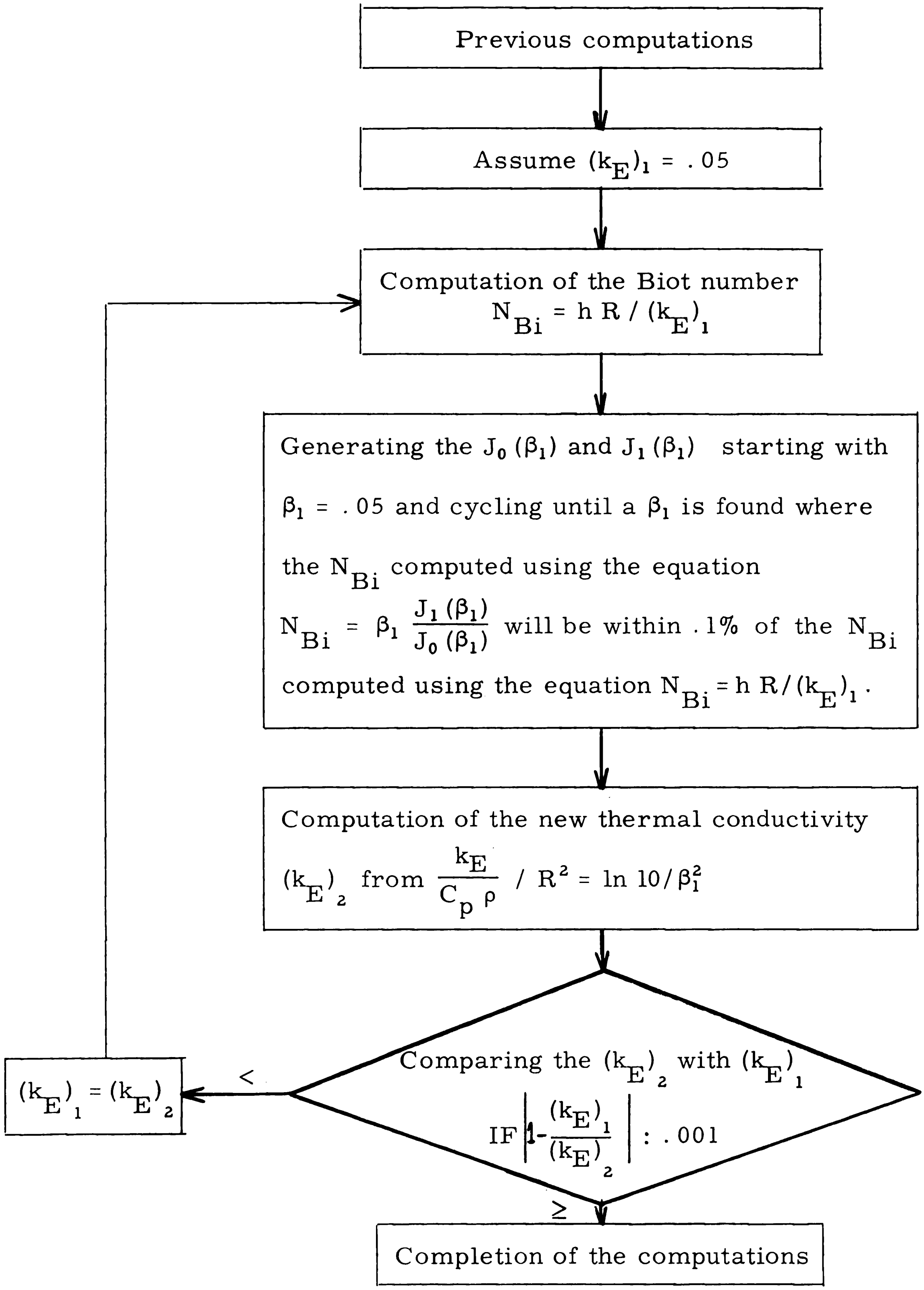

thermal properties of the single components and their respective concentrations. This expression developed in section 3.7 will hold for any two-component system, providing the system will fulfill the requirements posed in the above mentioned section. We think that the air-sucrose solutions foam system as well as the apple flesh evaluated in this study can be considered to be such a system, and we, therefore, shall in the following discussion check and compare the magnitude of the predicted thermal conductivity, k_T, calculated from equation (3.7.5) with that obtained from the experimental results with respect to various parameters. We propose that agreement between the magnitudes of the values calculated from the developed expression and these values obtained from the experimental data, evaluated from a few points of view, will prove that the basic assumptions used to develop the expression and the reasoning behind the development are in agreement. As long as the magnitudes of our comparisons are about the same, we should not be disturbed if the experimental results differ moderately from those obtained using the developed expression. If the values obtained in the several comparisons are of about the same magnitude, this agreement will take care of the most important part, the identity of the functional groups. A proportionality constant, if needed, will take care of any deviation of the results, if any.

Table 6.1 is the condensed input-output of program COND. It contains all the basic input information and most of the output results of this study.

Table 6.1. Input-output of the experimental data.

Test No.	Sample **	% Sugar w/w	Tube size	% air v/v	f min	N_{BI}	Media*	k_E $\frac{Btu}{hr\ ft°F}$	k_T $\frac{Btu}{hr\ ft°F}$	ST	α_E $\frac{ft}{hr^2}$	α_T $\frac{ft}{hr^2}$	j_c	Tj_c	SJ
40	SUCROSE	1.5	1.0	0.0	6.9	132	2	0.360	0.348	1.03416	0.00581	0.00562	1.050	1.602	0.6555
42	SUCROSE	1.5	1.5	0.0	15.8	218	2	0.358	0.348	1.02685	0.00577	0.00562	1.650	1.602	1.0300
44	SUCROSE	1.5	2.0	0.0	28.6	322	2	0.353	0.348	1.01377	0.00570	0.00562	1.633	1.602	1.0196
82	SUCROSE	1.5	1.0	5.0	7.1	143	2	0.332	0.330	1.00611	0.00564	0.00561	1.167	1.602	0.7284
84	SUCROSE	1.5	1.5	5.0	16.1	234	2	0.333	0.330	1.00934	0.00566	0.00561	1.583	1.602	0.9884
86	SUCROSE	1.5	2.0	5.0	29.5	350	2	0.325	0.330	0.98455	0.00552	0.00561	1.533	1.602	0.9572
100	SUCROSE	1.5	1.0	15.0	6.8	152	2	0.312	0.291	1.07314	0.00593	0.00553	1.667	1.602	1.0405
102	SUCROSE	1.5	1.5	15.0	15.9	259	2	0.302	0.291	1.03641	0.00573	0.00553	1.750	1.602	1.0924
104	SUCROSE	1.5	2.0	15.0	28.5	378	2	0.301	0.291	1.03381	0.00571	0.00553	1.667	1.602	1.0404
94	SUCROSE	1.5	1.0	20.0	7.3	175	2	0.271	0.271	1.00075	0.00547	0.00547	1.650	1.602	1.0301
96	SUCROSE	1.5	1.5	20.0	16.1	279	2	0.280	0.271	1.03344	0.00565	0.00547	1.717	1.602	1.0716
98	SUCROSE	1.5	2.0	20.0	28.5	401	2	0.283	0.271	1.04406	0.00571	0.00547	1.717	1.602	1.0716
88	SUCROSE	1.5	1.0	25.0	7.3	187	2	0.254	0.251	1.01140	0.00547	0.00541	1.550	1.602	0.9676
90	SUCROSE	1.5	1.5	25.0	16.4	303	2	0.258	0.251	1.02548	0.00555	0.00541	1.550	1.602	0.9676
92	SUCROSE	1.5	2.0	25.0	29.5	443	2	0.256	0.251	1.01965	0.00551	0.00541	1.600	1.602	0.9988
47	SUCROSE	8.0	1.0	0.0	7.1	138	2	0.345	0.336	1.02804	0.00565	0.00549	1.550	1.602	0.9677
49	SUCROSE	8.0	1.5	0.0	16.2	227	2	0.344	0.336	1.02470	0.00563	0.00549	1.667	1.602	1.0404
51	SUCROSE	8.0	2.0	0.0	29.3	334	2	0.340	0.336	1.01259	0.00556	0.00549	1.680	1.602	0.9988
113	SUCROSE	8.0	1.0	5.0	7.2	147	2	0.323	0.318	1.01500	0.00556	0.00548	1.617	1.602	1.0093
115	SUCROSE	8.0	1.5	5.0	16.5	243	2	0.321	0.318	1.00762	0.00552	0.00548	1.183	1.602	0.7387
117	SUCROSE	8.0	2.0	5.0	29.8	358	2	0.318	0.318	0.99733	0.00546	0.00548	1.633	1.602	1.0196
127	SUCROSE	8.0	1.0	16.0	7.2	167	2	0.285	0.277	1.03015	0.00555	0.00539	1.833	1.602	1.1445
129	SUCROSE	8.0	1.5	16.0	16.0	267	2	0.292	0.277	1.05551	0.00569	0.00539	1.550	1.602	0.9676
131	SUCROSE	8.0	2.0	16.0	29.2	397	2	0.286	0.277	1.03407	0.00557	0.00539	1.550	1.602	0.9676
121	SUCROSE	8.0	1.0	20.0	7.4	180	2	0.264	0.262	1.00960	0.00540	0.00535	1.667	1.602	1.0405
123	SUCROSE	8.0	1.5	20.0	16.5	289	2	0.270	0.262	1.03127	0.00551	0.00535	1.550	1.602	0.9676
125	SUCROSE	8.0	2.0	20.0	30.2	431	2	0.264	0.262	1.00757	0.00539	0.00535	1.650	1.602	1.0300
53	SUCROSE	16.0	1.0	0.0	7.3	143	2	0.332	0.321	1.03572	0.00553	0.00533	1.700	1.602	1.0613
55	SUCROSE	16.0	1.5	0.0	17.5	250	2	0.313	0.321	0.97562	0.00520	0.00533	1.533	1.602	0.9572
57	SUCROSE	16.0	2.0	0.0	29.7	345	2	0.330	0.321	1.02805	0.00548	0.00533	1.650	1.602	1.0300
136	SUCROSE	16.0	1.0	8.0	7.3	158	2	0.301	0.294	1.02566	0.00544	0.00531	1.167	1.602	0.7284
134	SUCROSE	16.0	1.5	8.0	16.9	262	2	0.298	0.294	1.01515	0.00539	0.00531	1.600	1.602	0.9988
133	SUCROSE	16.0	2.0	8.0	29.8	376	2	0.302	0.294	1.02946	0.00546	0.00531	1.617	1.602	1.0092
145	SUCROSE	16.0	1.0	20.0	7.4	183	2	0.260	0.250	1.03824	0.00540	0.00520	1.633	1.602	1.0197
147	SUCROSE	16.0	1.5	20.0	17.8	318	2	0.246	0.250	0.98266	0.00511	0.00520	1.583	1.602	0.9884
149	SUCROSE	16.0	2.0	20.0	30.8	447	2	0.254	0.250	1.01599	0.00528	0.00520	1.633	1.602	1.0196
139	SUCROSE	16.0	1.0	30.0	7.5	213	2	0.224	0.214	1.04593	0.00532	0.00508	1.733	1.602	1.0821
141	SUCROSE	16.0	1.5	30.0	17.1	349	2	0.224	0.214	1.04535	0.00531	0.00508	1.717	1.602	1.0716
143	SUCROSE	16.0	2.0	30.0	29.5	490	2	0.232	0.214	1.08425	0.00551	0.00508	1.667	1.602	1.0404
59	SUCROSE	24.0	1.0	0.0	7.6	153	2	0.311	0.306	1.01725	0.00527	0.00518	1.667	1.602	1.0405
61	SUCROSE	24.0	1.5	0.0	18.0	262	2	0.299	0.306	0.97707	0.00506	0.00518	1.517	1.602	0.9468
63	SUCROSE	24.0	2.0	0.0	30.4	359	2	0.316	0.306	1.03474	0.00536	0.00518	1.633	1.602	1.0196
151	SUCROSE	24.0	1.0	12.0	7.6	168	2	0.283	0.266	1.06249	0.00526	0.00495	1.583	1.602	0.9885
155	SUCROSE	24.0	1.5	12.0	18.0	287	2	0.272	0.266	1.02101	0.00505	0.00495	1.633	1.602	1.0196
153	SUCROSE	24.0	2.0	12.0	30.4	395	2	0.288	0.266	1.08148	0.00535	0.00495	1.667	1.602	1.0404
157	SUCROSE	24.0	1.0	27.0	7.8	209	2	0.228	0.214	1.06382	0.00511	0.00481	1.667	1.602	1.0405
159	SUCROSE	24.0	1.5	27.0	17.4	335	2	0.233	0.214	1.08676	0.00522	0.00481	1.667	1.602	1.0404
161	SUCROSE	24.0	2.0	27.0	31.2	489	2	0.232	0.214	1.08423	0.00521	0.00481	1.667	1.602	1.0404
41	SUCROSE	1.5	1.0	0.0	7.3	95	1	0.341	0.334	1.01973	0.00550	0.00540	1.117	1.601	0.6973
43	SUCROSE	1.5	1.5	0.0	17.2	160	1	0.330	0.334	0.98570	0.00532	0.00540	1.500	1.602	0.9364
45	SUCROSE	1.5	2.0	0.0	30.1	287	1	0.335	0.334	1.00299	0.00541	0.00540	1.550	1.602	0.9676
83	SUCROSE	1.5	1.0	5.0	7.4	101	1	0.320	0.317	1.01110	0.00545	0.00538	1.100	1.602	0.6868
85	SUCROSE	1.5	1.5	5.0	17.5	171	1	0.307	0.317	0.97016	0.00522	0.00538	1.467	1.602	0.9156
87	SUCROSE	1.5	2.0	5.0	31.3	314	1	0.306	0.317	0.96707	0.00521	0.00538	1.500	1.602	0.9364
101	SUCROSE	1.5	1.0	15.0	7.9	121	1	0.268	0.279	0.95815	0.00508	0.00531	1.500	1.602	0.9365
103	SUCROSE	1.5	1.5	15.0	17.7	194	1	0.272	0.279	0.97214	0.00516	0.00531	1.550	1.602	0.9676
105	SUCROSE	1.5	2.0	15.0	31.4	353	1	0.273	0.279	0.97763	0.00519	0.00531	1.500	1.602	0.9364
95	SUCROSE	1.5	1.0	20.0	8.2	134	1	0.242	0.260	0.93110	0.00489	0.00525	1.483	1.602	0.9261
97	SUCROSE	1.5	1.5	20.0	18.6	216	1	0.243	0.260	0.93355	0.00490	0.00525	1.500	1.602	0.9364
99	SUCROSE	1.5	2.0	20.0	33.4	399	1	0.242	0.260	0.92788	0.00487	0.00525	1.467	1.602	0.9156
89	SUCROSE	1.5	1.0	25.0	8.4	146	1	0.222	0.241	0.91809	0.00477	0.00519	1.333	1.602	0.8324
91	SUCROSE	1.5	1.5	25.0	19.3	240	1	0.219	0.241	0.90909	0.00472	0.00519	1.283	1.602	0.8011
93	SUCROSE	1.5	2.0	25.0	34.0	433	1	0.222	0.241	0.92147	0.00478	0.00519	1.433	1.602	0.8947
46	SUCROSE	8.0	1.0	0.0	7.6	100	1	0.324	0.323	1.00555	0.00530	0.00527	1.550	1.602	0.9678
48	SUCROSE	8.0	1.5	0.0	17.5	165	1	0.320	0.323	0.99113	0.00523	0.00527	1.583	1.602	0.9885
50	SUCROSE	8.0	2.0	0.0	30.6	294	1	0.326	0.323	1.01052	0.00533	0.00527	1.567	1.602	0.9780
114	SUCROSE	8.0	1.0	5.0	7.8	107	1	0.302	0.306	0.98685	0.00519	0.00526	1.500	1.602	0.9366
116	SUCROSE	8.0	1.5	5.0	16.9	167	1	0.314	0.306	1.02829	0.00541	0.00526	1.167	1.602	0.7283
118	SUCROSE	8.0	2.0	5.0	31.3	318	1	0.303	0.306	0.98954	0.00521	0.00526	1.550	1.602	0.9676
128	SUCROSE	8.0	1.0	16.0	8.1	127	1	0.255	0.266	0.95707	0.00495	0.00518	1.500	1.602	0.9365

Test No.	Sample **	% Sugar w/w	Tube size	% air v/v	f min	N_{Bi}	Media*	k_E $\frac{Btu}{hr\ ft°F}$	k_T $\frac{Btu}{hr\ ft°F}$	ST	α_E $\frac{ft}{hr^2}$	α_T $\frac{ft}{hr^2}$	J_c	TJ_c	SJ
136	SUCROSE	8.0	1.5	16.0	18.0	202	1	0.260	0.266	0.97940	0.00507	0.00518	1.417	1.602	0.8844
132	SUCROSE	8.0	2.0	16.0	33.0	380	1	0.253	0.266	0.95308	0.00493	0.00518	1.383	1.602	0.8635
122	SUCROSE	8.0	1.0	20.0	8.1	134	1	0.242	0.251	0.96414	0.00495	0.00513	1.500	1.602	0.9365
124	SUCROSE	8.0	1.5	20.0	18.5	218	1	0.241	0.251	0.95999	0.00493	0.00513	1.500	1.602	0.9364
126	SUCROSE	8.0	2.0	20.0	31.8	385	1	0.251	0.251	0.99703	0.00512	0.00513	1.500	1.602	0.9364
52	SUCROSE	16.0	1.0	0.0	7.9	106	1	0.306	0.308	0.99453	0.00510	0.00512	1.567	1.602	0.9782
54	SUCROSE	16.0	1.5	0.0	17.9	171	1	0.308	0.308	0.99961	0.00512	0.00512	1.583	1.602	0.9885
56	SUCROSE	16.0	2.0	0.0	31.7	312	1	0.309	0.308	1.00357	0.00514	0.00512	1.550	1.602	0.9676
137	SUCROSE	16.0	1.0	8.0	7.9	115	1	0.281	0.282	0.99822	0.00509	0.00510	1.267	1.602	0.7909
135	SUCROSE	16.0	1.5	8.0	18.3	190	1	0.277	0.282	0.98166	0.00500	0.00510	1.500	1.602	0.9364
138	SUCROSE	16.0	2.0	8.0	31.6	338	1	0.285	0.282	1.01150	0.00516	0.00510	1.533	1.602	0.9572
146	SUCROSE	16.0	1.0	20.0	7.9	133	1	0.244	0.240	1.01678	0.00508	0.00499	1.533	1.602	0.9573
148	SUCROSE	16.0	1.5	20.0	19.0	228	1	0.231	0.240	0.96093	0.00480	0.00499	1.633	1.602	1.0196
150	SUCROSE	16.0	2.0	20.0	31.5	388	1	0.249	0.240	1.03510	0.00517	0.00499	1.417	1.602	0.8843
140	SUCROSE	16.0	1.0	30.0	8.1	155	1	0.209	0.206	1.01814	0.00497	0.00488	1.483	1.602	0.9260
142	SUCROSE	16.0	1.5	30.0	19.4	266	1	0.198	0.206	0.96110	0.00469	0.00488	1.500	1.602	0.9364
144	SUCROSE	16.0	2.0	30.0	33.7	474	1	0.203	0.206	0.98985	0.00483	0.00488	1.517	1.602	0.9468
58	SUCROSE	24.0	1.0	0.0	7.9	108	1	0.301	0.294	1.02435	0.00509	0.00497	1.550	1.602	0.9678
60	SUCROSE	24.0	1.5	0.0	19.0	185	1	0.284	0.294	0.96673	0.00481	0.00497	1.667	1.602	1.0405
62	SUCROSE	24.0	2.0	0.0	32.4	324	1	0.297	0.294	1.01142	0.00503	0.00497	1.550	1.602	0.9676
152	SUCROSE	24.0	1.0	12.0	7.9	119	1	0.273	0.256	1.06937	0.00509	0.00475	1.467	1.602	0.9157
156	SUCROSE	24.0	1.5	12.0	19.0	204	1	0.258	0.256	1.00990	0.00480	0.00475	1.500	1.602	0.9364
154	SUCROSE	24.0	2.0	12.0	32.4	357	1	0.270	0.256	1.05702	0.00503	0.00475	1.467	1.602	0.9156
158	SUCROSE	24.0	1.0	27.0	8.6	155	1	0.209	0.206	1.01366	0.00468	0.00462	1.517	1.602	0.9469
160	SUCROSE	24.0	1.5	27.0	18.5	240	1	0.219	0.206	1.06376	0.00491	0.00462	1.550	1.602	0.9676
162	SUCROSE	24.0	2.0	27.0	34.4	457	1	0.211	0.206	1.02407	0.00473	0.00462	1.500	1.602	0.9364
3	POTATO R	18.4	1.0	0.0	7.3	144	2	0.330	0.316	1.04461	0.00553	0.00529	1.750	1.602	1.0926
6	POTATO R	18.4	1.5	0.0	16.5	237	2	0.330	0.316	1.04416	0.00552	0.00529	1.633	1.602	1.0196
1	POTATO R	18.4	2.0	0.0	30.8	359	2	0.317	0.316	1.00131	0.00530	0.00529	1.633	1.602	1.0196
21	AP.+AIR1	14.4	1.0	26.5	7.8	210	2	0.227	0.229	0.99285	0.00511	0.00515	1.650	1.602	1.0300
23	AP.+AIR1	14.4	1.5	26.5	18.8	364	2	0.214	0.229	0.93833	0.00483	0.00515	1.650	1.602	1.0300
30	AP.+AIR2	14.4	1.0	26.5	7.9	212	2	0.224	0.229	0.98142	0.00505	0.00515	1.500	1.602	0.9364
33	AP.+AIR2	14.4	1.5	26.5	19.4	376	2	0.208	0.229	0.90916	0.00468	0.00515	1.683	1.602	1.0508
25	AP.-AIR1	14.4	1.0	0.0	8.0	158	2	0.302	0.324	0.93264	0.00500	0.00536	1.633	1.602	1.0197
27	AP.-AIR1	14.4	1.5	0.0	16.9	240	2	0.326	0.324	1.00538	0.00539	0.00536	1.567	1.602	0.9780
35	AP.-AIR1	14.4	1.0	0.0	8.2	162	2	0.295	0.324	0.90962	0.00488	0.00536	1.650	1.602	1.0301
37	AP.-AIR1	14.4	1.5	0.0	17.5	249	2	0.314	0.324	0.97064	0.00520	0.00536	1.600	1.602	0.9988
600	AP.SAUCE	21.2	1.0	0.0	7.6	152	2	0.312	0.311	1.00420	0.00527	0.00524	1.633	1.602	1.0197
602	AP.SAUCE	21.2	1.5	0.0	17.8	257	2	0.304	0.311	0.97821	0.00513	0.00524	1.583	1.602	0.9884
604	AP.SAUCE	21.2	2.0	0.0	31.0	365	2	0.311	0.311	1.00156	0.00525	0.00524	1.533	1.602	0.9572
4	POTATO R	18.4	1.0	0.0	7.7	104	1	0.313	0.304	1.02954	0.00523	0.00508	1.583	1.602	0.9886
7	POTATO R	18.4	1.5	0.0	17.0	163	1	0.322	0.304	1.05918	0.00538	0.00508	1.583	1.602	0.9885
2	POTATO R	18.4	2.0	0.0	33.0	326	1	0.295	0.304	0.97207	0.00494	0.00508	1.383	1.602	0.8635
20	AP.+AIR1	14.4	1.0	26.5	9.3	170	1	0.191	0.220	0.86898	0.00430	0.00495	1.383	1.602	0.8636
22	AP.+AIR1	14.4	1.5	26.5	21.6	281	1	0.187	0.220	0.85176	0.00421	0.00495	1.500	1.602	0.9364
31	AP.+AIR2	14.4	1.0	26.5	8.8	161	1	0.202	0.220	0.91896	0.00455	0.00495	1.717	1.602	1.0717
32	AP.+AIR2	14.4	1.5	26.5	21.4	279	1	0.189	0.220	0.85978	0.00425	0.00495	1.500	1.602	0.9364
24	AP.-AIR1	14.4	1.0	0.0	7.9	105	1	0.308	0.311	0.98952	0.00510	0.00515	1.583	1.602	0.9886
26	AP.-AIR1	14.4	1.5	0.0	17.6	168	1	0.314	0.311	1.00885	0.00520	0.00515	1.500	1.602	0.9364
34	AP.-AIR1	14.4	1.0	0.0	8.4	112	1	0.289	0.311	0.92959	0.00479	0.00515	1.500	1.602	0.9366
36	AP.-AIR1	14.4	1.5	0.0	18.5	176	1	0.298	0.311	0.95922	0.00494	0.00515	1.633	1.602	1.0197
601	AP.SAUCE	21.2	1.0	0.0	7.8	107	1	0.304	0.299	1.01784	0.00513	0.00504	1.500	1.602	0.9366
603	AP.SAUCE	21.2	1.5	0.0	18.2	177	1	0.298	0.299	0.99679	0.00502	0.00504	1.533	1.602	0.9572
605	AP.SAUCE	21.2	2.0	0.0	31.4	313	1	0.308	0.299	1.03047	0.00519	0.00504	1.583	1.602	0.9884

* Media -- 1-cooling, 2-heating

** Sample

SUCROSE - Sugar matrix
POTATO R - Raw potato flesh
AP.+AIR 1 - Raw apple flesh experiment 1
AP.+AIR 2 - Raw apple flesh experiment 2
AP.-AIR 1 - Deaerated apple flesh of experiment 1
AP.-AIR 2 - Deaerated apple flesh of experiment 2
AP.SAUCE - Apple sauce

All the points appearing in the figures in this section are experimental points and their best fit (least square method) first degree polynomial appears in the form of solid lines. The broken lines are the results of the prediction equations.

Sucrose matrix

We would like to point out that although the developed expression in orthogonal coordinates (equation 3.7.5) is very close to the form of $k = b\ AIR + d$, its real form is of a second degree equation. Since the difference between the first degree form and the second degree, as obtained by the least squares method, was very small, we decided to present the developed expression in the form of a first degree equation, so comparison between its values and the experimental results (which are expressed in the first degree form) could be made on the basis of slope and intercept with the ordinate. In Figures 6.2, 6.3, 6.4 and 6.5 the experimental thermal conductivity, k_E (which is the average of the experimental thermal conductivity for the three sizes of the stainless steel tubings), and the predicted thermal conductivity, k_T (according to the developed expression, equation (3.7.5) are plotted, for cooling and heating, versus the amount of air for 1.5, 8, 16 and 24 percent sucrose respectively. A polynomial of the first degree, having the form $k = b$ $AIR + d$ (b and d are constants, AIR = percent air v/v), for all cases was calculated by the least square method. The constants for these

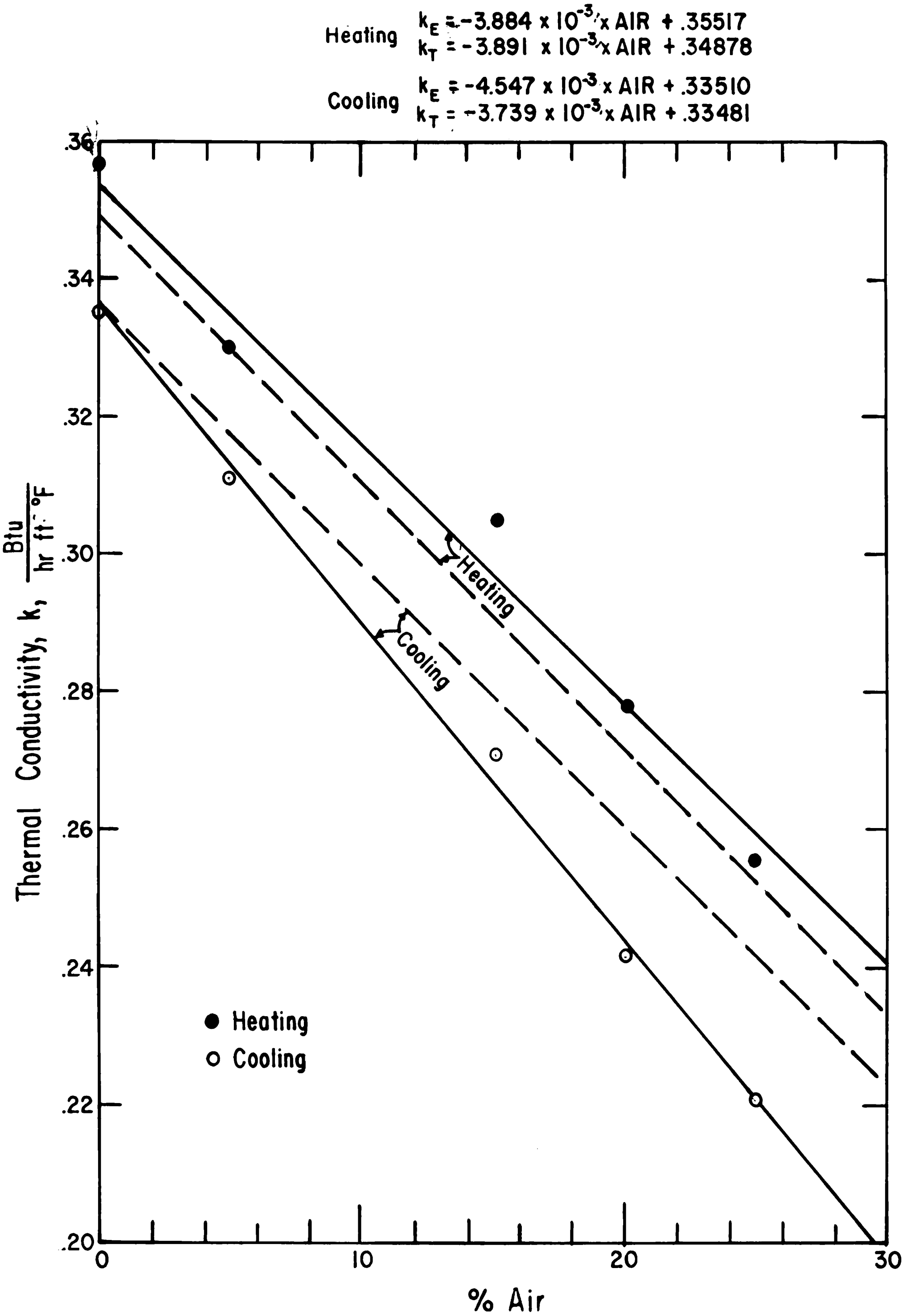

Figure 6.2. Experimental (data points and solid lines) and predicted (broken lines) thermal conductivity vs. percent air in heating and cooling of 1.5% sugar solution.

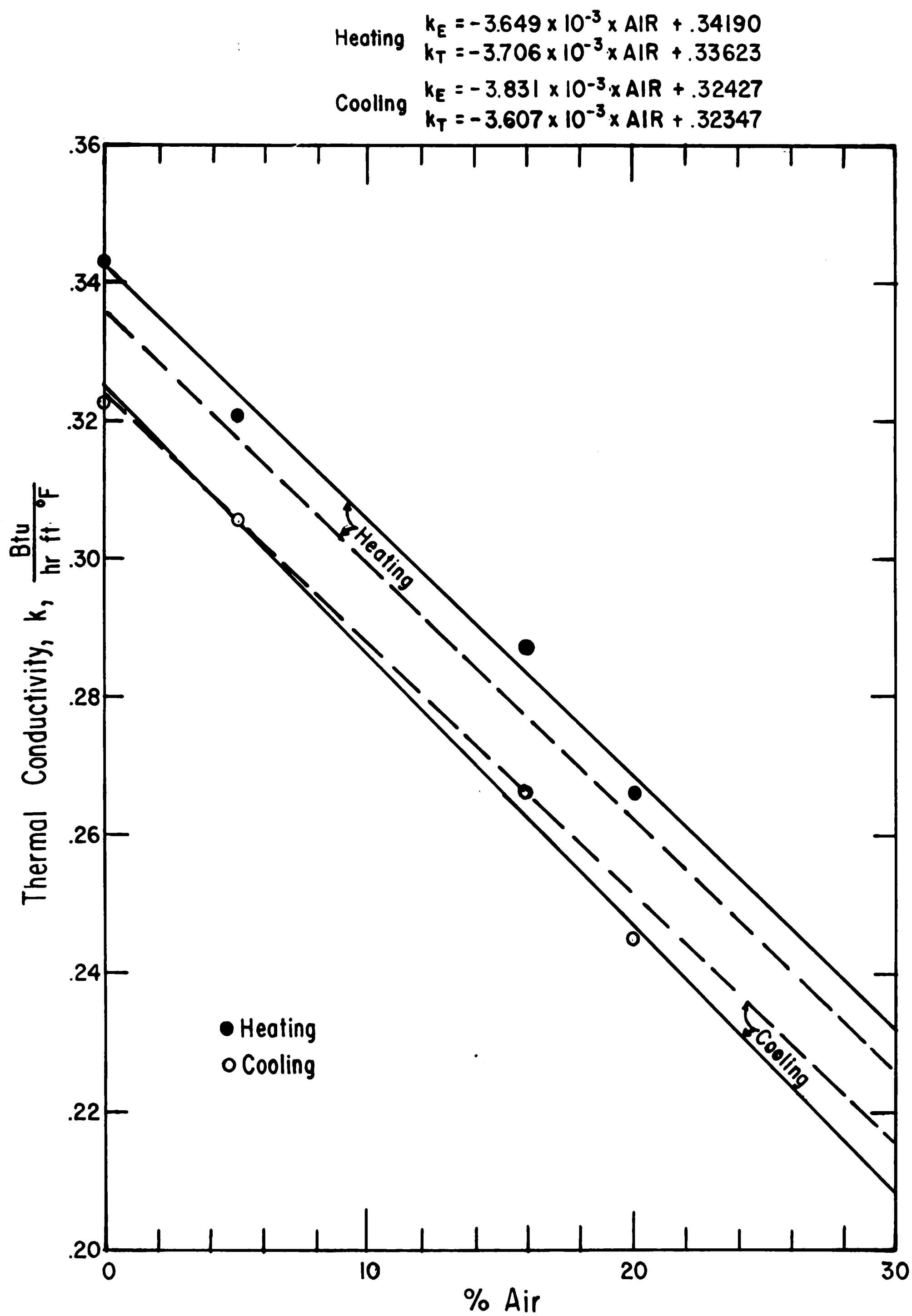

Figure 6. 3. Experimental (data points and solid lines) and predicted (broken lines) thermal conductivity vs. percent air in heating and cooling of 8% sugar solution.

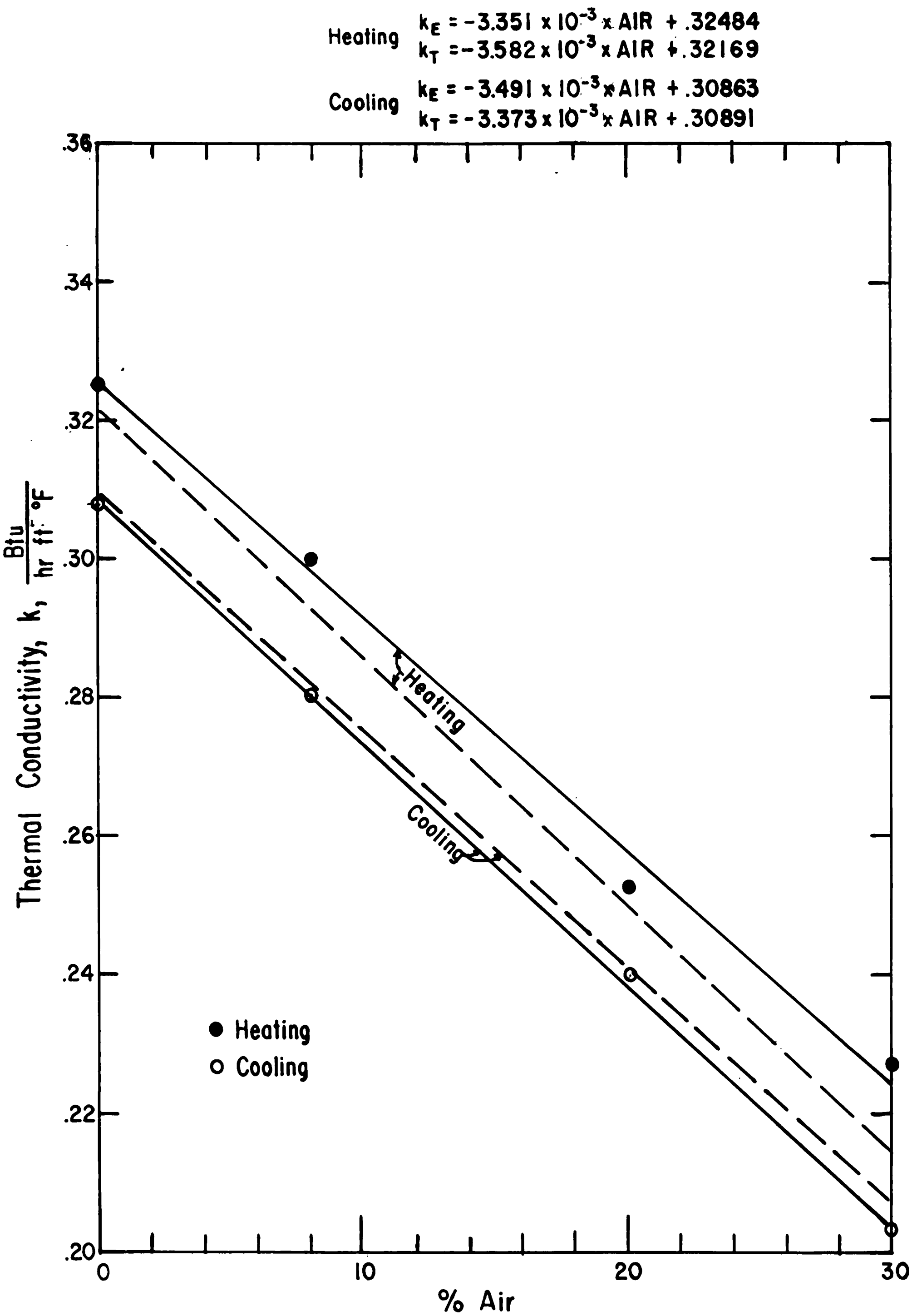

Figure 6. 4. Experimental (data points and solid lines) and predicted (broken lines) thermal conductivity vs. percent air in heating and cooling in 16% sugar solution.

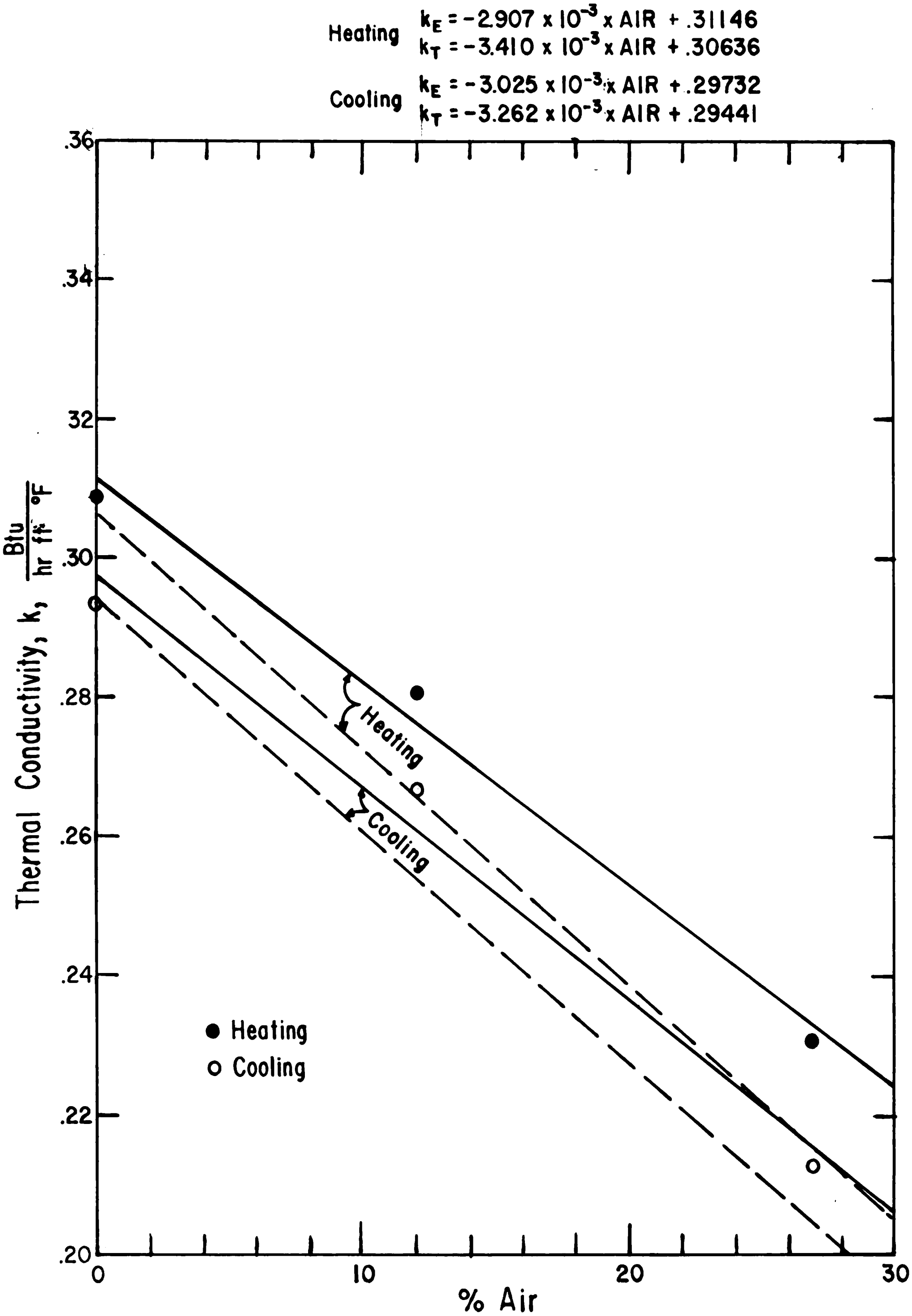

Figure 6.5. Experimental (data points and solid lines) and predicted (broken lines) thermal conductivity vs. percent air in heating and cooling of 24% sugar solution.

polynomials are tabulated in Table 6.2. By inspection of Figures 6.2, 6.3, 6.4, and 6.5, we can see that in all cases the cooling lines are lower than the respective heating lines. This is to be expected for both the theoretical and the experimental lines, since when $k_d \ll k_c$ the thermal conductivity of the two component system is dependent (see equation 3.7.6) in a linear fashion on the thermal conductivity of the continuous phase (the sucrose solution), k_L, which itself is proportional to the temperature.

In all the above mentioned figures (except for the 1.5 percent sugar case), the experimental line for cooling is more or less parallel (within 5%) to the respective experimental heating line. This parallel relationship between the experimental heating and cooling lines is satisfactory due to the fact that the change in the thermal property for the sugar system is almost linear with respect to temperature. Therefore, we can expect the lines for the experimental heating and cooling to have the same slope, but be shifted with respect to their intersection with the ordinate.

ST is the ratio between the experimental thermal conductivity, k_E, for each experiment and its predicted value, k_T, and SJ is the ratio between the experimental lag factor j_c for each experiment and its predicted value. The average values of ST and SJ and their standard deviations for the various experimental groups as computed from Table 6.1 are tabulated in Table 6.3.

Table 6.2. Coefficients of the equation of the thermal conductivity k_E and k_T with respect to air for various sucrose concentrations.

The equation has the form of k = b AIR + d

Sucrose concentration	Heating				Cooling			
	Experimental k_E		Predicted k_T		Experimental k_E		Predicted k_T	
	10^3 b	d	10^3 b	d	10^3 b	d	10^3 b	d
1.5	-3.844	.35517	-3.891	.34878	-4.547	.33510	-3.739	.33481
8.0	-3.649	.34190	-3.706	.33623	-3.831	.32427	-3.607	.32347
16.0	-3.351	.32484	-3.582	.32169	-3.491	.30863	-3.373	.30891
24.0	-2.907	.31146	-3.410	.30636	-3.025	.29732	-3.262	.29441

Table 6.3. The average ST = k_E/k_T and the average SJ = j_c/Tj_c and their standard deviation.

	ST = k_E/k_T		SJ = J_c/Tj_c	
	Average	Standard deviation	Average	Standard deviation
All the experiments	1.0003	.0450	.9641	.0852
Sucrose matrix--- heating experiments	1.0282	.0265	.9944	.0940
Sucrose matrix-- cooling experiment	.9894	.0369	.9250	.0757
All the experiments beside the sucrose matrix	.9690	.0548	.9811	.0506

From Table 6.3 it can be seen that the average ST for the sucrose matrix is slightly larger than 1 for heating, and slightly smaller than 1 for cooling. The average ST for the whole study is surprisingly 1.0004. The divergence of the average SJ from 1.0 and the standard deviation of the SJ are greater than those of the ST. This higher divergency of SJ should not be surprising since the errors in the measurement of the lag factor, j_c, are well known and are discussed in section (3.2). It is interesting to note from Table 6.1 that the theoretical lag factor, Tj_c, for all experiments has the same value of 1.602 which is an asymptotic value of high N_{Bi} system. This again shows the impossibility of using the lag factor, j_c, as a characteristic variable in a high N_{Bi} system, even if the possibilities for experimental error in its determination were eliminated.

Figure 6.6 shows the relationship in the sucrose matrix between the amount of air and w, where w is a dimensionless ratio between thermal conductivity of the foamed sucrose solution, k, and the thermal conductivity of the same sucrose solution having zero air, $(k)_{zero\ air}$, i.e. $w = k/(k)_{zero\ air}$. w has limits of $0 < w \leq 1$.

From Figure 6.6 we can see that the scattering of experimental points around the experimental least-square line is approximately proportional to the amount of air. This is quite expected since the greater the amount of air entrapped in the sample the more complicated the system and the larger are the probably discrepancies with respect to

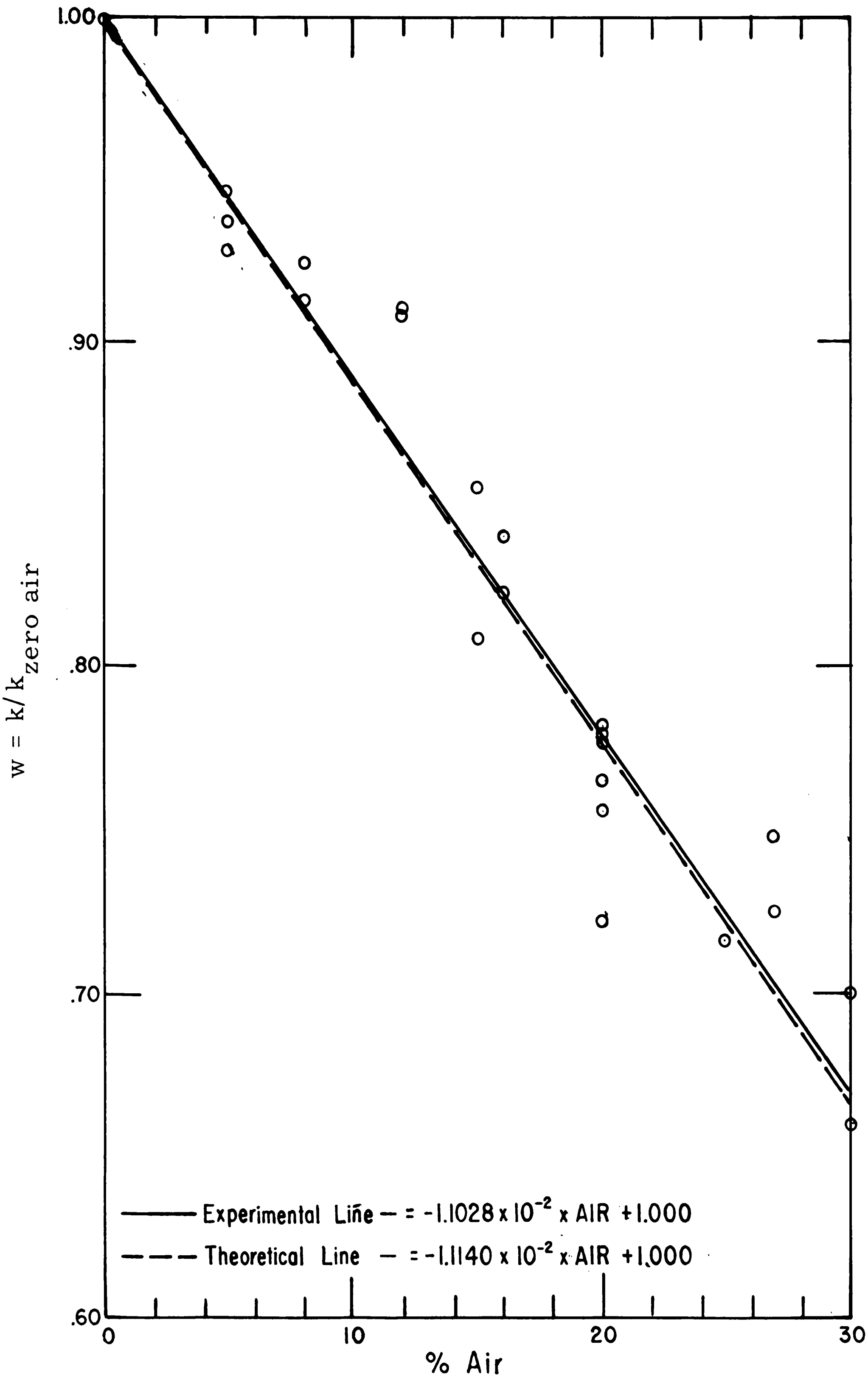

Figure 6.6. The ratio w vs. % air for all the sucrose matrix experiments.

air distribution and liquid phase continuity. However, we are very pleased and even surprised to see that the predicted line obtained by plotting the amount of air versus $k_T/(k_T)_{zero\ air}$ almost coincides with the experimental line. The equations of the lines are:

Experimental line	$k_E/(k_E)_{zero\ air} = -1.1028 \times 10^{-2}\ AIR + 1.000$	(6.1.1)
Predicted line	$k_T/(k_T)_{zero\ air} = -1.1140 \times 10^{-2}\ AIR + 1.000$	(6.1.1)

The experimental thermal conductivity, k_E, and the predicted thermal conductivity, k_T, of the air-sucrose solutions foam for both heating and cooling are plotted versus the amount of air in Figures 6.7 and 6.8. From these graphs and from the table of coefficients (Table 6.2) we observe that the slope b, of both the experimental lines and the predicted lines decreases when the sugar concentration increases. This common behavior of the predicted and the experimental lines is expected and more than welcome, so to speak: since as the sugar concentration increases the thermal conductivity of the continuous phase, k_L, decreases and since the thermal conductivity of the dispersed phase (air), k_A, is constant, the difference between k_L and k_A will be smaller and the thermal conductivity of the sucrose solution foam, k_E, ($k_L \geq k_E \geq k_A$) will be, therefore, less air-dependent (i.e. slope presented in k_E: AIR coordinates is smaller). The fact that the magnitude of change for both the experimental and the predicted lines is the same supports the validity

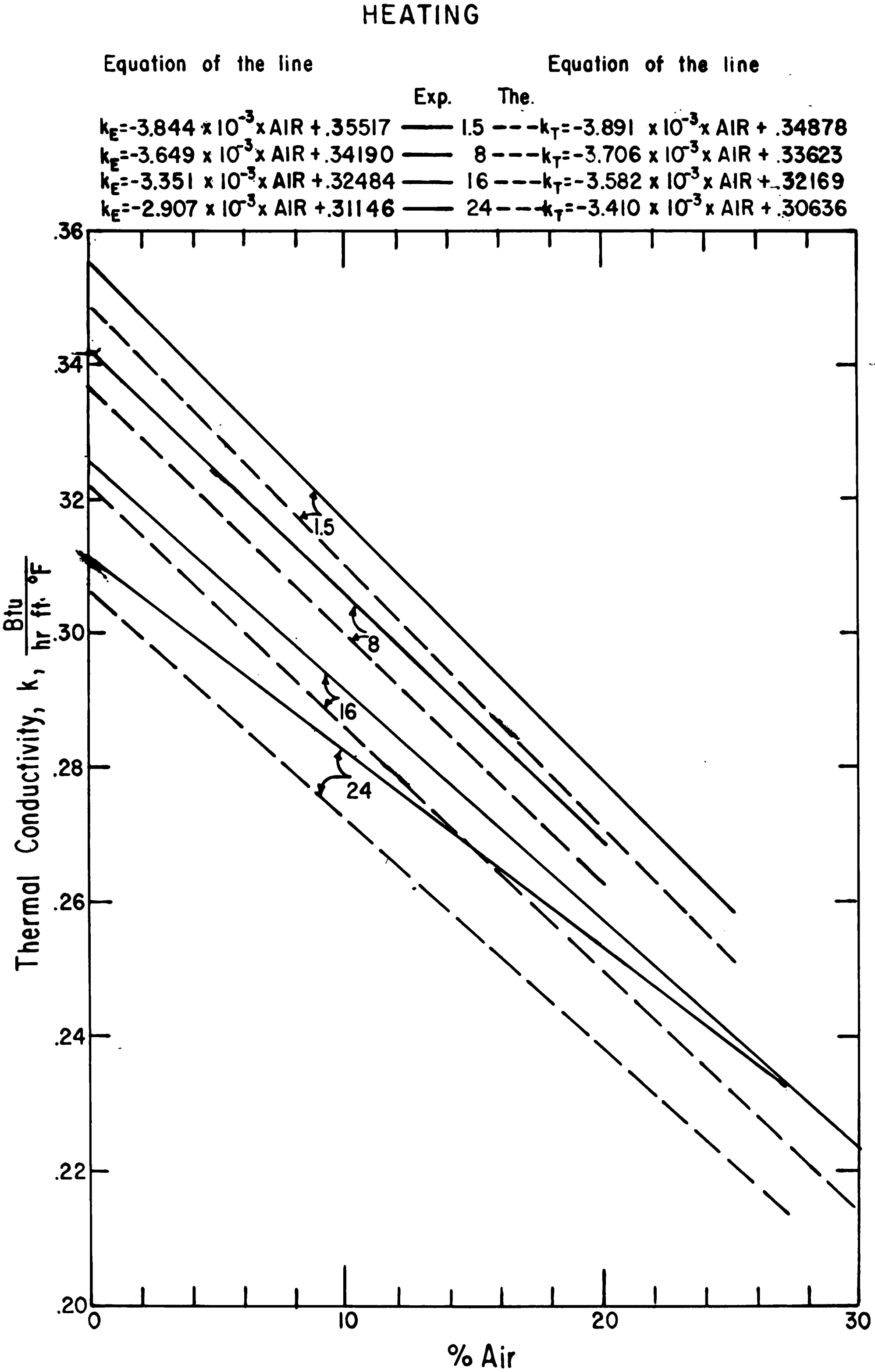

Figure 6.7. Summary of the heating results. Experimental (solid lines) and predicted (broken lines) thermal conductivity vs. percent air in heating.

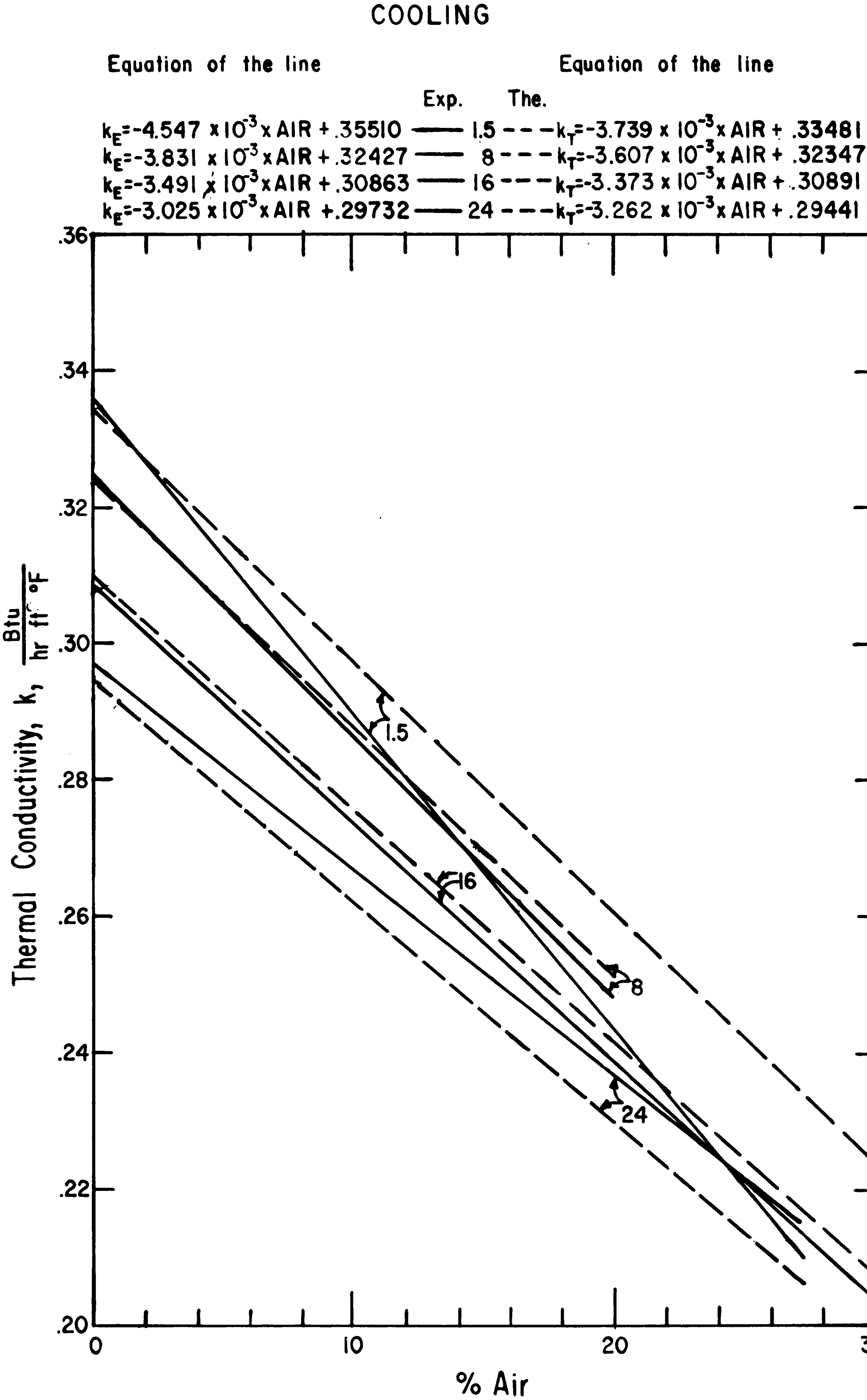

Figure 6.8. Summary of the cooling results. Experimental (solid lines) and predicted (broken lines) thermal conductivity vs. percent air in cooling.

of the equations developed for the two phase system. The value of the constant d is inversely proportional to the sucrose concentration; this is obvious since d, the intercept of the curve with the ordinate, is the thermal conductivity for zero air.

The functional group $\frac{f\alpha}{R^2}$ throughout our study approaches a constant value. It has been noted above that all the experiments were performed in a high N_{Bi} system (well over 100). In these N_{Bi} regions the $\frac{f\alpha}{R^2}$ becomes a constant and is different for each geometrical shape (see equation 3.5.1).

$$\frac{f\alpha}{R^2} = \text{constant}$$

$$\log f = 2 \log R + \text{constant} \tag{6.1.3}$$

or taken between limits

$$\log (f_1/f_2) = 2 \log (R_1/R_2) \tag{6.1.4}$$

or the slope of the straight line obtained when f is plotted vs. R on a log-log scale is constant (E = 2). Since each set of experiments consisted of three values of f and three values of R, we obtained three slopes, E_{1-2}, E_{2-3} and E_{1-3}. The slopes, E, for all the air-sucrose solutions foam matrix, their various average and standard deviations were computed and the computer output is presented in Table 6.4.

From Table 6.4 we can observe that the slope, E, is generally about 2. As a matter of fact, the average E for the heating matrix, cooling matrix, or the total matrix, is about 1.98-1.99. We would like

Table 6.4. The constant $E \sim 2$ for the sucrose matrix

Media*	Sample	% Sugar w/w	% Air v/v	f_1 min	f_2 min	f_3 min	log f_1	log f_2	log f_3	E_{1-2}	E_{2-3}	E_{1-3}	Average
2	SUCROSE	1.5	0.0	6.9	15.8	28.6	0.8388	1.1987	1.4564	2.0030	2.0340	2.0158	2.0176
2	SUCROSE	1.5	5.0	7.1	16.1	29.5	0.8513	1.2068	1.4698	1.9794	2.0757	2.0192	2.0248
2	SUCROSE	1.5	15.0	6.8	15.9	28.5	0.8293	1.2014	1.4548	2.0714	2.0004	2.0420	2.0379
2	SUCROSE	1.5	20.0	7.3	16.1	28.5	0.8633	1.2068	1.4548	1.9122	1.9575	1.9310	1.9336
2	SUCROSE	1.5	25.0	7.3	16.4	29.5	0.8633	1.2148	1.4698	1.9568	2.0124	1.9798	1.9830
2	SUCROSE	8.0	0.0	7.1	16.2	29.3	0.8513	1.2095	1.4669	1.9943	2.0312	2.0096	2.0117
2	SUCROSE	8.0	5.0	7.2	16.5	29.8	0.8573	1.2175	1.4742	2.0049	2.0263	2.0137	2.0150
2	SUCROSE	8.0	16.0	7.2	16.0	29.2	0.8573	1.2041	1.4654	1.9305	2.0620	1.9849	1.9925
2	SUCROSE	8.0	20.0	7.4	16.5	30.2	0.8692	1.2175	1.4800	1.9386	2.0720	1.9938	2.0015
2	SUCROSE	16.0	0.0	7.3	17.5	29.7	0.8603	1.2430	1.4728	2.1304	1.8131	1.9992	1.9809
2	SUCROSE	16.0	8.0	7.3	16.9	29.8	0.8663	1.2279	1.4742	2.0129	1.9442	1.9845	1.9805
2	SUCROSE	16.0	20.0	7.4	17.8	30.8	0.8692	1.2504	1.4886	2.1220	1.8795	2.0217	2.0077
2	SUCROSE	16.0	30.0	7.5	17.1	29.5	0.8751	1.2330	1.4698	1.9926	1.8692	1.9415	1.9344
2	SUCROSE	24.0	0.0	7.6	18.0	30.4	0.8808	1.2553	1.4829	2.0845	1.7964	1.9654	1.9488
2	SUCROSE	24.0	12.0	7.6	18.0	30.4	0.8808	1.2553	1.4829	2.0845	1.7964	1.9654	1.9488
2	SUCROSE	24.0	27.0	7.8	17.4	31.2	0.8921	1.2405	1.4942	1.9398	2.0016	1.9654	1.9689
1	SUCROSE	1.5	0.0	7.3	17.2	30.1	0.8651	1.2355	1.4790	2.0621	1.9216	2.0040	1.9959
1	SUCROSE	1.5	5.0	7.4	17.5	31.3	0.8692	1.2430	1.4955	2.0809	1.9929	2.0445	2.0395
1	SUCROSE	1.5	15.0	7.9	17.7	31.4	0.8976	1.2480	1.4969	1.9503	1.9649	1.9563	1.9572
1	SUCROSE	1.5	20.0	8.2	18.6	33.4	0.9138	1.2695	1.5237	1.9801	2.0066	1.9911	1.9926
1	SUCROSE	1.5	25.0	8.4	19.3	34.0	0.9243	1.2856	1.5315	2.0112	1.9410	1.9821	1.9781
1	SUCROSE	8.0	0.0	7.6	17.5	30.6	0.8808	1.2430	1.4857	2.0164	1.9154	1.9746	1.9688
1	SUCROSE	8.0	5.0	7.8	16.9	31.3	0.8893	1.2279	1.4955	1.8848	2.1125	1.9790	1.9921
1	SUCROSE	8.0	16.0	8.1	18.0	33.0	0.9085	1.2553	1.5185	1.9305	2.0777	1.9914	1.9998
1	SUCROSE	8.0	20.0	8.1	18.5	31.8	0.9085	1.2672	1.5024	1.9967	1.8568	1.9389	1.9308
1	SUCROSE	16.0	0.0	7.9	17.9	31.7	0.8976	1.2516	1.5011	1.9707	1.9686	1.9698	1.9697
1	SUCROSE	16.0	8.0	7.9	18.3	31.6	0.8976	1.2613	1.4997	2.0243	1.8818	1.9654	1.9571
1	SUCROSE	16.0	20.0	7.9	19.0	31.5	0.8976	1.2788	1.4983	2.1217	1.7329	1.9609	1.9385
1	SUCROSE	16.0	30.0	8.1	19.4	33.7	0.9058	1.2878	1.5270	2.1265	1.8878	2.0278	2.0140
1	SUCROSE	24.0	0.0	7.9	19.0	32.4	0.8976	1.2788	1.5105	2.1217	1.8294	2.0008	1.9840
1	SUCROSE	24.0	12.0	7.9	19.0	32.4	0.8976	1.2788	1.5105	2.1217	1.8294	2.0008	1.9840
1	SUCROSE	24.0	27.0	8.6	18.5	34.4	0.9320	1.2683	1.5366	1.8725	2.1169	1.9736	1.9877

The average E value for all the sucrose matrix $E = 1.98367 \pm 0.02928$

The average E value for the heating sucrose matrix $E = 1.98672 \pm 0.03161$

The average E value for the cooling sucrose matrix $E = 1.98061 \pm 0.02640$

* Media -- 1-cooling, 2-heating

to point out that the value of E should be just below 2, because E approaches 2 from below as $N_{Bi} \rightarrow \infty$.

Carbohydrate sample

The carbohydrate type products which were examined in this system were raw potato flesh, raw apple flesh and apple sauce. The experimental data associated with these experiments are tabulated in the main input-output table (Table 6.1). In Figure 6.9 the experimental thermal conductivity, k_E, for each case (each point on the figure represents the average value for the various cylinder sizes) is plotted versus the predicted thermal conductivity, k_E, using equation (3.7.5).

From Figure 6.9 we can see that the experimental thermal conductivity, k_E, of the apple sauce and the raw potato are about the same as their respective predicted thermal conductivity, k_T. As far as the apple flesh is concerned the experimental thermal conductivity, k_E, was lower than the predicted values. One of the major probable reasons for this discrepancy is the inaccuracy of the diameter of the apple flesh with respect to the stainless steel tube. From this standpoint, both the air-sucrose solutions foam and the apple sauce have the most accurate shape because they take the shape of the tube when they are poured; whereas, the rigid plugs of apple flesh did not conform exactly to the shape of the tube.

It is interesting to see from Figure 6.9 the increase in the thermal

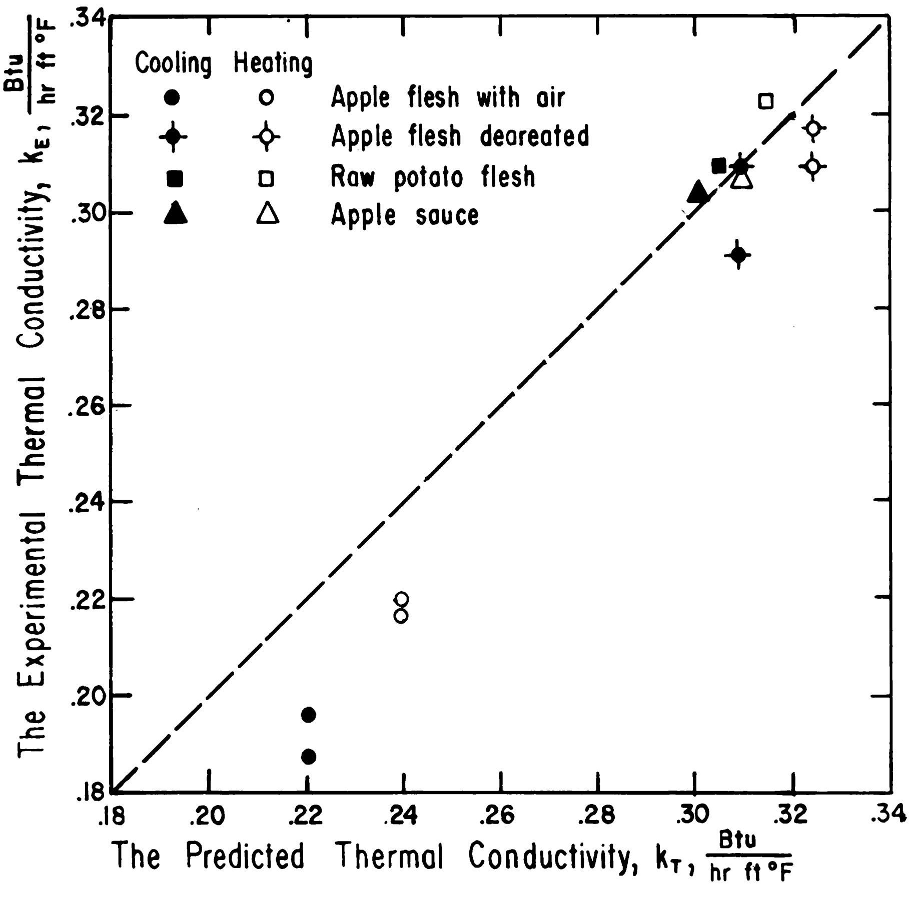

Figure 6.9. The predicted thermal conductivity, k_T, vs. the experimental thermal conductivity, k_E, for the carbohydrates type products.

conductivity of the raw apple flesh after the air was deaerated and replaced by liquid. This increase was expected from our theoretical equation which takes into account the thermal properties of the individual phases and the percentage of air. The determination and comparison of the thermal conductivity of the raw apple flesh to the deaerated product demonstrates again that the thermal conductivity of raw apple flesh cannot be approximated (as was done in the past by a few researchers) by using Anderson approach (equation 6.1.5). The Anderson's equation says that the thermal conductivity of a carbohydrate type fruit is the same as the thermal conductivity of a sucrose solution having the same percent of carbohydrates as the fruit. The Anderson thermal conductivity prediction equation agrees with sucrose solution data of Riedel (1951), and presumably agrees with data on other foodstuffs not containing air. Since as much as 25% of the apple volume may be intercellular spaces the Anderson equation is not applicable. Calculation of the thermal conductivity of our apple according to the Anderson approach will approximate the thermal conductivity of an apple, if the air is replaced with liquid having the same concentration of carbohydrates as the apple juice.

$$k = (\%\ \text{moisture}/100)\,k_w + .15\,(100 - \%\ \text{moisture})/100 \qquad (6.1.5)$$

It is worthwhile mentioning that one of the basic results of the development of an overall thermal conductivity of the two-component homogeneous isotropic system is that as long as the dispersed particles are randomly dispersed and small enough in comparison to the whole unit, they do not necessarily have to be of a single geometry nor of a single size. If the dispersed particles are small and randomly distributed, the area void fraction for any cross section of the system will be the same. This means that the thermal conductivity of the two-component system is a function of the thermal conductivities of the individual components and the volumetric void fraction only, and independent of the size or the shape of the particles in the dispersed phase. The air-sucrose solutions foam are systems where the dispersed phase (air) is found in various sizes of one single shape (sphere). The spherical particles are quite small (see section 5.6) which not only satisfies the requirements for elimination of free convection (see section 5.5), and having a small ratio between the individual particle size and the system size, but increases indirectly (by having more dispersal particles) the chances of the particle being randomly distributed. In the case of the apple flesh the air is dispersed to form intercellular channels having sizes of .3 mm up to 1 mm (Reeve, 1954). The air channel size in the apple flesh, as in the case of the air-sucrose solutions foam, obviously fulfill the basic requirements with respect to size and random distribution. It is interesting to note that the air channels in the apple flesh are not closed type cells (as in the case of air-sucrose solutions foam) but are inter-connected to one another

(otherwise deaeration would not be possible!).

It has been mentioned that the experimental system was designed to have a large N_{Bi}, so that the $d\alpha / dN_{Bi}$ or its equivalent dk_E / dN_{Bi} would be as small as possible. By using the modified program COND we computed the projected change of the experimental thermal conductivity, k_E, should the film coefficient change. In other words what was the $\frac{\Delta k_E}{\Delta h}$ of our system? Two examples were computed and the results are shown in Table 6.5 where the new thermal conductivity of the reference point $(k_E)_{RV}$ were tabulated vs the percent change in the film coefficient with respect to the actual experiment condition. From Table 6.5 we can see that the film coefficient in our system is so high that even if a change would occur which will cause the film coefficient to be reduced by 50% or to be doubled its assumed value (evaluated from the copper and aluminum cylinders), the error in such extrame changes (which are very unlikely to happen) in the determination of the experimental thermal conductivity, k_E, will not exceed .4%. Practically we can say that in our system $\frac{\Delta k_E}{\Delta h} \approx 0$. (See also 3.4, 3.5.)

Beef lean meat

A few experiments were done with raw meat. The average thermal conductivity and diffusivity for the three tubing diameters are tabulated in Table 6.6. The specific heat of the raw meat used in the computation of the thermal conductivity from the thermal diffusivity

Table 6.5. The influence of changing the film coefficient h on the experimental thermal conductivity, k_E

	$100 \frac{h}{h_{RV^*}}$	h $\frac{BTU}{hr\ ft^2\ °F}$	β_1	N_{Bi}	α_E $\frac{ft}{hr^2}$	k_E $\frac{BTU}{hr\ ft\ °F}$	$\frac{k_E}{(k_E)_{RV^*}}$
Test No. 40							
	40,00	468,00	2,358717	51,62	0,0059517	0.368705	1,024015
	50.00	585.00	2,368177	65,09	0,0059043	0.365497	1,015107
	60.00	702.00	2,374394	78,50	0,0058734	0.363673	1,010041
	70.00	819,00	2,378808	91,91	0,0058516	0.362377	1,006441
	80,00	936.00	2,382104	105,32	0,0058354	0.361408	1,003751
	90,00	1053,00	2,384659	118,74	0,0058229	0.360657	1,001665
	100,00	1170,00	2,386697	132,15	0,0058130	0.360058	1,000000
	110,00	1287,00	2,388362	145,56	0,0058049	0.359568	0,998641
	120,00	1404,00	2,389746	158,97	0,0057982	0.359161	0,997509
	130,00	1521,00	2,390916	172,39	0,0057925	0.358817	0,996553
	140,00	1638,00	2,391917	185,80	0,0057877	0.358522	0,995735
	150,00	1755,00	2,392784	199,22	0,0057835	0.358267	0,995026
	160,00	1872,00	2,393542	212,64	0,0057798	0.358044	0,994406
	170,00	1989,00	2,394210	226,05	0,0057766	0,357847	0,993861
	180,00	2106,00	2,394803	239,46	0,0057737	0.357673	0,993375
	190,00	2223.00	2,395334	252,88	0,0057712	0.357516	0,992941
	200,00	2340.00	2,395811	266,29	0,0057689	0.357376	0,992551
	210,00	2457,00	2,396242	279,69	0,0057668	0.357248	0,992197
	220,00	2574,00	2,396634	293,10	0,0057649	0.357133	0,991877
	230,00	2691.00	2,396992	306,52	0,0057632	0.357028	0,991584
	240,00	2808.00	2,397320	319,94	0,0057616	0.356931	0,991316
	250,00	2925.00	2.397622	333,38	0.0057601	0.356842	0,991070
Test No. 154							
	40,00	468.00	2,387881	141,42	0,0050693	0.272481	1,008433
	50,00	585,00	2.391297	177,26	0,0050548	0.271719	1,005611
	60.00	702.00	2,393568	213,13	0.0050452	0.271212	1,003737
	70,00	819.00	2,395185	248,97	0,0050384	0.270851	1,002400
	80,00	936,00	2,396396	284,81	0.0050333	0.270581	1,001399
	90,00	1053,00	2,397337	320,67	0,0050294	0.270370	1,000622
	100,00	1170,00	2,398089	356,53	0,0050262	0.270202	1,000000
	110,00	1287,00	2,398704	392,40	0,0050237	0.270065	0,999492
	120,00	1404,00	2,399216	428,27	0,0050215	0.269951	0,999069
	130,00	1521,00	2,399649	464,15	0,0050197	0.269854	0,998711
	140,00	1638,00	2,400019	499,92	0,0050182	0.269771	0,998405
	150,00	1755,00	2,400341	535,86	0,0050168	0.269700	0,998139
	160,00	1872,00	2,400622	571,73	0,0050156	0.269637	0,997907
	170,00	1989,00	2,400870	607.61	0.0050146	0.269582	0,997702
	180,00	2106,00	2,401090	643.44	0,0050137	0.269532	0,997520
	190,00	2223,00	2,401287	679,30	0,0050129	0.269488	0,997357
	200,00	2340,00	2,401464	715.10	0,0050121	0.269449	0,997210
	210,00	2457,00	2,401624	750,87	0,0050114	0.269413	0,997078
	220,00	2574,00	2,401770	786,79	0,0050108	0.269380	0,996957
	230,00	2691,00	2,401903	822,63	0.0050103	0.269351	0,996847
	240,00	2808,00	2,402025	858,50	0.0050098	0.269323	0,996746
	250,00	2925,00	2,402137	894,30	0,0050093	0.269298	0,996654

*Reference value corresponds to the actual experiment conditions

Table 6.6. The thermal diffusivity, the thermal conductivity and the j value for the raw meat flesh

Heat flow in respect to grains	Media	Average thermal diffusivity ft^2/hr	Average thermal conductivity Btu/hr ft °F	Average j_c	SJ = j_c/Tj_c
Perpendicular	Heating	.00361	.200	1.47	.863
Perpendicular	Cooling	.00404	.223	1.48	.913
Parallel	Heating	.00454	.251	1.56	.974
Parallel	Cooling	.00490	.271	1.55	.970

was taken arbitrarily from the literature to be .82 Btu/lb °F. The specific gravity for the raw meat was experimentally found to be 1.08.

It is difficult to evaluate the thermal properties of raw meat in a temperature range above the freezing point. The problems involved start with the difficulty of obtaining the needed accurate shape, loss of liquid and other problems yield unpredictable discrepancies in the results due to the fact that raw meat above the freezing point is a relatively soft nonhomogeneous material. These are probably the reasons why the thermal properties of raw meat in most cases have been evaluated for the temperature range below the freezing point.

The main purpose of the raw meat experiments was to get some idea of the thermal properties and to understand the system and the problems involved. We would like to point out again that in this study the thermal diffusivity was found directly from the experimental data and the thermal conductivity was evaluated by picking an arbitrary value (from the literature) for the specific heat. The parameters in the lean meat test were cooling and heating; heat flow in the direction parallel and perpendicular to the meat grain. The values of the thermal conductivity, the thermal diffusivity and j_c of the lean meat tests are tabulated in Table 6.6. From Table 6.6 we can observe that there is no appreciable difference between the thermal conductivity for heating or cooling in the respective raw material.

Before going further we would like to point out that our so-called "heat flow parallel to the meat fibers" is far from being parallel. The reason for this is that the heat flow in our system is radial heat flow. The meat fibers in order to be considered parallel to heat flow should be arranged in radial form, i.e. the fibers will represent the radii - like sun rays. This situation does not occur in meat, and as the fiber arrangement can be assumed to be parallel in rectangular coordinates, we actually find that the direction of the fibers with respect to the heat flow varies from being completely perpendicular to completely parallel. The value of the thermal conductivity, in the so-called perpendicular direction will be, obviously, some value between the value of the thermal conductivity in the parallel direction and the value of the thermal conductivity in the perpendicular direction.

From Table 6.6 we can see that the thermal conductivity when the heat flow was parallel to the meat fibers is larger for both cooling and heating than the thermal conductivity in the so-called perpendicular direction. The phenomena of meat flesh having a higher thermal conductivity in the direction parallel to the fibers than in the perpendicular direction was observed before by a few researchers, among them Lentz (1961) and Miller (1963). We would like to point out that the analysis we have made in section 3.7 shows that in the fibrous (or layered) homogeneous system the thermal conductivity in the direction parallel to the fibers is always larger than the thermal conductivity in the direction perpendicular to the fibers. We were quite satisfied that both the extensive experimental investigations of Lentz (1961) and Miller (1963) with respect to the thermal conductivity of meat and the few results that we have obtained in this study confirm the analysis.

7. SUMMARY

The study consisted of two phases, a laboratory study followed by a theoretical study. The conclusions reached in this study are as follows:

1) By dimensional analysis we showed that: $\frac{f\,\alpha}{R^2} = \lambda\, N_{Bi}^{\eta}$ and from the exact solution that for high and low N_{Bi} λ and η approach constant values.

2) The evaluation of the film coefficient h should be carried out in a system where the N_{Bi} is small as possible. When $N_{Bi} > 10$, h is very sensitive to changes or errors in either the physical or geometric properties of the overall system. On the other hand evaluation of the thermal diffusivity, α, should be done in a system with a high N_{Bi} so that the root value β_1 is insensitive to N_{Bi} (or h).

3) In the high N_{Bi} system f is independent of N_{Bi} (or h), and is proportional to $C_p\, \rho / k$ (reciprocal of the thermal diffusivity) and R^2. In low N_{Bi} system, the f is inversely proportional to N_{Bi} (or h) but directly proportional to $C_p\, \rho$ (heat capacity) and R.

4) The ratio between f values of a sphere to an infinite cylinder to an infinite slab is 1: 1.5-1.7 : 3-4 respectively (the low ratio values are for the high N_{Bi} systems and the large ratio values are for the low N_{Bi} systems).

5) The mass-average temperature can be expressed as a function of the temperature at the geometric center $T_m = T_1 - K(T_1 - T_c)$, where $K = j_m / j_c$.

6) The overall thermal conductivity of three dimensional homogeneous isotropic system, two dimensional anisotropic fibrous system and one dimensional anisotropic layered system was expressed as a function of the thermal conductivity of the individual components and the relative proportion of the components.

7) The thermal conductivity of a homogeneous fibrous (or layered) system is always larger in the direction parallel to the fibers (or layers) rather than in the direction perpendicular to the fibers (or layers). In fact, in such systems, the maximum and minimum overall system thermal conductivity will be in the direction parallel and perpendicular to the fibers (or layers) respectively.

8) In the layered system the ratio between the thermal conductivity in the direction parallel to the layers to the thermal conductivity in the direction perpendicular to the layers with respect to the void fraction, P, will reach a maximum value when $P = .5$.

9) The experimental thermal conductivity of an air-sucrose solutions foam agreed with the values and particularly with the various magnitudes of the predicted expression for the two-component three-dimensional dispersion system. This prediction equation for the overall system thermal conductivity of the two-component three-dimensional homogeneous-isotropic system as a function of the thermal conductivities of the single components and their proportion, should hold for many other systems such as butter (water dispersed in fat), ice cream, or insulation materials.

APPENDIX 1

Transient heat conduction in infinite slab (see 2. 3)

$$\frac{(T - T_1)}{(T_0 - T_1)} = \sum_{i=1}^{\infty} \frac{2 \sin \beta_i}{\beta_i + \sin \beta_i \cos \beta_i} \cos \left(\beta_i \frac{r}{R}\right) e^{-\frac{\beta_i^2 \alpha t}{R^2}} \qquad (A.1)$$

root equation: $N_{Bi} = \beta_i \tan \beta_i$ (A.2)

1st term approximation:

$$\log \frac{(T - T_1)}{(T_0 - T_1)} = \frac{-\beta_1^2 \alpha t}{(\ln 10) R^2} + \log \left[\left(\frac{2 \sin \beta_1}{\beta_1 + \sin \beta_1 \cos \beta_1} \right) \cos \left(\beta_1 \frac{r}{R}\right) \right] \qquad (A.3)$$

$$j = \frac{2 \sin \beta_1}{\beta_1 + \sin \beta_1 \cos \beta_1} \cos \left(\beta_1 \frac{r}{R}\right) \qquad \frac{f \alpha}{R^2} = \frac{\ln 10}{\beta_1^2}$$

$$j_c = \frac{2 \sin \beta_1}{\beta_1 + \sin \beta_1 \cos \beta_1} \qquad (A.4)$$

$$j_m = \frac{2 \sin^2 \beta_1}{\beta_1 (\beta_1 + \sin \beta_1 \cos \beta_1)} = j_c \left(\frac{\sin \beta_1}{\beta_1} \right) \qquad (A.5)$$

$$j_s = \frac{2 \sin^2 \beta_1}{\beta_1 + \sin \beta_1 \cos \beta_1} \cos \beta_1 = j_c \cos \beta_1 \qquad (A.6)$$

Table A. 1. Numerical solution for infinite slab (equation A.3).

β_1	N_{Bi}	$f\alpha/R^2$	j_c	j_m	j_s
0.000	0.00000	∞	1.000000	1.000000	1.000000
0.020	0.00040	5756.46273	1.000067	1.000000	0.999867
0.030	0.00090	2558.42788	1.000150	1.000000	0.999700
0.040	0.00160	1439.11568	1.000267	1.000000	0.999467
0.050	0.00250	921.03404	1.000417	1.000000	0.999166
0.070	0.00491	469.91533	1.000817	0.999999	0.998366
0.090	0.00812	284.26976	1.001350	0.999999	0.997297
0.110	0.01215	190.29629	1.002016	0.999997	0.995960
0.130	0.01700	136.24764	1.002816	0.999994	0.994354
0.150	0.02267	102.33712	1.003749	0.999989	0.992478
0.220	0.04920	47.57407	1.008059	0.999947	0.983763
0.290	0.08654	27.37913	1.013993	0.999840	0.971653
0.360	0.13551	17.76686	1.021540	0.999618	0.956056
0.430	0.19721	12.45314	1.030683	0.999213	0.936856
0.500	0.27315	9.21034	1.041397	0.998545	0.913912
0.570	0.36535	7.08706	1.053643	0.997508	0.887063
0.600	0.41048	6.39607	1.059347	0.996921	0.874317
0.720	0.63149	4.44172	1.084756	0.993432	0.815526
0.840	0.93713	3.26330	1.113883	0.987435	0.743476
0.960	1.37122	2.49846	1.145865	0.977794	0.657176
1.080	2.02091	1.97410	1.179331	0.963074	0.555852
1.200	3.08658	1.59902	1.212226	0.941535	0.439259
1.320	5.15242	1.32150	1.241615	0.911190	0.308138
1.340	5.70253	1.28235	1.245911	0.905131	0.285006
1.380	7.14486	1.20909	1.253804	0.892067	0.237772
1.420	9.34519	1.14193	1.260617	0.877684	0.189377
1.460	13.12337	1.08021	1.266162	0.861916	0.139999
1.500	21.15213	1.02337	1.270241	0.844706	0.089853
1.540	49.99015	0.97090	1.272652	0.826005	0.039187
1.550	74.52165	0.95841	1.272969	0.821093	0.026471
1.554	92.51153	0.95348	1.273063	0.819101	0.021382
1.558	121.74704	0.94859	1.273136	0.817094	0.016291
1.562	177.56954	0.94374	1.273191	0.815071	0.011199
1.566	326.49735	0.93893	1.273225	0.813033	0.006107
1.570	1971.55200	0.93415	1.273239	0.810980	0.001014
$\pi/2$	∞	$4 \ln 10/\pi^2$	$4/\pi$	$8/\pi^2$	0.000000

Transient heat conduction in infinite cylinder (see 2. 3)

$$\frac{(T - T_1)}{(T_0 - T_1)} = \sum_{i=1}^{\infty} \left(\frac{2}{\beta_i}\right) \frac{J_1(\beta_i)}{J_0^2(\beta_i) + J_1^2(\beta_i)} \; J_0\left(\beta_i \frac{r}{R}\right) e^{-\frac{\beta_i^2 \alpha t}{R^2}} \qquad (A.7)$$

root equation: $$N_{Bi} = \beta_i \frac{J_1(\beta_i)}{J_0(\beta_i)} \qquad (A.8)$$

1st term approximation:

$$\log \frac{(T - T_1)}{(T_0 - T_1)} = \frac{-\beta_1^2 \alpha t}{(\ln 10) R^2} + \log \left[\frac{2 J_1(\beta_1)}{\beta_1 [J_0^2(\beta_1) + J_1^2(\beta_1)]} \; J_0\left(\beta_1 \frac{r}{R}\right) \right] \qquad (A.9)$$

$$j = \frac{2 J_1(\beta_1)}{\beta_1 [J_0^2(\beta_1) + J_1^2(\beta_1)]} \; J_0\left(\beta_1 \frac{r}{R}\right) \qquad \frac{f \alpha}{R^2} = \frac{\ln 10}{\beta_1^2}$$

$$j_c = \frac{2 J_1(\beta_1)}{\beta_1 [J_0^2(\beta_1) + J_1^2(\beta_1)]} \qquad (A.10)$$

$$j_m = \frac{4 J_1^2(\beta_1)}{\beta_1^2 [J_0^2(\beta_1) + J_1^2(\beta_1)]} = j_c \frac{2 J_1(\beta_1)}{\beta_1} \qquad (A.11)$$

$$j_s = \frac{2 J_1(\beta_1)}{\beta_1 [J_0^2(\beta_1) + J_1^2(\beta_1)]} \; J_0(\beta_1) = j_c \; J_0(\beta_1) \qquad (A.12)$$

Table A.2. Numerical solution for infinite cylinder (equation A.9).

β_1	N_{Bi}	$f\alpha/R^2$	j_c	j_m	j_s
0.000	0.00000	∞	1.00000	1.00000	1.00000
0.020	0.00020	5756.46273	1.000050	1.000000	0.999950
0.030	0.00045	2558.42788	1.000113	1.000000	0.999887
0.040	0.00080	1439.11568	1.000200	1.000000	0.999800
0.050	0.00125	921.03404	1.000313	1.000000	0.999687
0.060	0.00180	639.60697	1.000450	1.000000	0.999550
0.080	0.00320	359.77892	1.000800	1.000000	0.999200
0.100	0.00501	230.25851	1.001251	0.999999	0.998749
0.120	0.00721	159.90174	1.001801	0.999999	0.998198
0.140	0.00982	117.47883	1.002452	0.999998	0.997546
0.150	0.01128	102.33712	1.002815	0.999997	0.997182
0.200	0.02010	57.56463	1.005008	0.999992	0.994983
0.250	0.03150	36.84136	1.007833	0.999979	0.992147
0.300	0.04551	25.58428	1.011292	0.999957	0.988665
0.350	0.06221	18.79661	1.015390	0.999921	0.984531
0.400	0.08164	14.39116	1.020131	0.999864	0.979732
0.450	0.10390	11.37079	1.025521	0.999781	0.974258
0.600	0.18862	6.39607	1.045648	0.999294	0.953636
0.750	0.30308	4.09348	1.071851	0.998232	0.926339
0.900	0.45244	2.84270	1.104323	0.996221	0.891767
1.050	0.64445	2.08851	1.143220	0.992743	0.849178
1.200	0.89095	1.59902	1.188591	0.987103	0.797702
1.400	1.33848	1.17479	1.258814	0.974588	0.713565
1.600	2.00226	0.89945	1.338607	0.953583	0.609605
1.800	3.07874	0.71067	1.423969	0.920069	0.484130
2.000	5.15184	0.57565	1.506837	0.869031	0.337367
2.200	11.08276	0.47574	1.573174	0.795115	0.173619
2.230	13.11904	0.46303	1.580484	0.781771	0.148169
2.270	17.22961	0.44685	1.588787	0.763017	0.114099
2.310	24.78411	0.43151	1.595250	0.743155	0.080002
2.360	53.11172	0.41342	1.600416	0.716769	0.037582
2.370	68.52477	0.40994	1.601027	0.711286	0.029152
2.380	96.34846	0.40650	1.601490	0.705734	0.020745
2.390	161.69599	0.40311	1.601800	0.700115	0.012366
2.400	497.85003	0.39975	1.601956	0.694428	0.004017
2.404825	∞	0.39815	1.601975	0.691560	0.000000

Transient heat conduction in sphere (see 2.3)

$$\frac{(T - T_1)}{(T_0 - T_1)} = \sum_{i=1}^{\infty} \frac{2(\sin\beta_i - \beta_i\cos\beta_i)}{\beta_i - \sin\beta_i\cos\beta_i} \frac{\sin(\beta_i \frac{r}{R})}{\beta_i \frac{r}{R}} e^{-\frac{\beta_i^2 \alpha t}{R^2}} \qquad (A.13)$$

root equation: $N_{Bi} = 1 - \beta_i \cot\beta_i$ (A.14)

1st term approximation: (A.15)

$$\log\frac{(T - T_1)}{(T_0 - T_1)} = \frac{-\beta_1^2 \alpha t}{(\ln 10) R^2} + \log\left[\left[\frac{2(\sin\beta_1 - \beta_1\cos\beta_1)}{\beta_1 - \sin\beta_1\cos\beta_1}\right]\left[\frac{\sin(\beta_1 \frac{r}{R})}{\beta_1 \frac{r}{R}}\right] \right]$$

$$j = \left[\frac{2(\sin\beta_1 - \beta_1\cos\beta_1)}{\beta_1 - \sin\beta_1\cos\beta_1}\right]\left[\frac{\sin(\beta_1 \frac{r}{R})}{\beta_1 \frac{r}{R}}\right] \qquad \frac{f\alpha}{R^2} = \frac{\ln 10}{\beta_1^2}$$

$$j_c = \frac{2(\sin\beta_1 - \beta_1\cos\beta_1)}{\beta_1 - \sin\beta_1\cos\beta_1} \qquad (A.16)$$

$$j_m = j_c \frac{3}{\beta_1^3}(\sin\beta_1 - \beta_1\cos\beta_1) \qquad (A.17)$$

$$j_s = \left[\frac{2(\sin\beta_1 - \beta_1\cos\beta_1)}{\beta_1 - \sin\beta_1\cos\beta_1}\right]\left[\frac{\sin\beta_1}{\beta_1}\right] = j_c \frac{\sin\beta_1}{\beta_1} \qquad (A.18)$$

Table A. 3. Numerical solution for sphere (equation A. 15).

β_1	N_{Bi}	$f\alpha/R^2$	j_c	j_m	j_s
0.000	0.00000	∞	1.00000	1.00000	1.00000
0.020	0.00013	5756.46273	1.000040	1.000000	0.999973
0.030	0.00030	2558.42788	1.000090	1.000000	0.999940
0.040	0.00053	1439.11568	1.000160	1.000000	0.999893
0.050	0.00083	912.03404	1.000250	1.000000	0.999833
0.060	0.00120	639.60697	1.000360	1.000000	0.999760
0.085	0.00241	318.69690	1.000723	1.000000	0.999518
0.110	0.00404	190.29629	1.001211	1.000000	0.999193
0.135	0.00608	126.34212	1.001824	0.999999	0.998784
0.160	0.00855	89.94473	1.002563	0.999999	0.998291
0.180	0.01082	71.06744	1.003245	0.999998	0.997836
0.260	0.02264	34.06191	1.006781	0.999991	0.995476
0.340	0.03883	19.91856	1.011620	0.999974	0.992242
0.420	0.05950	13.05320	1.017781	0.999940	0.988121
0.500	0.08476	9.21034	1.025283	0.999878	0.983093
0.600	0.12298	6.39607	1.036586	0.999745	0.975500
0.800	0.22303	3.59779	1.065847	0.999174	0.955740
1.000	0.35791	2.30259	1.104494	0.997917	0.929400
1.200	0.53346	1.59902	1.153260	0.995507	0.895736
1.400	0.75853	1.17479	1.212969	0.991278	0.853800
1.650	1.13096	0.84576	1.304219	0.981982	0.787958
1.950	1.77705	0.60555	1.439317	0.961328	0.685676
2.250	2.81653	0.45483	1.600330	0.923671	0.553411
2.550	4.79541	0.35411	1.775242	0.858958	0.388245
2.850	10.49531	0.28348	1.930778	0.754951	0.194757
2.910	13.33971	0.27191	1.954322	0.728485	0.154148
2.970	18.13822	0.26104	1.973801	0.700028	0.113478
3.030	28.03952	0.25080	1.988439	0.669592	0.073081
3.090	60.83910	0.24116	1.997426	0.637227	0.033336
3.110	99.40785	0.23806	1.999022	0.626026	0.020304
3.116	122.72711	0.23715	1.999356	0.622626	0.016420
3.122	160.32505	0.23624	1.999621	0.619209	0.012548
3.128	231.11014	0.23533	1.999817	0.615774	0.008690
3.134	413.75948	0.23443	1.999943	0.612321	0.004845
3.140	1972.55075	0.23354	1.999997	0.608851	0.001014
π	∞	$\ln 10/\pi^2$	2.00000	$6/\pi^2$	0.00000

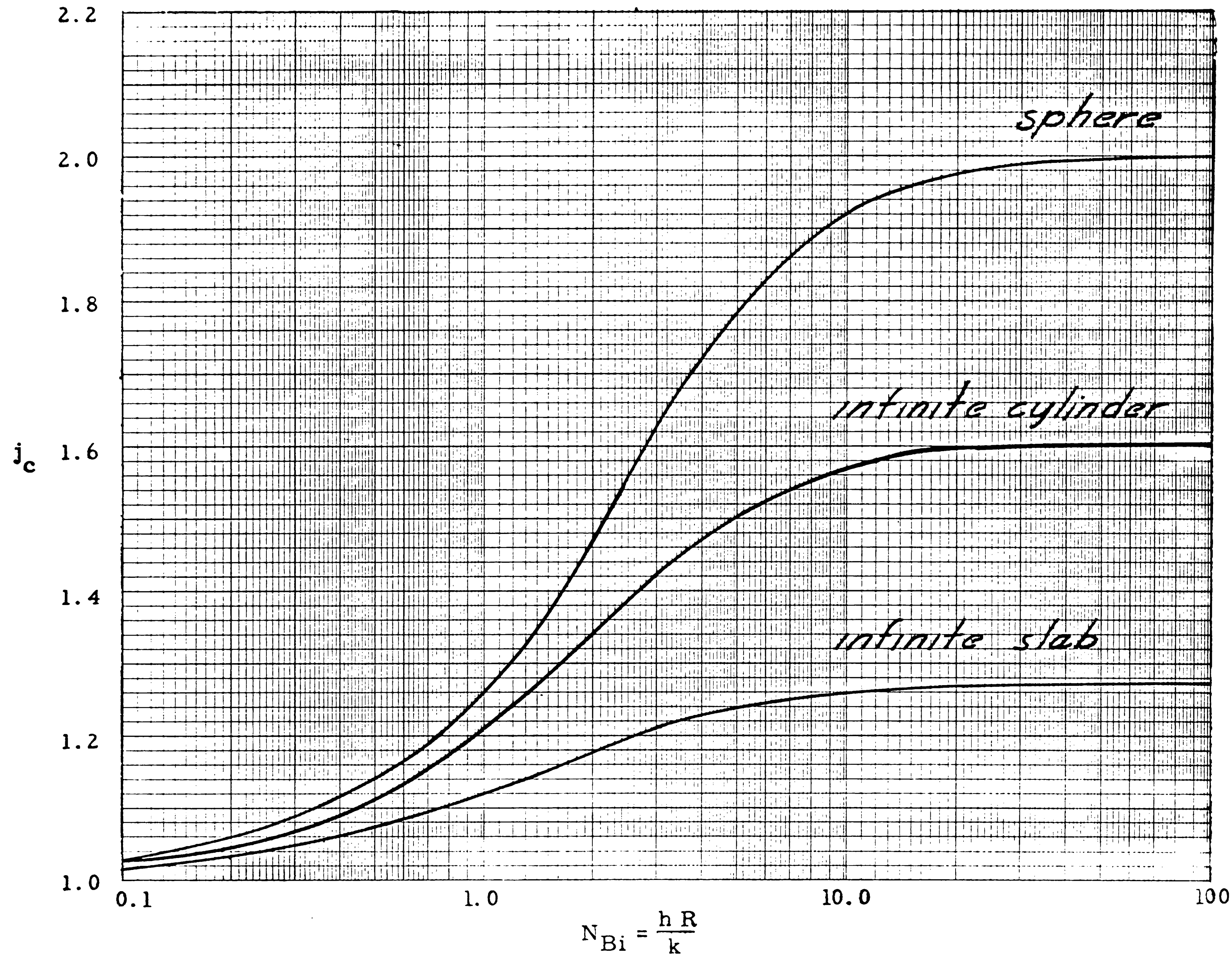

Figure A.1. j_c vs N_{Bi} for infinite slab, infinite cylinder and sphere.

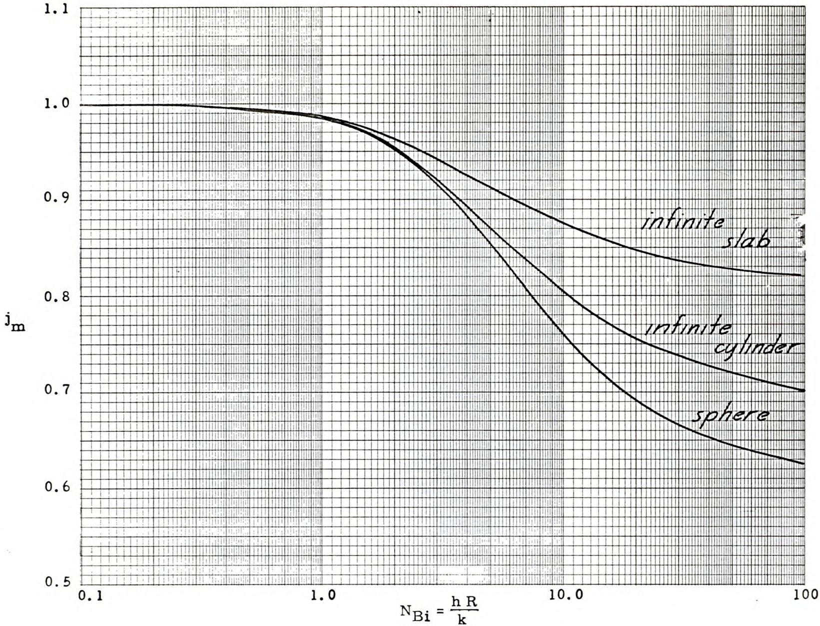

Figure A.2. j_m vs N_{Bi} for infinite slab, infinite cylinder and sphere.

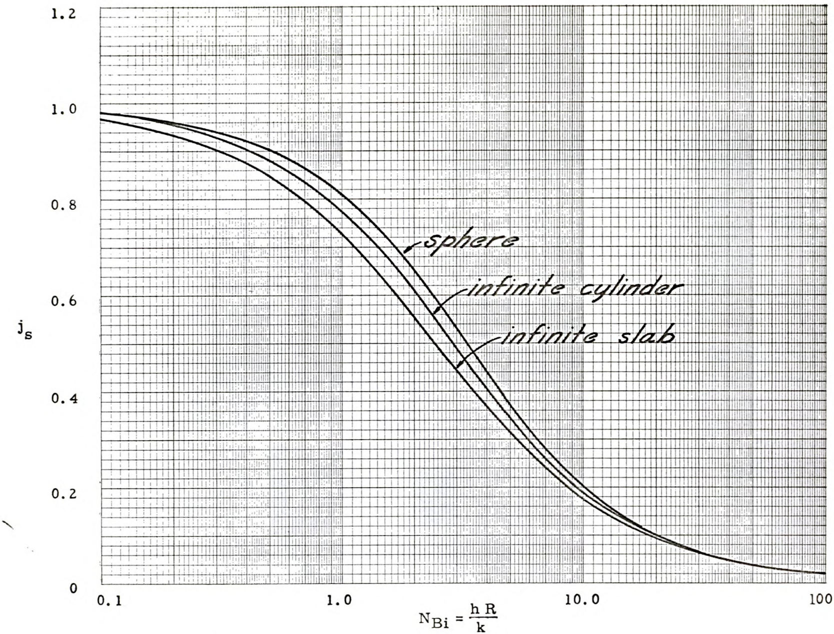

Figure A.3. j_s vs N_{Bi} for infinite slab, infinite cylinder and sphere.

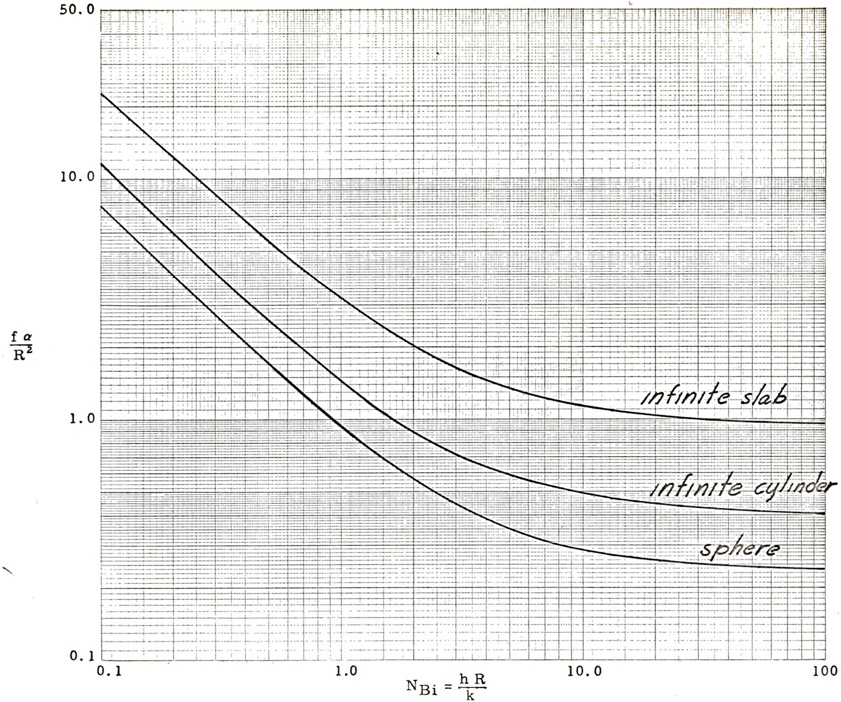

Figure A.4. N_{Bi} vs $f\alpha / R^2$ for infinite slab, infinite cylinder and sphere.

REFERENCES

Anderson, S. A. 1959. Automatic Refrigeration. MacLaren and Son. for Donfoss, Dordobork, Denmark.

A.O.A.C. 1960. Official Methods of Analysis. 9th Ed. Assoc. Offic. Agr. Chemists, Washington, D.C.

Ball, C. O. 1923. Thermal process time for canned food. National Research Council Bull. 37.

Bennett, A. H. 1964. Precooling fruits and vegetables. Trans. ASAE, 7, 3, 265.

Bennett, A. H., Chance, W. G. and R. H. Cubbedge. 1962. Estimating thermal conductivity of fruit and vegetable components. The Fitch method. ASHRAE Journal 9, 1962.

Bennett, A. H., Chance, W. G. and R. H. Cubbedge. 1964. Thermal conductivity of Valencia orange and Mrash grapefruit rind and juice vesicles. 1964 ASHRAE 71st Annual Meeting, Cleveland, Ohio.

Briggs, D. K. H. 1957. Thermal conductivity of liquids. Ind. Eng. Chem. 49, 418.

Charm, S. 1963. A method for experimentally evaluating heat-transfer coefficients in freezers and thermal conductivity of frozen foods. Food Technol. 17 (10), 93.

Charm, S. E. 1963. The Fundamentals of Food Engineering. AVI Publishing Co., Inc., p. 539.

Dickerson, R. J. 1965. An apparatus for the measurement of thermal diffusivity of foods. Food Technol. 19 (5), 198.

Fitch, A. L. 1935. A new thermal conductivity apparatus. American Physics Teacher, 3, 135.

Gane, R. 1936. The thermal conductivity of the tissue of fruits. Report of Food Investigations Board, London, 211.

Graham, L., M. Karel and S. A. Goldblith. 1964. Thermal conductivity of some freeze dried fish. Food Technol. 18 (10), 121.

Harper, J. C. 1962. Transport properties of gases in porous media at reduced pressures with reference to freeze-drying. A.I.Ch.E. Journal 8, 298.

Hildebrand, F. B. 1963. Advanced Calculus for Engineers. 3rd Ed., Prentice-Hall, Inc., London, p. 151.

Homig, P. Principles of Sugar Technology. 1953. Elsevier Publishing Co., vol. 1, ch. 2.

Howard, O. T., and L. W. Aurand. 1963. Food Composition and Analysis. D. Van Nostrand Co., Inc., ch. 8.

International Critical Tables 1929. McGraw-Hill Book Co., Inc., 5:214.

Jason, A. C., and R. A. K. Long. 1955. The specific heat and the thermal conductivity of fish muscle. Proc. Intern. Congr. Refrig. 9th Congr. 1, 2160.

Kopelman, I., Blaisdell, J. L. and I. J. Pflug. 1966. The influence of fruit size and coolant velocity on the cooling of Jonathan apples in water and air. Paper to be presented at January (1966) ASHRAE National Meeting, Houston.

Lentz, C. P. 1961. Thermal conductivity of meats, fats, gelatin gels and ice. Food Technol. 15 (5), 243.

Mannheim, H. C., M. P. Steinberg, and A. I. Nelson. 1955. Determinations of enthalpies involved in food freezing. Food Technol. 9, 556.

McAdams, W. H. 1954. Heat Transmission, 3rd Ed., McGraw-Hill Book Co., New York.

Miller, H. L. and J. E. Sunderland. 1963. Thermal conductivity of beef. Food Technol. 17 (4), 124.

Moline, S. W., J. A. Sawdye, A. J. Short and A. P. Rinfret. 1961. Thermal properties of food at low temperatures. I. Specific Heat. Food Technol. 15 (5), 228.

Ordinanz, W. O. 1946. Specific heat of foods in cooling. Food Industries 18, 101.

Pflug, I. J., J. L. Blaisdell. 1963. Methods of analysis of precooling data. ASHRAE Journal 5, 33.

Pflug, I. J., Blaisdell, J. L. and Kopelman, I. 1965. Procedure for developing temperature-time cooling curves for objects that can be approximated by the geometries of sphere, infinite plate or infinite cylinder. ASHRAE Transaction 31.

Poppendiek, H. F. 1953. Transient and steady state heat transfer in irradiated citrus fruit. ASME Transactions, 75, 421.

Reeve, R. M. H. 1953. Histological investigations of texture in apples. II. Structure and intercellular spaces. Food Res. 18, 604.

Reeve, R. M. and Leinbach, L. R. 1953. Histological investigations of texture in apples. I. Composition and influence of heat on structure. Food Res. 18, 592.

Riedel, L. 1951. Wärmeleit fähigkeits messungen an Mischungen verschiedener organischer Verbendungen mit Wasser. Chem. Ing. Tech. 23:465.

Schneider, P. J. 1957. Conduction Heat Transfer. Addison-Wesley Publishing Co., Inc., 2nd Ed.

Short, B. E., W. R. Woolrich and L. H. Bartlett. 1942. Specific heat of foodstuffs. Refrig. Eng. 44, 385.

Siebel, E. 1892. Specific heats of various products. Ice and Refrig. 2, 256.

Smock, R. H. and Neubert, A. M. 1950. Apples and Apple Products. Interscience Publishers, New York.

Staph, H. E. and W. R. Woolrich. 1951. Specific heat and latent heats of foods in the freezing zone. Refrig. Eng. 59, 1.

Staph, H. E. 1949. Specific heat of foodstuffs. Refrig. Eng. 57, 767.

Stumbo, C. R. 1964. Estimation of the mass average temperature during heating or cooling of conduction heating products in cylindrical cans. Food Technol. 18 (12), 126.

Turrell, F. M. and R. L. Perry. 1957. Specific heat and heat conductivity of citrus fruits. Proc. ASHS, 70, 261.

Walters, R. E. and K. N. May. 1963. Thermal conductivity and density of chicken breast muscle and skin. Food Technol. 17 (6), 130.